IMPROVED FABRICATION AND QUALITY CONTROL OF SUBSTRATE INTEGRATED MICROELECTRODE ARRAYS

Bret E. Zim, B.S.

Thesis Prepared for the Degree of

MASTER OF SCIENCE

UNIVERSITY OF NORTH TEXAS

May 2000

APPROVED:

Guenter W. Gross, Major Professor
David C. Tam, Committee Member
Jeffrey A. Kelber, Committee Member
Earl G. Zimmerman, Chair of the Department of Biological Sciences
C. Neal Tate, Dean of the Robert B. Toulouse School of Graduate Studies

Zim, Bret E., Improved Fabrication and Quality Control of Substrate Integrated Microelectrode Arrays. Master of Science (Biology), May 2000, 119 pp., 10 tables, 38 figures, references, 26 titles.

Spontaneously active monolayer neuronal networks cultured on photoetched multimicroelectrode plates (MMEPs) offer great potential for use in studying neuronal networks. However, there are many problems associated with frequent, long-term use of MMEPs. The major problems include (1) polysiloxane insulation deterioration and breakdown, (2) and loss of gold at the gold electroplated indium-tin oxide (ITO) electrodes. The objective of this investigation was to correct these major problems. Quality control measures were employed to monitor MMEP fabrication variables. The phenotypes of polysiloxane degradation were identified and classified. Factors that were found to contribute most to insulation deterioration were (1) moisture contamination during MMEP insulation, (2) loss of the quartz barrier layer from excessive exposure to basic solutions, and (3) repetitive use in culture. As a result, the insulation equipment and methods were modified to control moisture-dependent insulation deterioration, and the KOH reprocessing solution was replaced with tetramethylguanidine to prevent damage to the quartz. The problems associated with gold electroplating were solved via the addition of a pulsed-DC application of gold in a new citrate buffered electroplating solution.

TABLE OF CONTENTS

Page

LIST OF TABLES

Table Page

LIST OF FIGURES

CHAPTER 1

INTRODUCTION

1.1 Electrophysiology Overview

Neuronal information processing can be organized into three categories: cellular processing, communications between cells, and functions expressed by whole networks. Measurements of the electrophysiological characteristics are necessary for understanding each of these categories (Kandel et al., 1991). However, the nervous system in vertebrates is so complicated that *in vivo* monitoring, particularly of multiple neurons, is difficult. One method of circumventing this problem is the use of dissociated primary cell cultures. Cultured neurons maintain most of their *in vivo* biochemical, electrophysiological and morphological characteristics. Thus, cell culture provides a very useful method for studying the physiology of neuronal systems.

The monitoring of single cell electrical activity is most often carried out in culture using saline-filled glass micropipettes. The electrodes are positioned inside the cell using a micromanipulator, and can thereafter record the action potentials of an active cell. However, it is difficult and very time consuming to work with several glass microelectrodes simultaneously *in vivo* or *in vitro.* This limits the number of possible recording sites and simultaneous, long-term recordings. Voltage sensitive dyes have been employed in the detection of the electrical activity of cells to avoid these problems

(Cohen and Salzberg, 1978, Grinvald et al, 1987, Wenner et al., 1996), but can introduce problems of toxicity, limiting the life of the culture.

An alternative to these methods is to use recording electrode arrays that are positioned outside the cell to detect the extracellular signal. Since the pioneering efforts by Thomas et al. in 1972, and the first recording of spike potentials with photoetched multimicroelectrode surfaces (Gross et al., 1977), steady progress has brought us to the point where the routine monitoring of the internal dynamics of mammalian networks is now possible (Pine, 1979, Israel et al., 1984, Connolly et al., 1990, Jimbo and Kawana, 1992, Nisch et al., 1994, Gross, 1994). The growth of networks on high density photoetched multimicroelectrode plates (MMEPs) is a unique feature of cell culture that holds the promise of allowing long-term, simultaneous monitoring of spike activity from visible cells continuously for weeks, and even months (Gross and Kowalski, 1991). The great advantage of such extracellular recording is that long-term recording from multiple sites can take place, and the simultaneous monitoring of signal traffic in the network is possible.

Spontaneously active monolayer networks on MMEPs offer great potential for use in studying neuronal network development, generation of spatio-temporal action potential patterns, and strategies of pattern processing and storage (Kamioka et al., 1996, Gross et al., 1997). These systems provide data about changes in their physical and chemical environments in terms of changes in burst and spike patterns. The controlled *in vitro* environment allows highly reproducible pharmacological manipulations with no homeostatic interference from other organs. The networks are isolated and do not receive

undefined input from other neural tissue (Gross et al., 1997). Thus, monolayer neural networks grown on MMEPs appear to function as unique and highly effective test systems for the evaluation of neuroactive substances. If applied for use as biosensors or as a pre-screening method, it can accelerate the development of new methods for the rapid detection of neurotoxic substances and also enhance drug development. Because MMEPs allow non-invasive, long-term monitoring of electrical activity and provide optical access for the observation of network growth, this approach should also facilitate the study of neuronal network development and studies of network structure and function.

1.2 MMEP Photolithography and Fabrication

All fabrication occurs in-house by the Center for Network Neuroscience (CNNS) staff. The techniques used to fabricate and prepare multimicroelectrode plates (MMEPs) are described elsewhere (Gross, 1979; Gross and Lucas, 1982; Gross et al., 1985; Gross and Kowalski, 1991). Briefly, the MMEPs consist of an array of photo-etched electrodes (Figure 1) onto which monolayer neuronal networks are grown. The plates (5 cm x 5 cm) are prepared from 1.2 mm thick indium-tin oxide (ITO) sputtered barrier glass (soda lime glass with a 200 Å minimum quartz layer and 1400 Å ITO layer, Applied Films Corp., Boulder, Co.). The 3C electrode conductor pattern consists of a central 0.8 mm^2 recording matrix of 64 microelectrodes (4 rows, 16 columns), and the 4A array contains a central 1.2 mm^2 recording matrix of 64 equidistant microelectrodes (8 rows, 8 columns), as shown in Figure 1. Photoetching is performed utilizing standard methods. Fabrication continues with a series of quality control methods, which include labeling, sanding, and

MMEPs Y3C and Y4A Microelectrode Arrays

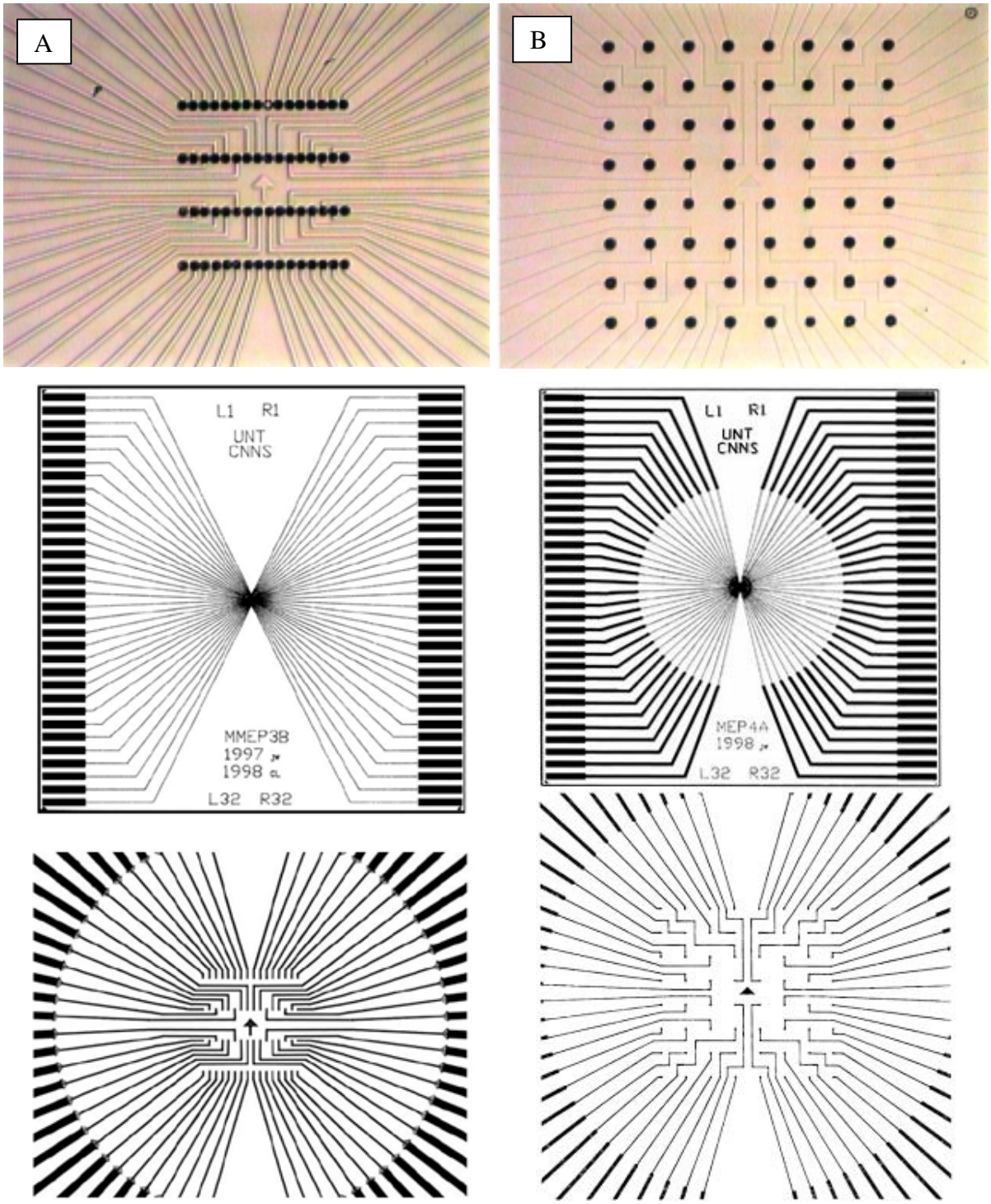

Figure 1: (A) MMEP 3C with 64 conductors terminating in a 0.8 mm^2 recording area in 4 rows of 16 columns. Electrode spacing in columns (lateral) is 40 µm (center-to-center); between rows 200 µm. Electrode area is roughly 225 μm^2. (B) MMEP 4A with 64 conductors terminating in a 1.2 mm^2 recording area of 8 rows by 8 columns. Electrode spacing is equidistant at 150 µm. Electrode area is roughly 900 μm^2.

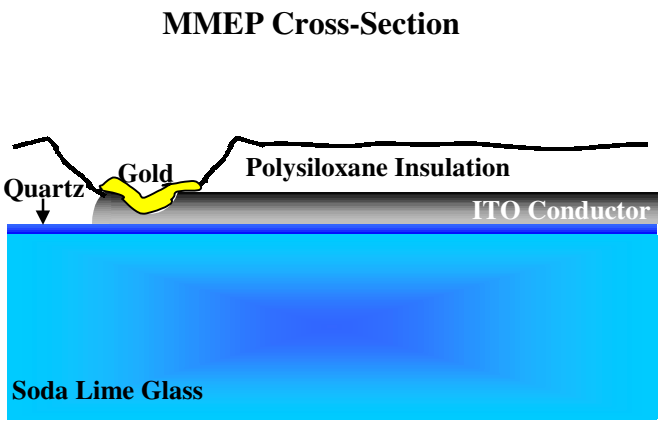

Figure 2: A cross-section of a multimicroelectrode plate (MMEP) showing the layers of components. The 1.2 mm thick indium-tin oxide (ITO) sputtered barrier glass consists of soda lime glass with a 200 Å quartz layer and a 1400 Å ITO layer. After photoetching, the MMEP is spin-insulated with a 2-5 µm layer of polysiloxane. The ITO electrode tip is exposed via laser deinsulation and gold electroplated.

checking for coupled electrodes. The plates are spin-insulated with a 2-5 µm thick layer of polysiloxane resin (Dow Corning 648) yielding a shunt impedance of approximately 15 MΩ. Each microelectrode in the matrix is deinsulated with a single laser pulse (Gross, 1979). This results in about a 20 µm diameter crater at the end of each 10 µm wide ITO conductor. Low recording crater impedances of 1-2 MΩ are achieved by electroplating a thin layer of gold on each exposed ITO tip (Gross et al., 1985). Figure 2 shows a cross-section of a fabricated MMEP.

1.3 Cell Culture

Dissociated tissue cultures are prepared according to the basic method established by Ransom et al. (1977). Embryos are obtained from timed pregnancy Hsd:ICR mice at 14.5 to 18 days gestational age. The tissue is dissociated enzymatically and mechanically, seeded onto MMEPs, and maintained under Minimal Essential Medium (MEM) supplemented with 10% horse serum and 10% fetal bovine serum (MEM 10/10)

for the first 7 days. Thereafter, the use of fetal bovine serum is discontinued and the cultures are maintained in MEM supplemented with 10% horse serum (MEM 10). Seeding concentrations range from 250 to 600 thousand cells per mL. Each MMEP is seeded with 0.5 mL MEM 10/10 containing the dispersed cells. The applied MEM 10/10 is confined to a 4 cm^2 area by a silicone gasket.

Before seeding, the hydrophobic MMEP insulation is prepared to allow maximum cell adhesion. Direct butane flaming (1 sec) oxidizes the methyl groups of the polysiloxane to hydroxyl groups and forms a hydrophilic surface conducive to cell adhesion. Two adhesion areas, a centrally located recording island (typically 2-6 mm in diameter) and a separate, off-center "medium conditioning area" measuring approximately 1 cm x 2 cm are always formed before cells are seeded. Polylysine and laminin adheres only to the flamed regions and are used to enhance cell attachment and growth.

The cultures are incubated at 37°C in a 10% $C0_2$ atmosphere until ready for use, generally three weeks to three months after seeding. Cells are nourished twice a week with MEM containing 10% horse serum. Further descriptions of procedures for cell culture and maintenance can be found in other publications (Gross and Lucas, 1982; Gross et al., 1985; Gross and Kowalski, 1991).

The central island of the MMEP culture, which overlays the recording electrode matrix, typically develops a confluent glial carpet. Intermixed and atop this carpet, a monolayer neural network forms. Among the network, neuronal somata generally are found on top of the carpet, and axonal processes are found both below and at the surface

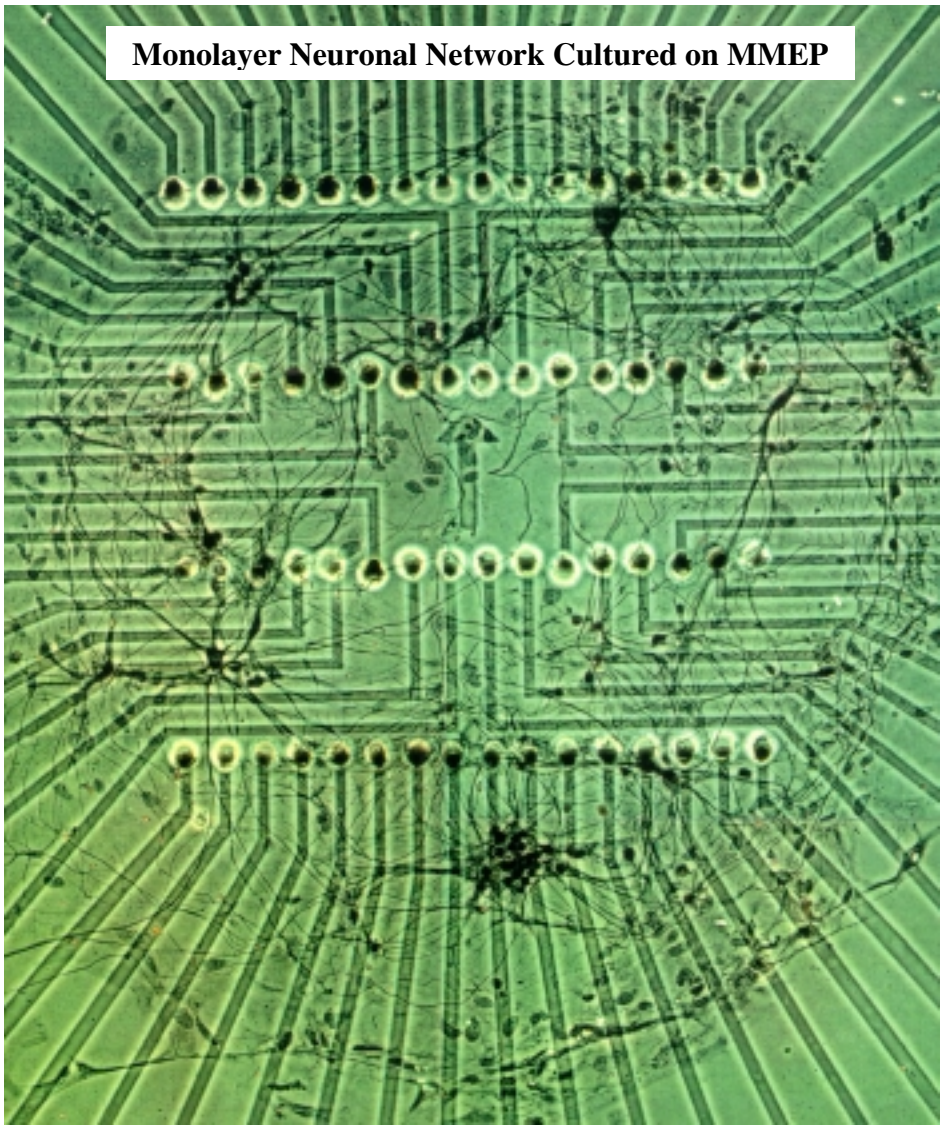

Figure 3: Low density monolayer network consisting of approximately 90 neurons growing over a 64 multimicroelectrode plate (MMEP Y3B) recording matrix 25 days after seeding. The ITO conductors in center are 1000 Å thick and 12 µm wide. Loots modified Bodian Stain (Gross, 1994)

of the glial layer (Figure 3). Previous unpublished work suggests that basic network morphology is established by 15 days *in vitro* and that, on MMEPs, networks can remain

viable, stable, spontaneously active, and pharmacologically responsive for more than six months (Gross, 1994). MMEP fabrication and tissue culture facilities at the CNNS represent a standard support infrastructure for research.

1.4 Data Acquisition and Analysis

The following arrangement allows for the simultaneous recording of spontaneous extracellular spike activity. The MMEP is placed on a base plate and pressed in place by a silicone 0-ring attached to a stainless steel chamber (Figure 4). The culture is maintained at 37°C by heating the base plate and at a pH of approximately 7.4 under a humidified 10% $C0_2$ atmosphere. A plastic cap covers the chamber and is equipped with lines carrying 10% $C0_2$ and a heating unit to prevent condensation on the cap. This allows for maintenance of the pH, osmolarity control, and prevention of culture contamination. pH is monitored by a phenol red indicator in the medium. A peach color signifies a pH around 7.4, which is optimal for culture survival and maintaining stable activity. Chamber components are sterilized via autoclaving and UV light exposure prior to each experiment.

Analysis of subtle aspects of network dynamics incorporating spike separation and spike pattern statistics are performed on a third generation version of the hardware sold by Plexon Inc., Dallas. The statistics on single unit or network activity are generated with a data analysis program package with the hardware. The ability to isolate and monitor single units, as opposed to the multi-unit analysis is essential to understand and characterize individual neurons.

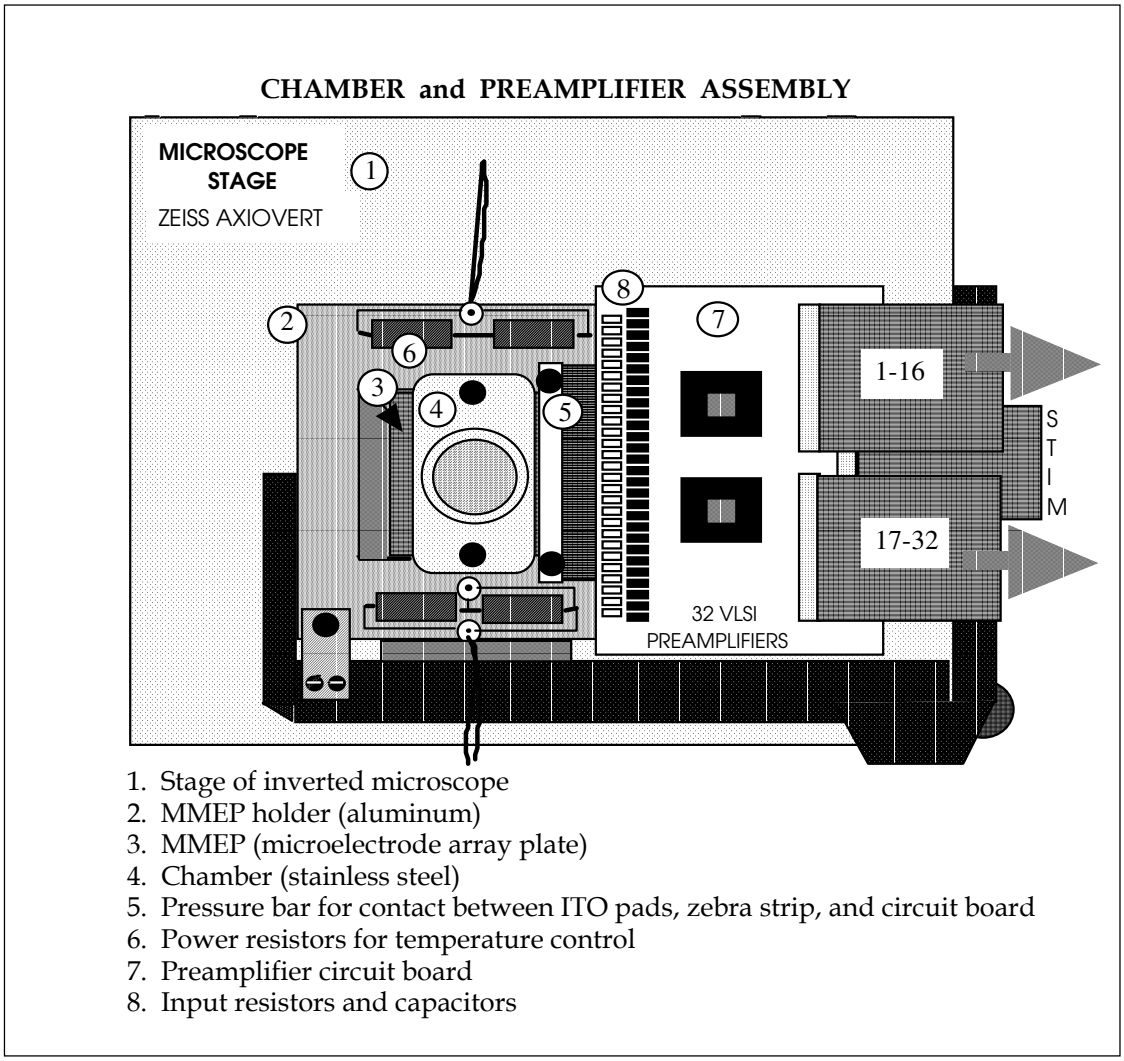

Figure 4: The experimental chamber on the stage of an inverted microscope. 32 preamplifiers are shown attached to the right side of the MMEP. A plastic cap utilized to maintain a 90% air/10% CO_2 atmosphere is not shown. (CNNS Archives)

Figure 5 shows a schematic of the experimental arrangement. Activity is recorded by a custom multi-amplifier system (Plexon Inc.) consisting of 2 sets of 32 preamplifiers connected to 64 second-stage amplifiers. Total system gain is 10K. Signal

Multichannel Recording Workstation

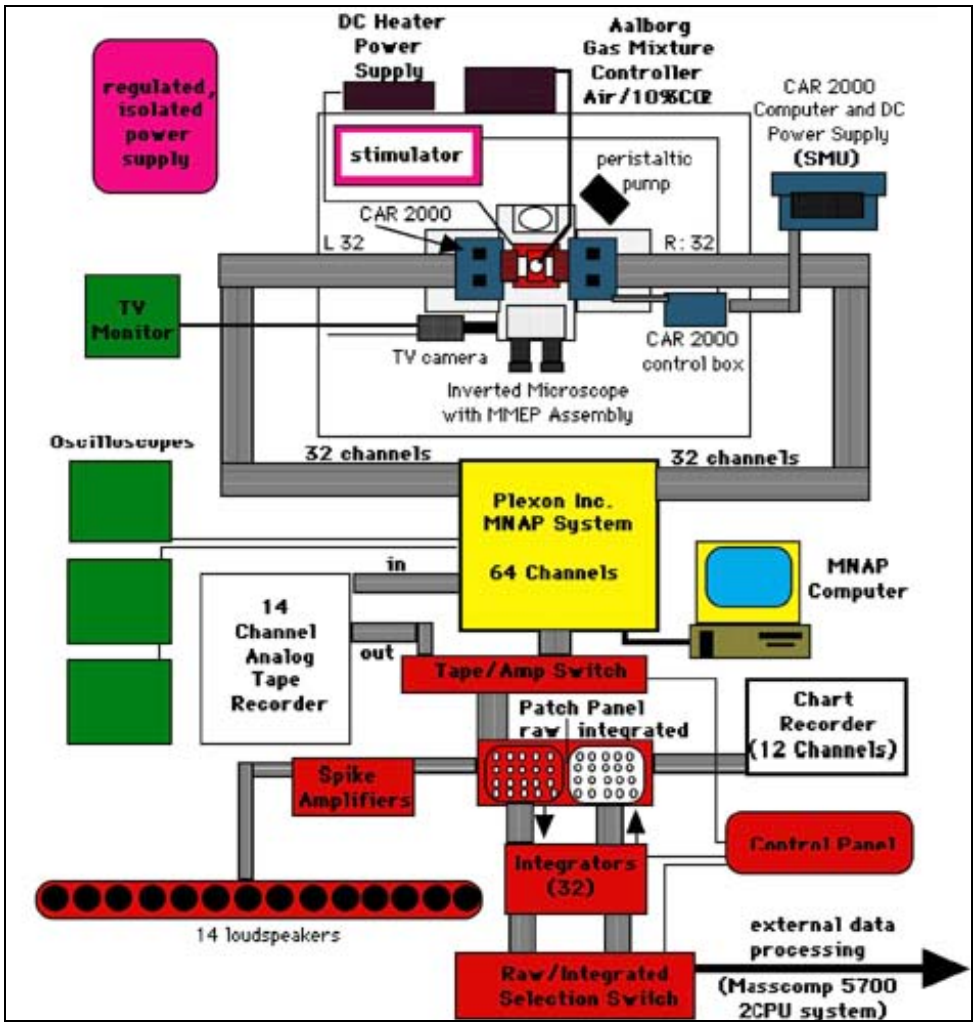

Figure 5: The network is mounted in a special recording chamber on an inverted microscope and connected to 2 sets of 32 VLSI preamplifiers (SMU, Dallas) in a Faraday cage. Spike train data is fed to 64 second stage amps (MNAP system, Plexon Inc., Dallas). All channels can be scanned, selected, and independently assigned to (a) 4 oscilloscope traces, (b) 32 patch panel locations, (c) 14 tape recorder channels, (d) 14 computer channels (to a Masscomp 5700). The 32 patch panel channels are integrated (analog RC circuits) and assigned to another 32 patch panel locations (left and right sides, respectively, of a 64 connector panel). Selected integrated panels (12) are displayed on a strip chart recorder. Raw data channels 1-14 are assigned to the analog tape recorder and to 14 speaker amplifiers. The MNAP system also allows 32 channels to be digitized in real time for spike separation and spike statistics. (CNNS Archives)

output from the amplifiers is selected and can be distributed to a 32-channel patch panel from which all channels are then integrated (analog RC circuits), 12 of the 32 integrated signals can be assigned to a 12 pen strip chart recorder. Fourteen raw data channels can be assigned to a Racal Store 14DS tape recorder, and 14 raw data channels can also be assigned to a Masscomp 5700 computer for off-line burst analysis. Sixteen channels can be assigned to speaker amplifiers for auditory feedback. Channels for recording are selected based on the best signal-to-noise ratios.

1.5 Objectives of Study

The objectives of this research focus on two topics, polysiloxane insulation and gold electroplating. Both procedures are utilized during MMEP fabrication and are essential for developing functional microelectrode arrays that are capable of recording from, or stimulating cultured neural networks grown on MMEPs. However, we have encountered long-term problems associated with the polysiloxane insulation and the gold electroplating. These major problems encompass (1) deterioration and breakdown of the polysiloxane insulation accompanied by the loss of optical clarity, and (2) a decline in electrode performance due to gold loss. Therefore, the focus of this investigation was to characterize and correct the problems associated with polysiloxane insulation degradation and gold electroplating, and improve the methodology. Both these MMEP fabrications procedures are thoroughly examined in this report.

CHAPTER 2

POLYSILOXANE INSULATION

2.1 Introduction

2.1.1 Insulation Criteria

The insulation layer is one of the most critical components of the microelectrode. The properties of the insulation must fulfill many stringent criteria necessary for its particular application. In general, insulation for microelectronic devices, including semiconductors, should be flexible at high and low temperatures, contain favorable electrical properties over a wide operating temperature range, provide protection from moisture, dirt and other atmospheric contaminants, and pass or block light transmission. These attributes are essential for most semiconductor protective coatings.

For the special application of recording from neuronal networks, the insulation must have the following characteristics (Gross 1979). The material needs to be biocompatible and biologically inert. The insulation material must be easy to apply as a thin uniform layer to the electrode plate and allow convenient reproducible deinsulation of the electrode tips during the fabrication process. Since the preferred deinsulation method is the exposure of ITO with single laser shots, the material must break from pressure induced by vaporizing metal in the laser focus (Gross, 1979). However, if the insulation material is too brittle, it will crack during autoclaving or flaming. If the material is too elastic, then breakthrough via single laser shots cannot be achieved. The

DOW CORNING 648 - Semiconductor Junction Coating			
Typical Properties		**Product Specifications**	
Physical		***Physical***	
Appearance	Clear	Color, APHA. maximum	250
Flash Point	85º F (29º C)	Viscosity at 77º F (25º C), cP	80-140
Viscosity. immediately after curing agent. cP	N/A	Pot Life at 77º F (25º C), hrs minimum	--
Mixing Ratio. base/curing agent. parts by weight	N/A	Specific Gravity at 77º F (25º C)	0.99 to 1.03
Durometer Hardness, Shore A. minimum	N/A	Solids Content. after 3 hrs at 275º F (135º C). percent minimum	49
Electrical			
Dielectric Constant, at 10^2 Hz 10^6 Hz	3.22 3.15	Solvent	Xylene
Dielectric Factor, at 10^2 Hz 10^6 Hz	0.008 0.004	Na, ppm maximum	2
Dielectric. Strength, volts/mil	1800	K, ppm maximum	2
Volume Resistivity, ohm-cm x 10^{15}	26	Other metals, ppm maximum	[1]
		Shelf Life at 77º F (25º C), months	6

[1]1ppm max: Ag, Al, Be, Bi, Ca, Co, Cr, Cu, Fe, Ge, Mg, Mn, Mo, Ni, Pb, Sb, Su, T, V, Zr; 10ppm max: Ba, As, Zn; 50ppm max: P

Table 1: Dow Corning 648 (DC648) Semiconductor Protective Coating properties and specifications provided by technical services, Dow Corning Corporation, Midland, Michigan.

insulation must withstand sterilization via autoclaving and allow surface modification to facilitate cell adhesion. It must remain stable for a long period of time under warm saline (biological media). The material must have a low dielectric constant to provide the high impedance required for satisfactory electrical insulation. Good optics is also necessary for direct observation and for the application of many histochemical and imaging techniques. To meet this particular restrictive list of important criteria necessary for this special application, polysiloxane was selected in 1979. As a hydrophobic material,

polysiloxane adheres better to quartz than glass. Hence, the preferred substrate is "barrier glass" that features a 200Å minimum quartz layer on top of a soda-lime glass plate.

2.1.2 Dow Corning 648 (DC648) Polysiloxane

Polysiloxane refers to a class of silicone polymers comprised of a diverse profile of characteristics and uses. Polysiloxane resins form hydrophobic surfaces that remain stable for long periods of time. DC648 polysiloxane has been used routinely to insulate the multimicroelectrode plates (MMEPs) since the process was established by Gross at the Max Planck Institute for Psychiatry in Munich (Gross, 1979). Dow Corning manufactures DC648 Semiconductor Protective Coating as a silicone rigid resin (versus flexible elastomer) designed as a protective coating for semiconductor junctions in solid state devices of all types. The typical properties and product specifications are listed in Table 1. Other types of insulation materials, such as polyimide and HIPEC R-6101 polysiloxane, have been tested and will be discussed later.

In general, silicones are inorganic polymers in which the backbone is a chain of alternating silicon and oxygen atoms as illustrated in Figure 6. Each silicone has two

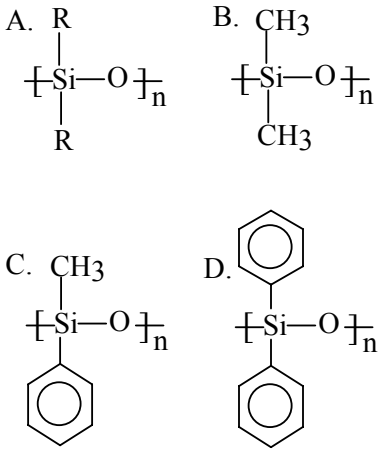

Figure 6: A. The general structure for polysiloxane polymers (silicones). The backbone consists of alternating silicon and oxygen atoms. Each silicone has two organic substituents attached to each silicon atom. B. The structure of polydimethylsiloxane, which is the primary component in DC648 polysiloxane insulation. C and D. The chemical structures for polymethylphenyl-siloxane and polydiphenylsiloxane, respectively.

groups attached to it, and these substituents can be any organic groups. The organic groups attached to the silicon atom via silicon-carbon bonds define the class of silicone. The most common silicone polymers are polydimethylsiloxane, polymethylphenyl-siloxane, and polydiphenylsiloxane. Silicones make good elastomers because the backbone chain is very flexible. Hence, the bonds between the silicon atom and the two adjacent oxygen atoms of the backbone are not rigid, and the bond angles are very flexible. Silicone elastomers are cross-linked fluids whose three-dimensional structure forms a matrix. The properties of this cross-linked matrix are defined by the organic substituents attached to the silicon atoms.

DC648 consists of a polydimethylsiloxane fluid dispersed in xylene. The cross-linking that occurs in curing results from an addition reaction between pendant vinyl groups and pendant dimethylsilyl groups catalyzed by a platinum complex present in concentrations of 3 to 10 ppm (Dow Corning, Technical Services). The reaction is illustrated in Figure 7. Incorporated in the fluid is a volatile polar unsaturated compound that reversibly complexes the Pt catalyst to inhibit cross-linking. In the initial stages of the cure, evaporation of the inhibitor frees the Pt catalyst to allow the addition cross-linking to occur.

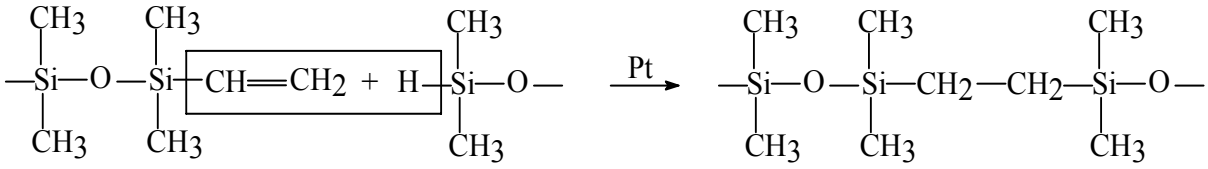

Figure 7: The DC648 polysiloxane cross-linking reaction that occurs during the curing process. The reaction mechanism occurs via an addition reaction between pendant vinyl groups and dimethylsilyl groups catalyzed by a platinum complex.

2.1.3 Polysiloxane Insulation Problems

The problems associated with DC648 polysiloxane insulation degradation on multimicroelectrode plates exhibit diverse phenotypes. A majority of these problems involve poor adhesion of the cured polysiloxane insulation layer to the ITO conductors or the quartz. The characteristics of most deterioration and breakdown that occurs with the ITO conductors range from numerous small granular bubbles to elongated blisters. Similar problems are seen with degradation associated with quartz regions, but the morphologies of the deformations differ. The phenotypes of the bubbles found over quartz regions vary in size and severity, and may hinder the optical analysis of network morphology. There are many other problems with the insulation such as cracking, particulate contamination, delamination, thickness, and surface hydrophobicity. The origins of these problems are unknown, but seem to arise from a variety of influences that range from poor methodology to basic wear and tear.

2.1.4 Polysiloxane Insulation Variables

To better understand the causes of DC648 breakdown, it is first necessary to identify all the variables that could contribute to deterioration of the polysiloxane insulation. These variables are listed in Table 2. They have been categorized into insulation and culture variables, and sub-divided into segments before, during and after the insulation or culturing process.

The contribution of each variable to insulation breakdown varies. Moreover, each variable may lead to a different phenotype of breakdown. The most significant variables that are believed to lead to common ailments of the insulation involve humidity and H_2O

Polysiloxane Insulation Deterioration Variables		
I. MMEP Insulation Variables	4. EtOH Reapplication (100%)	**II. MMEP Culture Variables**
	a. Purity	
Pre-Insulation	b. H_2O contamination	***Pre-Culture***
1. MMEP	c. Quantity	1. Pre-Cleaning
a. Surface cleanliness/residue	d. Spin removal time	a. Soak in dilute detergent
2. EtOH Solution (100%)	5. DC648 Application	b. Mechanical brushing
a. Purity	a. Purity	2. Sterilization
b. H_2O contamination	b. H_2O contamination	a. Autoclave
3. DC648 Polysiloxane	c. Viscosity	b. Oven dry
a. Purity	d. Temperature	3. Surface Modification
b. H_2O contamination	e. Quantity	a. Flaming
c. Age	f. Spin time	
4. N_2 Gas (UHP)		***Culture Development***
a. Purity	***Post-Insulation***	1. Incubation
b. H_2O contamination	1. Air-Dry/Laminar Flow Hood	a. Medium (MEM)
c. Flow rate	a. Environmental	b. Temperature
d. Flow dynamics	b. Time	c. Humidity
5. Spin Apparatus	2. Post-Spin QC Cleaning	
a. Particulate contamination	a. Particulate contamination	***Post-Culture***
	b. Time	1. Recording
Insulation	3. Oven/Cure	a. Stimulation
1. Environmental	a. Ramp and soak cycle	b. Mechanical abrasion
a. Humidity	b. Extent of cross-linking	2. MMEP Re-Use
b. Temperature	c. Contamination	a. Soak in H_2O
2. EtOH Spin Removal	4. Laser Deinsulation	b. 70% EtOH rinse
3. Taped-Edge Technique	a. Induced electrode oxidation	c. <5% Bleach rinse
a. H_2O contamination	5. Gold Electroplating	
b. Particulate contamination	a. CPGC solution chars.	
c. Other contamination	b. Electroplating current	

Table 2: All MMEP insulation and culture variables that possibly contribute to polysiloxane insulation deterioration and breakdown.

contamination at various stages of the insulation process. Culture variables such as autoclaving and flaming have also been shown to induce various types of deterioration. Another important factor to consider is the quality of the DC648 polysiloxane insulation. Here, the shelf-life, purity, and viscosity must be considered.

2.2 Materials and Methods

2.2.1 Equipment and Materials

All MMEP insulation was accomplished in clean room facilities at the Center for Network Neuroscience. The polysiloxane resin (DC648) was obtained from Dow Corning, Midland, MI. Denatured ethyl alcohol was purchased from Sigma Aldrich. Ultra high purity (UHP) compressed nitrogen gas was acquired from Air Liquide, Dallas, Texas. Headway Research of Garland, Texas, was the manufacturer of the photoresist spinner and controller used to insulate the MMEPs. The insulated MMEPs air dried in a laminar flow hood (Bellco Glass, Inc., Vineland, New Jersey). The curing was performed in a forced convection LFD Series 1-42 oven (Despatch Industries, Inc., Minneapolis, Minnesota). The mechanical thermocouple recorder used to monitor the curing cycle was obtained from Omega Engineering, Inc., Stanford, Connecticut.

2.2.2 Previous Insulation Methods

The previous techniques used to insulate the MMEPs have been described elsewhere (Gross, 1979, Gross et al.,1985, Gross and Kowalski, 1991). Briefly, the MMEPs were insulated by a spin application of DC648 polysiloxane resin. A 200 μL quantity of this substance was applied at a viscosity of approximately 100 cP to each MMEP spinning at approximately 4000 rpm. This procedure created a 1.5-2.0 μm thick insulation layer in the center 1/3 of the 5 cm x 5 cm glass electrode plate. In order to raise the shunt impedance of individual conductors from 5 MΩ to more than 25 MΩ, the spin application was followed by hand painting a thicker insulation layer to either side of

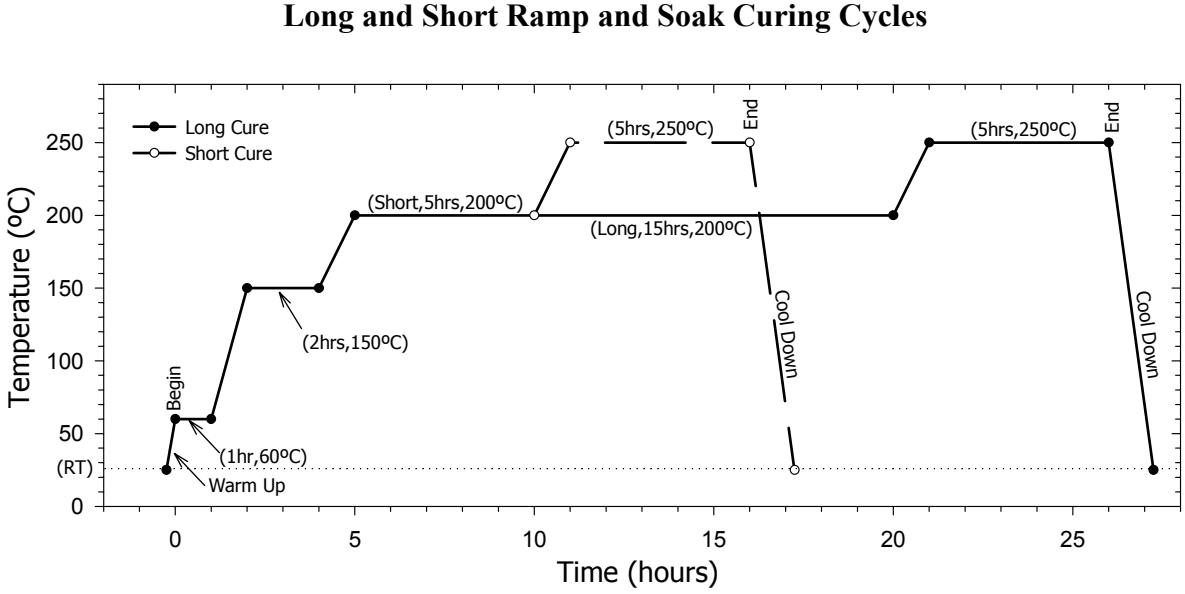

Figure 8: The long and short MMEP ramp and soak curing cycles. Both cycles begin at 60ºC, time 0, after a fifteen minute warm-up from room temperature (RT). The duration for each ramp (60-150ºC, 150-200ºC, 200-250ºC) is 1.00 hour. Both cycles begin the soak at 60ºC for 1.00 hour and continue at 150ºC for 2.00 hours. The long cure soaks 15.00 hours at 200ºC, and the short cure only 5.00 hours. Both cycles end after their 250ºC, 5.00 hour soak, respectively. Cool down requires about 1.25 hours to RT.

the recording matrix. This 10-15µm thick layer of DC648 was painted to within 1mm from the edge of the recording area and covered all conductors leading to the amplifier contact strips at the left and right edges of the MMEP. The thin insulation layer in the center had to be retained to allow laser deinsulation of the electrode tips.

These methods utilized two different ramp and soak curing cycles. A "short" curing cycle was administered after spinning the thin layer of insulation. Following the application of the thick layer, a "long" curing cycle was employed. A graph of temperature as a function of time for both ramp and soak curing cycles is represented in

Figure 8. Note the only difference between both cycles is the soak at 200ºC, where the long cure requires an additional ten hours over the short cure (fifteen versus five hours, respectively).

2.2.3 Quality Control

Quality control measures were created to study polysiloxane integrity and the problems associated with insulation deterioration and breakdown. Quality control renders vital feedback that helps to uncover many of the causes leading to breakdown. In addition, significant variables may be closely monitored and linked to the various deterioration types identified. As a result, MMEP insulation with polysiloxane can be improved considerably. The quality control measures used to investigate insulation degradation are the (1) MMEP Insulation and Curing Records, (2) MMEP Pre-culture Evaluations and MMEP Feedback Evaluations, and (3) Post Insulation Quality Control Assessment Protocol, Checklist, and Datasheet. Detailed descriptions for each polysiloxane insulation quality control measure are provided in Appendix A.

2.3 Results and Discussion

2.3.1 Insulation Degradation Classification

In conjunction with the abundant number of variables that may induce insulation imperfections, deterioration, and finally breakdown, there is a diverse set of degradation phenotypes. The observation of hundreds of used and new MMEPs has provided insight into the different types of degradation.

There are four classifications of degradation found with the polysiloxane (DC648) used to insulate the microelectrode plates. The first major class is associated with any deterioration or breakdown found on the indium-tin oxide (ITO) conductors. The second major classification involves those problems found at the quartz and polysiloxane interface. Delamination of the polysiloxane from the MMEP surface is a less common class of breakdown associated with the DC648 insulation. Any other forms of polysiloxane insulation degradation are categorized in class IV. The physical characteristics correlated with polysiloxane insulation degradation have been classified and are listed in Table 3. Note the degree or severity may vary considerably with every type of MMEP insulation deterioration and breakdown.

2.3.1.1 Class I Degradation Types

There were three types of class I insulation degradation associated with the ITO conductors. The most common types were IA and IB, seen in Figure 9 and 10 (respectively). The reasons for the different morphological characteristics of type IA and type IB were not clear, except that type IA was usually accompanied with type IB deterioration, hinting at a similar origin. Because the ITO electrodes comprised a small

Polysiloxane Insulation Deterioration and Breakdown Classification		
Class	Type	Figure
I. Deterioration Associated with the ITO Conductors		
I.	A. Numerous tiny to small granular bubbles, <2μm in diameter, uniformly spread across the entire surface of the ITO electrodes.	9
	B. Many small to large, elongated bubbles that may span the entire width of the ITO electrodes. They range in size from 1-100μm in length.	10
	C. Many small to medium granular bubbles, 0.5-2μm in diameter, lined up consistently along the edge of the ITO electrodes.	11
II. Deterioration Associated with Regions Over the Quartz		
II.	A. Thousands of tiny granular bubbles, <2μm in diameter, uniformly disbursed across the quartz, spaced equally.	12
	B. Numerous small to medium granular bubbles, 1-5μm in diameter, and large round amorphous bubbles, or blotches, of variable depth, 5-50μm in diameter, evenly distributed throughout the quartz.	13
	C. Same as IIB, but has progressed to be more severe with a greater number of the large round amorphous blotches. The optics is severely impaired.	14
III. Delamination		
III.	A. The delamination originates about the electrode tips at the laser deinsulation-ITO interface.	15
	B. Other types of delamination.	15
IV. Other Types of Deterioration		
IV.	A. Individual electrodes appear very dark, almost burnt, and fractured (oxidation induced).	16
	B. Volcano-like holes that are randomly distributed throughout the insulation.	17
	C. Other types not classified.	16

Table 3: The MMEP polysiloxane (DC648) insulation deterioration and breakdown classification scheme.

Type IA Polysiloxane Insulation Deterioration

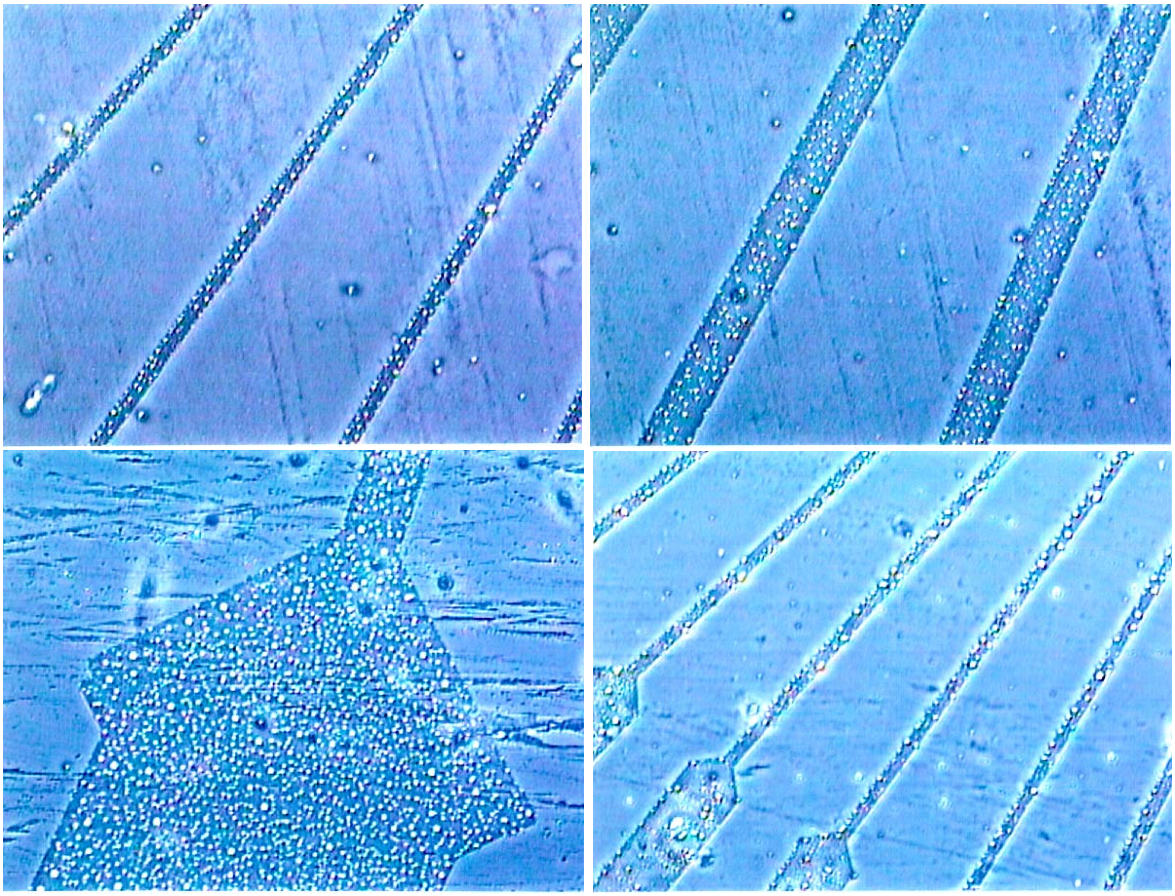

Figure 9: Type IA deterioration associated with the ITO conductors. Numerous tiny to small granular bubbles, <2µm in diameter, are uniformly spread across the entire surface of the ITO electrodes. Pictures were taken using phase contrast microscopy.

percentage of the surface area of the matrix, this class of insulation degradation did not significantly impair optical characteristics. However, a more severe type IB breakdown resulting in exposure of the ITO conductors, may alter the electrical properties of the conductors. Type IC exhibited deterioration along the edge of the conductors (Figure 11).

Type IB Polysiloxane Insulation Deterioration

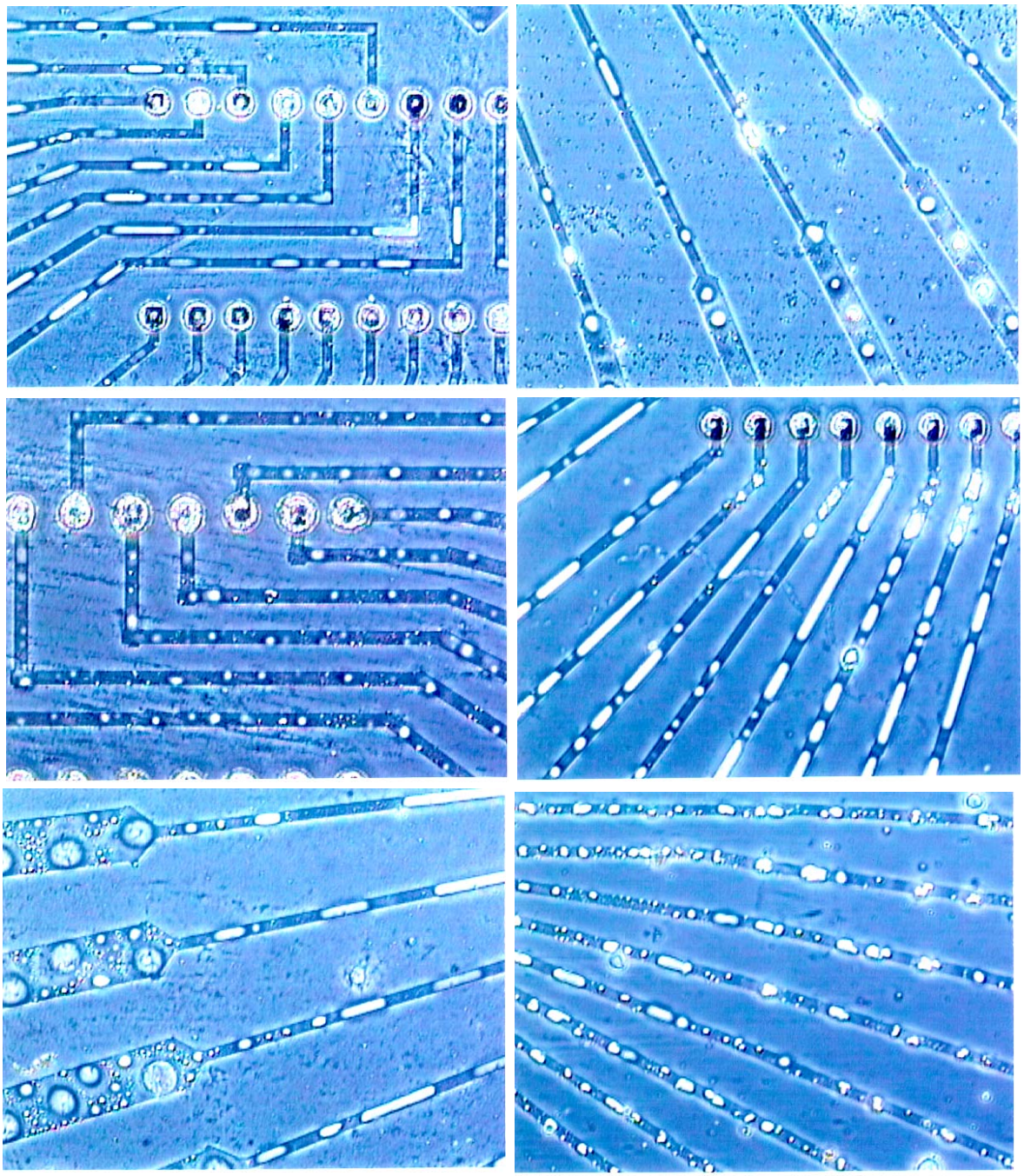

Figure 10: Type IB deterioration associated with the ITO conductors. Many small to large, elongated bubbles may span the entire width of the ITO electrodes. They range in size from 2-100µm in length. Pictures were taken using phase contrast microscopy.

Type IC Polysiloxane Insulation Deterioration

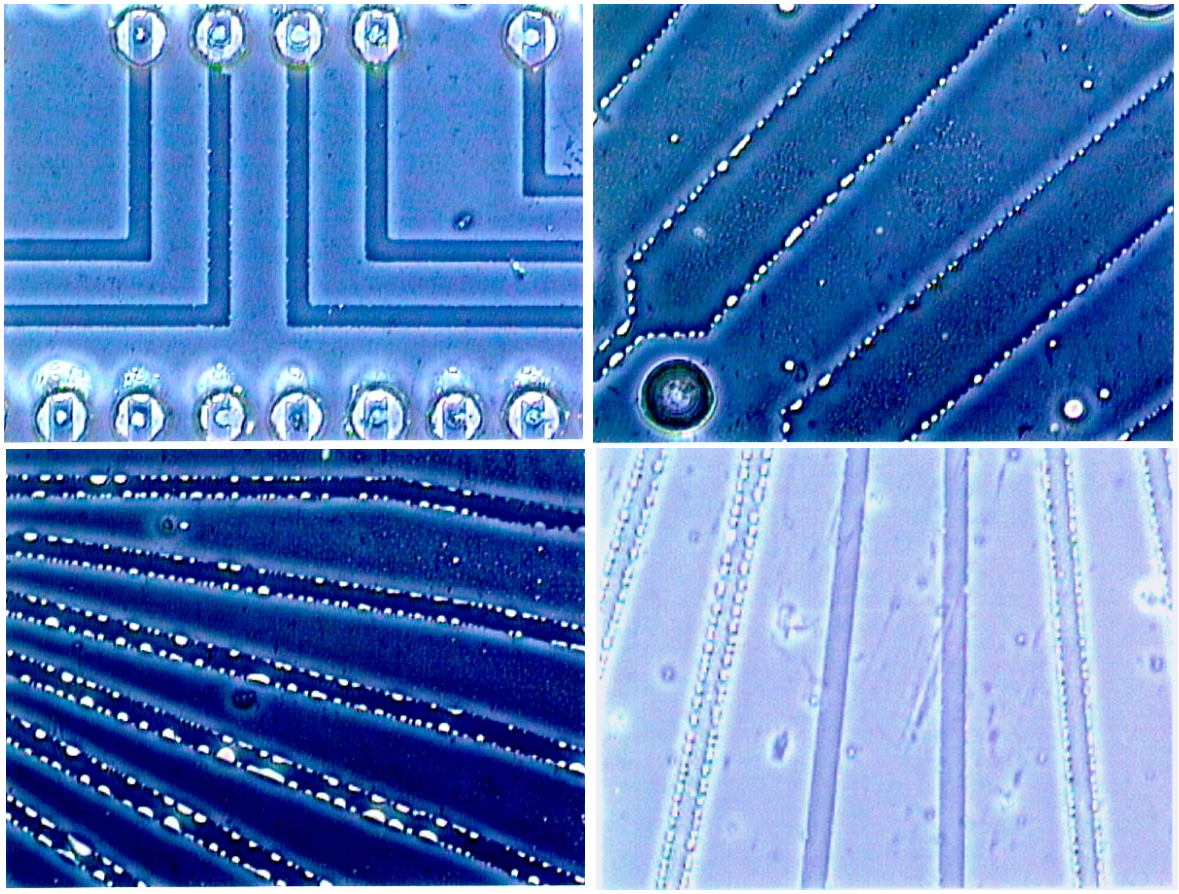

Figure 11: Type IC deterioration associated with the ITO conductors. There are many small to medium granular bubbles, 0.5-2µm in diameter, lined up consistently along the edge of the ITO electrodes. Pictures were taken using phase contrast microscopy.

2.3.1.2 Class II Degradation Types

Class II involved degradation observed over quartz regions. It was divided into three types of deterioration and breakdown that consisted of two phenotypes. Like type IA deterioration seen on the conductors, the less frequent type IIA (Figure 12)

Type IIA Polysiloxane Insulation Deterioration

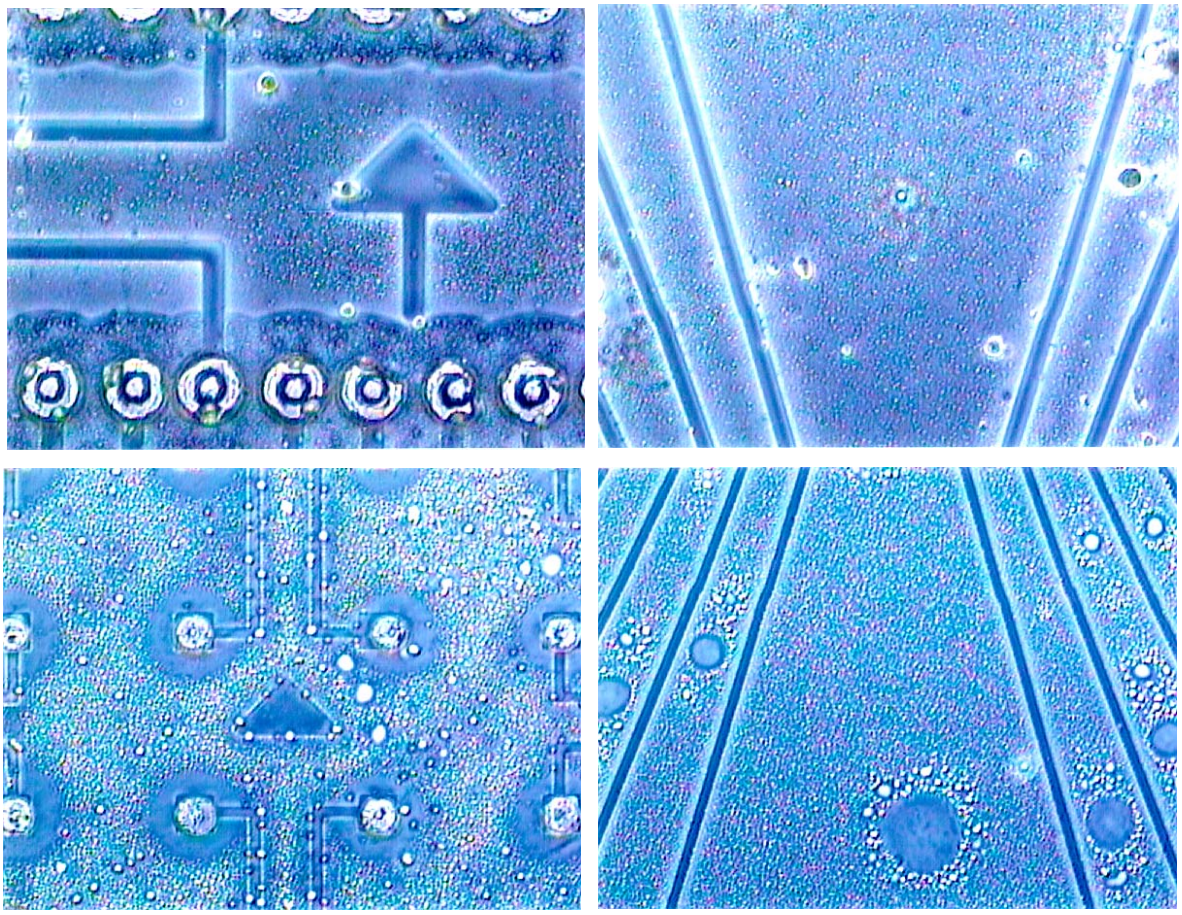

Figure 12: Type IIA deterioration associated with quartz regions. There are thousands of tiny granular bubbles, <2µm in diameter, uniformly distributed across the quartz, spaced equally. Pictures were taken using phase contrast microscopy.

morphology observed over quartz regions had a similar profile and was usually, but not always, accompanied by type IIB or IIC deterioration and breakdown (Figures 13 and 14). Type IIC breakdown was a more severe classification of type IIB, in which the poor optics due to excessive blotches completely interfered with visualization of network properties.

Type IIB Polysiloxane Insulation Deterioration

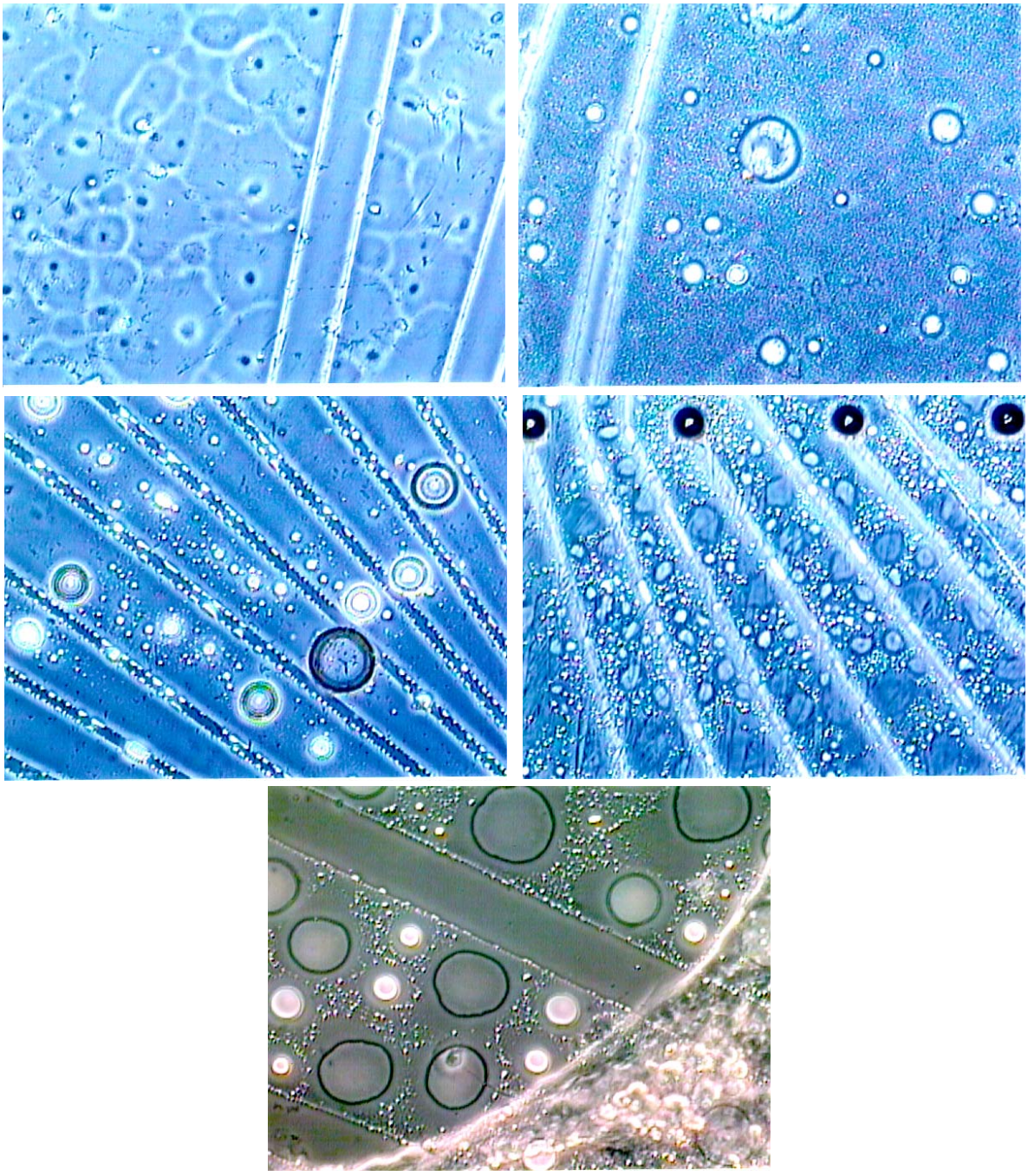

Figure 13: Type IIB deterioration associated with quartz regions. Numerous small to medium granular bubbles, 1-5µm in diameter, and large round amorphous bubbles, or blotches, of variable depth, 5-50µm in diameter, are evenly distributed throughout the quartz regions. Pictures were taken using phase contrast microscopy.

Type IIC Polysiloxane Insulation Deterioration

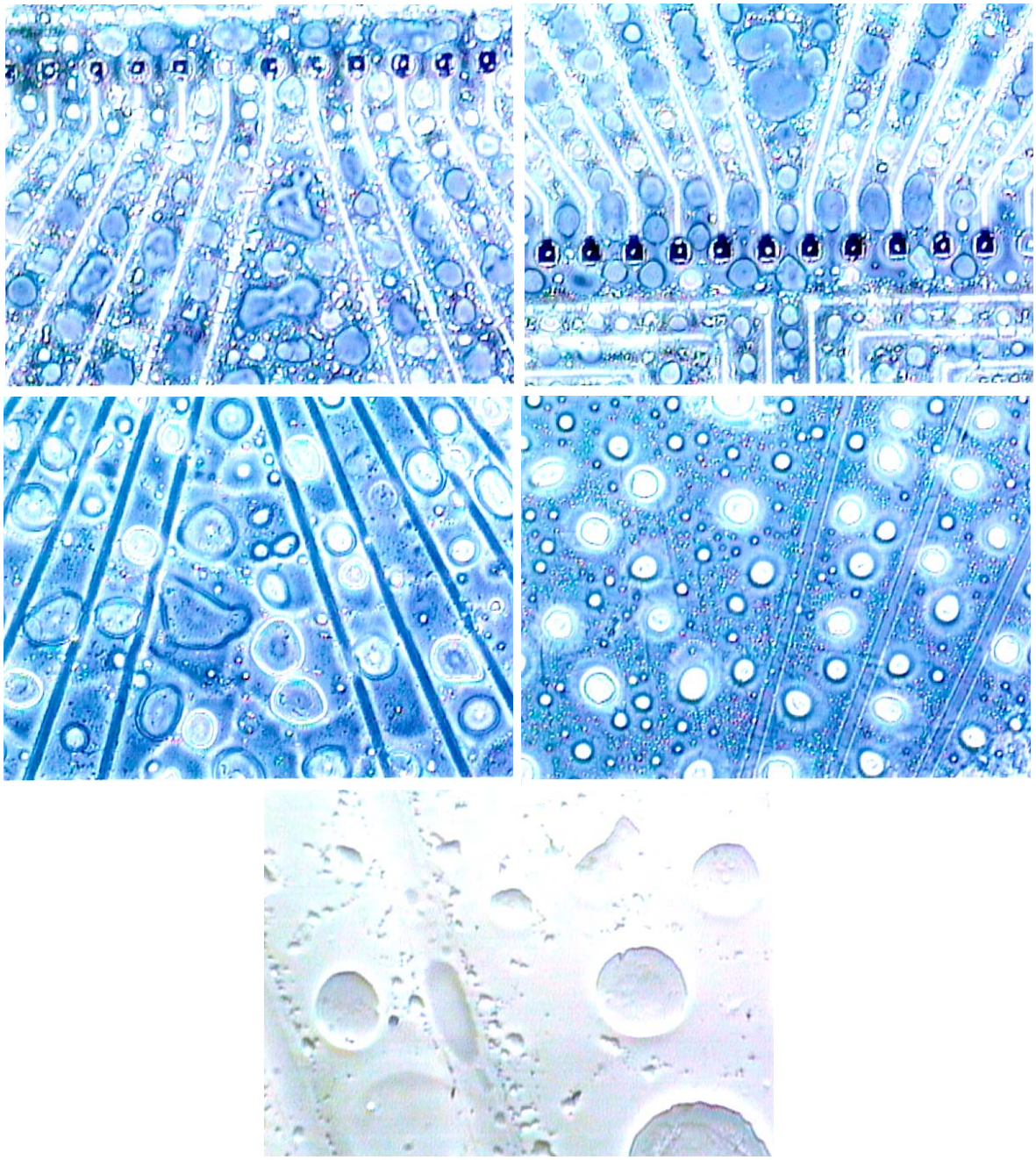

Figure 14: Type IIC deterioration associated with quartz regions. This is the same as IIB, but has progressed to be more severe with a greater number of the large round amorphous blotches. The optics are severely impaired. Pictures were taken using phase contrast and Hoffman modulation (bottom) microscopy.

2.3.1.3 Class III Degradation Types

Class III degradation refers to delamination seen either at the electrode tips or elsewhere on the insulation. Delamination about the electrode tips (type IIIA, Figure 15A) usually occurred in conjunction with severe cases of type IB deterioration along the conductors. The delamination originated at the craters where the laser deinsulation and repeated exposure to culture conditions may have weakened the adhesion of the cross-linked polysiloxane polymers with the quartz. Type IIIB (Figure 15B) delamination took place on any other regions of the MMEP surface, including both ITO conductors and quartz. The delamination looked like open blisters that left either ITO or quartz exposed. Type IIIB delamination was prevalent with severe cases of type IB and IIC degradation.

2.3.1.4 Class IV Degradation Types

Other types of imperfections and degradation were categorized in Class IV. Type IVA (Figure 16A), observed only twice, consisted of specific electrodes that appeared very dark, burnt, and fractured. The common type IVB contained morphological characteristics of an erupted volcano. Evidence of this was best visualized using high magnification phase contrast microscopy and Hoffman modulation, as depicted in Figure 17. The characteristics conformed to a porous indention penetrating the polysiloxane insulation layer, with raised edges around the perimeter. Remnants of insulation spots appeared near the lip of the crater as if they were spewed, like volcanic debris.

Class IVC consisted of various types of imperfections, deterioration, and breakdown. Particulate contaminants (dust, lint, etc.) were common imperfections (Figure 16B). Figure 16C shows cracked insulation, a breakdown usually associated with

Type IIIA and IIIB Polysiloxane Insulation Deterioration

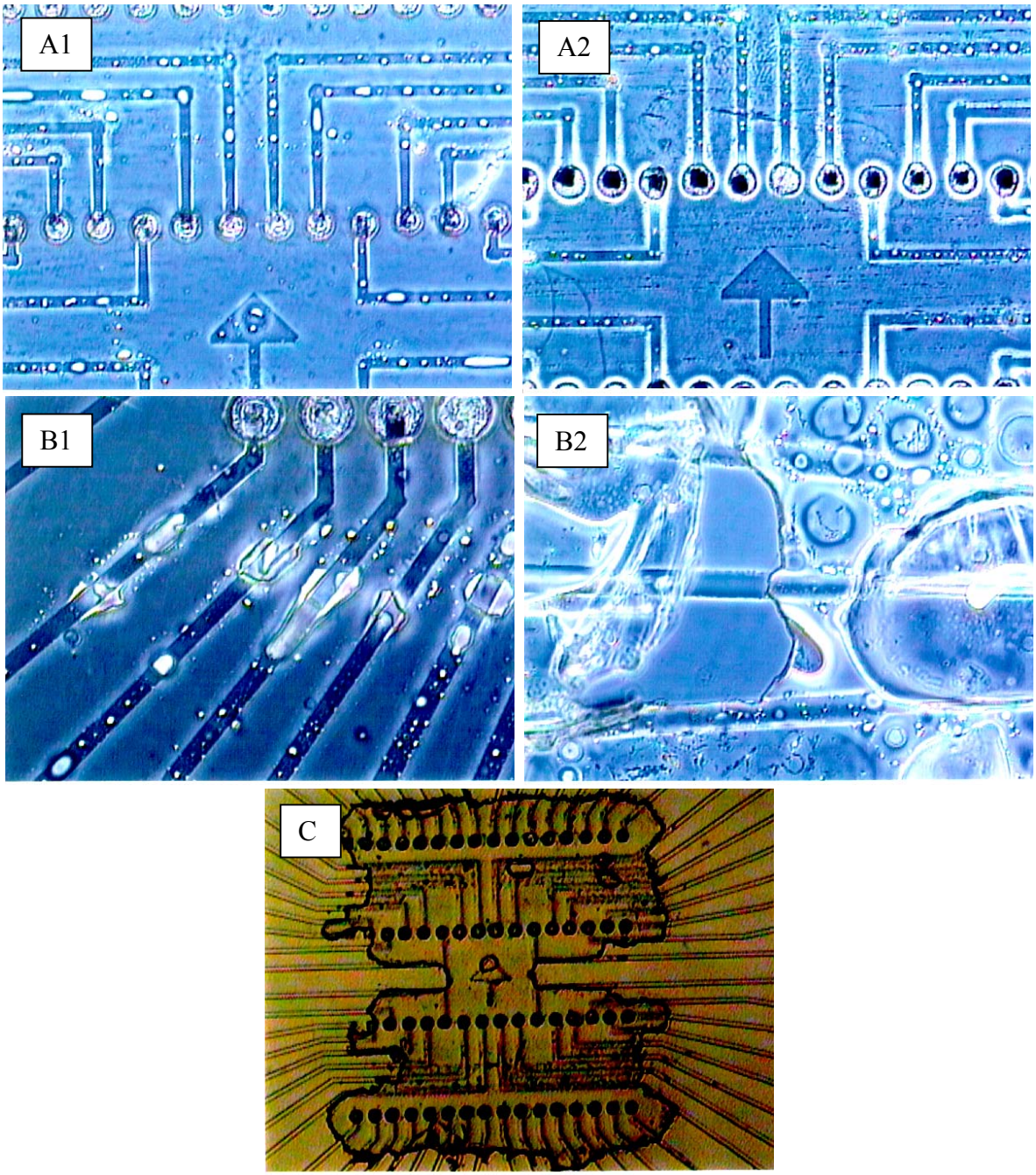

Figure 15: Type IIIA and IIIB deterioration. (A) The delamination originates about the electrode tips at the laser deinsulation-ITO interface (IIIA). (B) Other types of delamination (IIIB) caused by prolonged bleach exposure or (C) too thin a layer of insulation (1 μm). Pictures were taken using phase contrast microscopy.

Type IVA & IVC Polysiloxane Insulation Deterioration

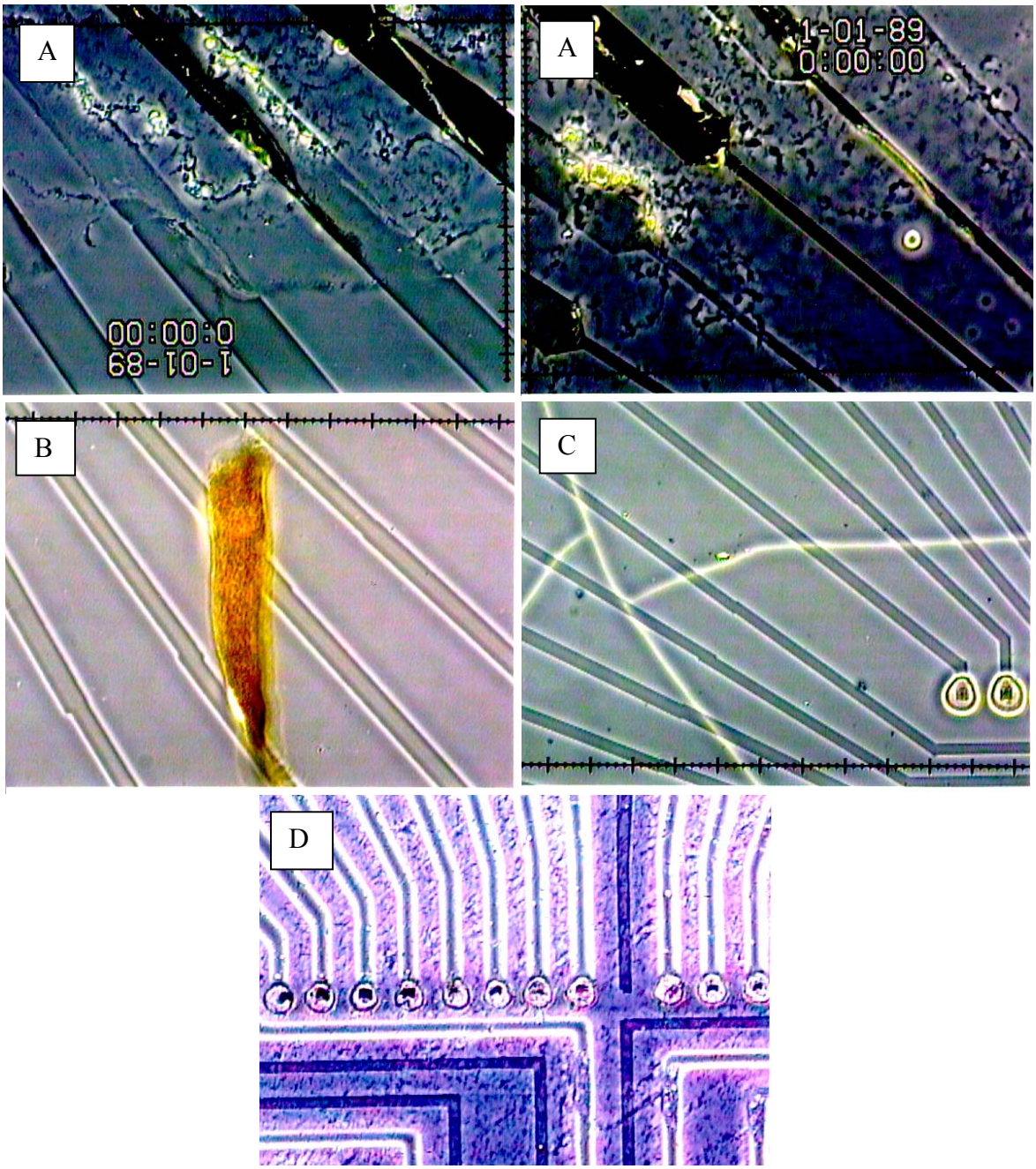

Figure 16: Type IVA and IVC deterioration. A. Individual electrodes appear very dark, almost burnt, and fractured .B. Common imperfection resulting from particulates contaminating the resin during insulation. C. Cracking that usually results from over-flaming. D. The halo phenomena seen only on deinsulated and exposed electrodes. The electrodes without the halo are not deinsulated because they are damaged or cut. Pictures were taken using phase contrast microscopy.

Type IVB Polysiloxane Insulation Deterioration

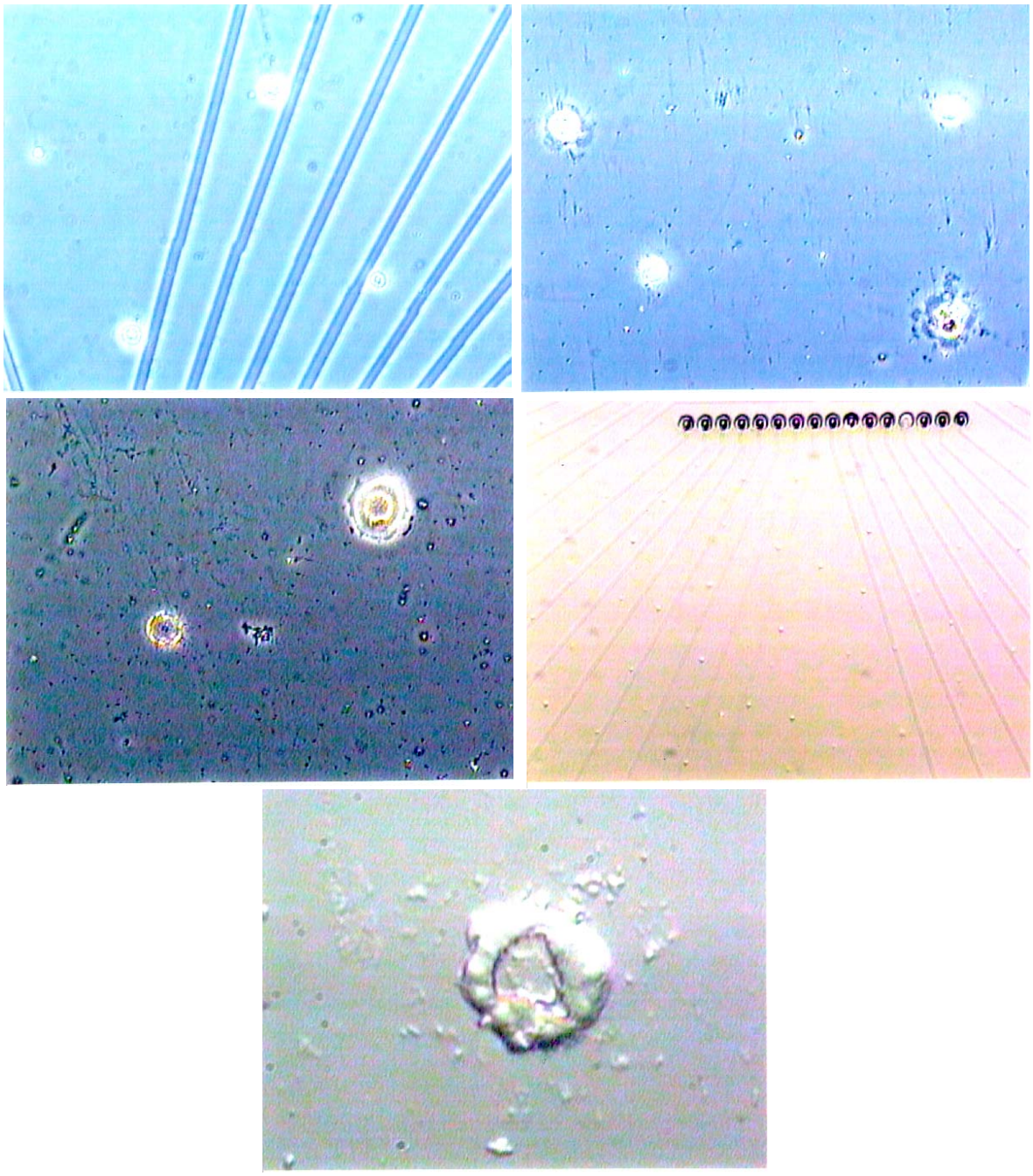

Figure 17: Type IVB deterioration where volcano-like holes are randomly distributed throughout the insulation. Pictures were taken using phase contrast and Hoffman modulation microscopy.

Summary of Insulation Deterioration and Breakdown Causes		
Class	**Causes**	**Probable Causes**
I	1. Flaming & Biological Media (Saline) 2. Bleach	1. EtOH "Out-gassing" 2. Autoclaving 3. DC648 Age
II	1. H_2O Contamination 2. KOH/EtOH (Quartz Removal) 3. Bleach 4. Biological Media, Saline 5. Contrad 70 Detergent (Quartz Removal) 6. Autoclaving	1. EtOH (pro-longed exposure) 2. Flaming 3. DC648 Age
III	1. Ultrasonication 2. Bleach	1. Repeated Culture Use
IV	1. Particulate Contamination	1. Flaming

Table 4: The causes have been proven to directly contribute to the different insulation deterioration and breakdown phenotypes. The probable causes are believed to contribute to insulation degradation.

over-flaming. Phase bright regions that appeared along the edges of the conductors, especially near the matrix, were termed "halo's" (Figure 16D).

2.3.2 Probable Causes of Insulation Degradation

The causes for the diverse phenotypes of insulation imperfections and degradation under each classification were investigated extensively. Experimental results and quality control feedback provided evidence for direct causes that led to many phenotypes of deterioration and breakdown. In some cases, only probable causes were postulated. These results are summarized in Table 4. Also, the MMEP Evaluation Database (Appendix A) was utilized to examine the frequency profile for each class of degradation exhibited by MMEPs (n=27) cycled through culture five times (Figure 18). Note these MMEPs were insulated after equipment and method modifications were made.

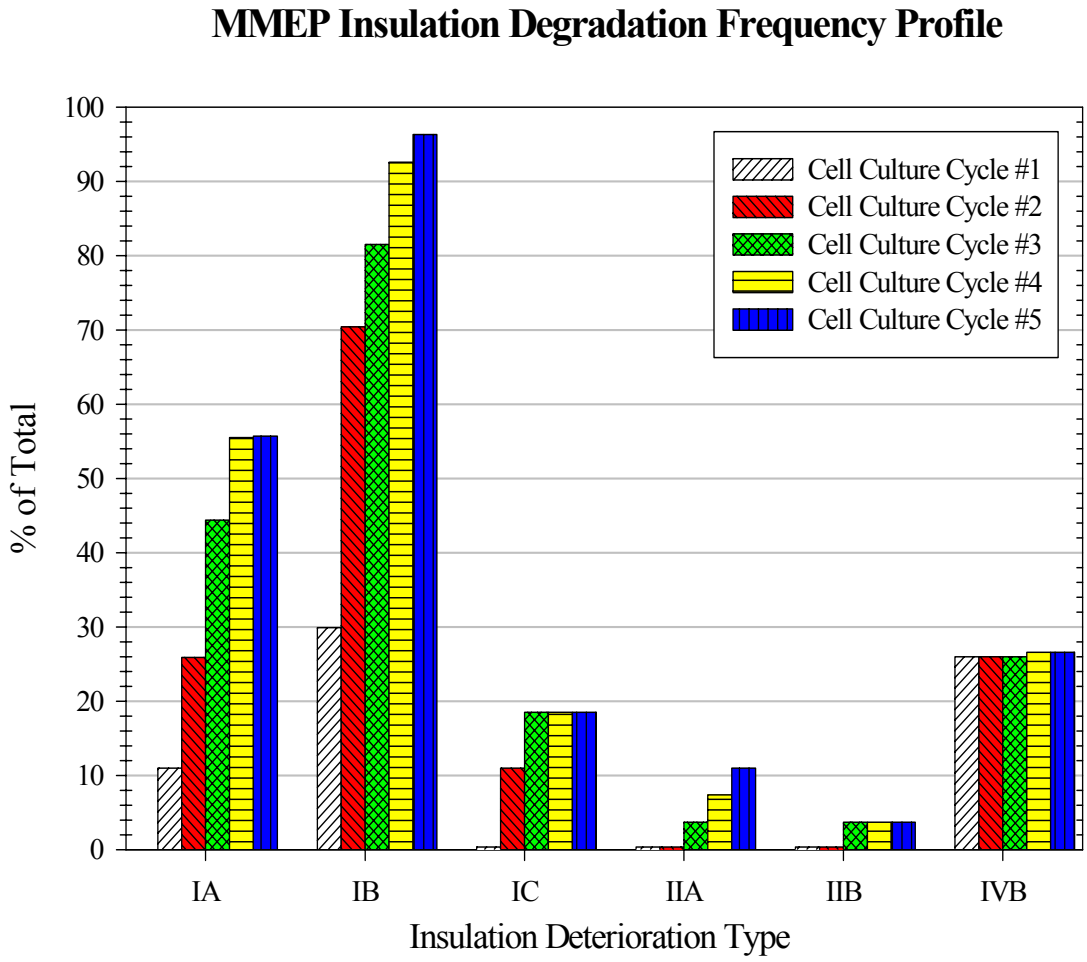

Figure 18: (n=27) The MMEP insulation deterioration and breakdown profile of 27 MMEP Y3C's cycled through cell culture a minimum of five times. All MMEPs were insulated after the spinner modifications. The MMEPs were evaluated after each cycle through cell culture and recorded into the MMEP Pre-Culture Evaluation Database. Type IA and IB (on the ITO electrodes) were the most common phenotypes of deterioration and were observed on about 10% and 30% (respectively) of the MMEPs following the first cell culture cycle. The degradation of IA and IB progressed steadily as a function of cell culture cycles (i.e. exposure to flaming and media). IC was usually observed in the presence of type IA and IIA. After minimizing moisture contamination using the new methodology, type IIA and IIB deterioration on the quartz was not frequently encountered. Type IIC or III(A or B) was not observed. Type IVB found on about 27% of the MMEPs was caused by particulate contamination during curing prior to cell culture use. Therefore, IVB is independent of the number of cell culture cycles.

2.3.2.1 Probable Causes for Class I Degradation

The causes for class I degradation were difficult to elucidate. Type IA and IB (Figures 9 and 10) were observed in the flaming region on the matrix of the MMEP after exposure to culture solvents, decontaminants, and repeated cycles through culture. This did not occur after flaming only once. Furthermore, we postulated that the adhesion of the hydrophobic polysiloxane to the hydrophilic ITO conductors was poor. The genesis for the rare type IC deterioration was unknown when it was exclusive from other types of degradation. Type IC deterioration (Figure 11) along the edge of the conductors frequently occurred in conjunction with type IA or IIA degradation, where the deterioration on the quartz occasionally appeared to push up against and over the raised edge of the conductor.

A. EtOH Out-gassing

One hypothesis for type IA was out-gassing of trapped EtOH in the ITO conductors upon exposure to high temperatures during flaming. The applied EtOH drops may have been absorbed by the ITO conductors and not allowed to completely evaporate before the application of the insulation. However, there were no conclusive results to support this postulate, because type IA had never been observed directly after flaming.

An experiment designed to force insulation deterioration by applying 100% EtOH to the surface of three MMEPs immediately before the polysiloxane resin, did not exhibit type IA deterioration after flaming (Table 5). Instead, these three MMEPs treated with EtOH showed signs of type IIB deterioration after autoclaving. The cause for type IIB degradation was H_2O contamination, and will be discussed later. Type IA deterioration

Forced Insulation Deterioration						
Batch #	**Treatment**	**MMEP #**	**Spin Order**	**Insulation Deterioration Type (Severity)**		
				Before Autoclaving	**After Autoclaving**	**After Flaming**
1	Control	Y3C374	1	None	IIB	No Change
		*Y3C379	6	None	IIB	No Change
		Y3C384	11	None	IIB	No Change
2	New DC648	Y3C375	2	None	None	None
		*Y3C380	7	IIB	IIB (increase)	No Change
		Y3C385	12	None	IIB	No Change
3	**H_20 Application**	Y3C376	3	**IIB**	IIB (increase)	No Change
		*Y3C381	8	**IIB**	IIB (increase)	No Change
		Y3C386	13	**IIB**	IIB (increase)	No Change
4	EtOH Application	Y3C377	4	None	IIB	No Change
		*Y3C382	9	None	IIB	No Change
		Y3C387	14	None	IIB	No Change
5	Direct N_2 Application	Y3C378	5	None	IIB	No Change
		*Y3C383	10	None	IIB	No Change
		Y3C388	15	IIB	IIB (increase)	No Change

Table 5: Summary of forced insulation deterioration experiments. Current insulation methods were used with exception to the treatments listed in the table and the spinner apparatus modifications (N_2 source directed into open spinner well, open neck, and no lid). All MMEPs were spun in numerical sequence from Y3C374 to Y3C388 at 4,400 rpm. The control consisted of stock DC648 that had been opened for approximately one year. The new DC648 came from fresh, unopened stock. Approximately 1 mL of UPH_2O and 100% EtOH (obtained from the biology stockroom) were applied immediately prior to DC648 application. Excess UPH_2O and EtOH were removed via a two-second spin at 4,400 rpm. Direct $UHPN_2$ was streamed directly over the matrix about ten seconds just before insulating. After a routine long cure, the second of the three MMEPs in each batch (indicated with an *) was cured with an additional long cure. All MMEPs were then subjected to autoclaving and flaming as outlined in the Quality Control Assessment, to force insulation deterioration.

was not observed after flaming in another experiment that compared two different types of EtOH (Table 6). Again, type IIB deterioration (moisture contamination) occurred after autoclaving. Hence, EtOH did not contribute to class I degradation, and EtOH out-gassing was not seen after flaming each MMEP once.

B. Flaming

It was deduced from the Pre-culture Evaluation Database that the more times a MMEP was flamed, the greater the possibility of the electrodes to exhibit type IA or IB deterioration and breakdown (Figure 18) in the flamed regions. However, this was not apparent after flaming only once in previous experiments, unless the MMEPs were exposed to biological media or saline. Over 90% of all MMEPs that cycled through culture at least three times exhibited type IA and/or IB degradation on the conductors (mostly type IB), which was concentrated around the flaming area of the matrix. This region was directly exposed to the flame. The evidence suggested that after the MMEPs have cycled through culture, they were more susceptible to type I deterioration on the conductors, which was dependent on flaming and exposure to biological media (or saline). An increase in the severity was correlated with increased uses or cycles of the MMEP through culture.

C. Culture Solvents

Insulation exposed to saline or biological media has already been shown to exhibit class I degradation when coupled with flaming and repeated cycles through culture (Figure 18). In addition, the evaluation database revealed hundreds of MMEPs that had a rectangular gasket ring encompassing a region consisting only of type IA and IB degradation. Here, deterioration and breakdown was observed on the ITO conductors that started at the matrix and spanned all the way to the inner perimeter of the gasket, where silicon grease was used to attach the gasket to the insulation. The gasket was used to contain the medium required for cell growth and maturation. This was observed on

MMEPs cycled through culture at least three times. Therefore, it was possible that further degradation, associated with the conductors, was caused by exposure to biological media. The areas on the insulation protected by the silicon grease and gasket showed minimal deterioration when compared to adjacent regions inside the gasket.

In some cases, the entire MMEP, except for the regions covered by the gasket, displayed type I degradation. They were said to contain a "gasket ring", where the protected areas under the silicon sealed gasket showed very little degradation. This scenario was similar to the situation just discussed, except the problems were also noticed outside the perimeter of the gasket ring. The most probable source for this occurred when the MMEPs were saturated for many hours in a DIH_2O bath and/or alkaline detergent after culture use. The MMEPs were subjected briefly to 70% EtOH when the cultures were contaminated with bacteria. Although there was no evidence that soaking in EtOH caused deterioration, there was clear evidence that EtOH mixed with other solvents did. KOH, tetramethylguanidine, or ethylene dichloride mixed with EtOH were reprocessing mixtures used to strip the insulation (MMEP reprocessing). Prolonged exposure to bleach, on the other hand, was known to cause Type I (also Types II and III) degradation of the insulation layer.

2.3.2.2 Probable Causes for Class II Degradation

The leading causes for class II (Figures 12, 13 and 14) degradation were H_2O contamination and damaged quartz. Other factors included prolonged exposure to media and ionic solutions, especially bleach. Feedback from the database indicated that class II was more common on reprocessed MMEPs, and rarely took place on new MMEPs. It

Forced Insulation Deterioration

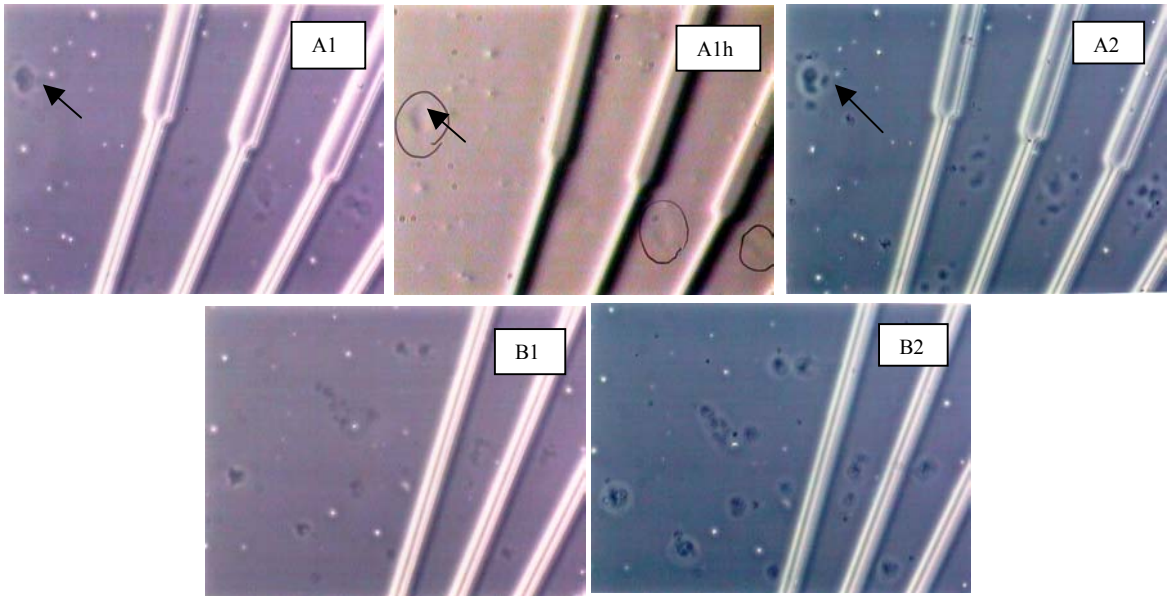

Figure 19: Progressive type IIB deterioration observed on two MMEPs (A:Y3C386 and B:Y3C381). Both MMEPs were pretreated with UPH_2O prior to spinning to force H_2O contamination. All of these MMEPs exhibited premature type IIB deterioration on quartz regions before autoclaving (A1, A1h (Hoffman modulation), and B1). The type IIB deterioration was worse after autoclaving (A2 and B2). Arrows define an example of this type IIB deterioration that gets worse after autoclaving. Note in A1h the arrow indicates a typical blotch seen in type IIB and IIC deterioration that appears to be a depression in the insulation surface. Pictures were taken using phase contrast and Hoffman modulation microscopy.

was proven that the reprocessing altered the quartz layer, leaving the surface more hydrophilic, and susceptible to breakdown. This is discussed in detail under MMEP Reprocessing.

A. H_2O Contamination

Of the insulation variables listed in Table 2, the most important, widespread variable was H_2O contamination. Moisture contamination that occurred just prior to the

spin-application of polysiloxane was the greatest cause proven to lead to type II deterioration and breakdown. At this critical time, we have demonstrated the possibility of water-contaminated air currents that were pulled down onto the top surface of the spinning MMEP, before the spinner apparatus was modified. The spinner modifications and airflow tests will be addressed under Spinner Apparatus Modifications in the next section. In fact, these humid air currents which contaminated the MMEP surface caused mild type IIB deterioration on the MMEPs as demonstrated by the forced insulation deterioration experiments (Table 5), as well as all other experiments which were conducted prior to spinner modifications (humidity control). After these significant modifications, this class of contamination was prevented and rarely occurred (Figure 18).

Evidence for type II deterioration induced by water contamination was shown in the forced insulation deterioration experiments (Table 5). The addition of ultra pure water (UPH_2O) immediately prior to DC648 application resulted in mild type IIB deterioration, observed both before and after autoclaving (Figure 19). Because all three MMEPs clearly displayed signs of deterioration before autoclaving, these results suggested that H_2O contamination contributed to type IIB insulation deterioration observed over quartz regions. After autoclaving, the type IIB degradation was worse. Flaming appeared to have no effect.

We hypothesized the EtOH acquired from the biology stockroom contained several contaminants, especially water. The biology stockroom received large drums of 100% EtOH from the chemistry stockroom where it was stored in bulk quantities. Then, the EtOH was transferred in 4L bottles for MMEP fabrication. Hence, there was ample

EtOH Comparison					
MMEP #	**Treatment**	**Insulation Deterioration Type (Severity)**			
		Before Autoclaving	**After Autoclaving**	**After Flaming**	**After Soaking in Ringers**
Y3C389	Reg EtOH	None	IIB	IIB (same)	IIB (increase)
Y3C390	New EtOH	None	IIB	IIB (same)	IIB (increase)
Y3C391	Reg EtOH	None	IIB	IIB (same)	**IIA,B (increase)**
Y3C392	New EtOH	None	IIB	IIB (same)	IIB (increase)
Y3C393	Reg EtOH	None	IIB	IIB (same)	**IIA,B (increase)**
Y3C395	New EtOH	None	IIB	IIB (same)	IIB (increase)

Table 6: Current insulation methods were used with exception to the spinner modifications (N_2 source directed into open spinner well, open neck, and no lid). All MMEPs were spun in sequence from Y3C389 to Y3C395 at 4,400 rpm, using a fresh stock of DC648. The controls consisted of regular EtOH supplied by the university. The new EtOH was obtained from Sigma and packaged in a sure-seal container. Approximately 1 mL of EtOH was applied to the matrix and spun at 4,400 rpm for ten seconds just prior to DC648 application. After a routine long cure, the MMEPs were subjected to autoclaving, flaming and soaking (Ringers for 48 hours) as outlined in the Quality Control Assessment, to force insulation deterioration.

chance for exposure to high humidity and water contamination. To determine if this EtOH was causing insulation degradation, we purchased pure denatured EtOH (Sigma) in a sure-seal container for comparison. A total of six MMEPs were insulated via alternate applications of both types of EtOH. Current methodology using the unmodified spinner was employed. Table 6 lists the experimental parameters and results.

Overall, the level of deterioration seen using the regular EtOH was more severe than with the pure EtOH. After completing the quality control assessment, all the MMEPs displayed the typical, mature profile of type IIB deterioration with blotches present. However, the two MMEPs, Y3C391 and Y3C393, that showed type IIA deterioration were treated with the university EtOH. The type IIA deterioration exhibited by these two MMEPs after soaking in Ringers solution, suggested contamination of the

EtOH. As a result, the pure EtOH obtained by Sigma was used for future MMEP fabrication. Since the unmodified spinner apparatus was used and humid air currents contaminated the surface of the MMEP, the usual mild type IIB resulted after autoclaving.

B. Autoclaving

Among the culture variables, autoclaving was clearly a trigger for initiating deterioration associated with quartz regions, especially if H_2O contamination was present. Deterioration that was already established before autoclaving, got worse as a result of autoclaving. Usually, the degradation phenotypes exhibited characteristics of premature classic type IIB breakdown.

The effects of autoclaving on type II deterioration and breakdown are clearly demonstrated in Figures 19 and 20. Figure 19 shows two MMEPs that exhibited mild type IIB deterioration before autoclaving. After autoclaving, the type IIB deterioration worsened. In Figure 20, no deterioration was observed until after autoclaving (premature type IIB). Tables 5 and 6 also provided evidence of this deterioration type induced or worsened by autoclaving. The synergistic effects of autoclaving with moisture contamination present was rare after spinner modifications were made.

From these observations, autoclaving was applied as an insulation quality control measure to new MMEPs immediately after insulating and curing. A single MMEP was randomly selected from a batch of insulated MMEPs to perform a qualitative analysis on insulation integrity. Signs of deterioration provided valuable feedback and indicated where breakdown occurred.

The Effect of Ringers Medium on Insulation Deterioration

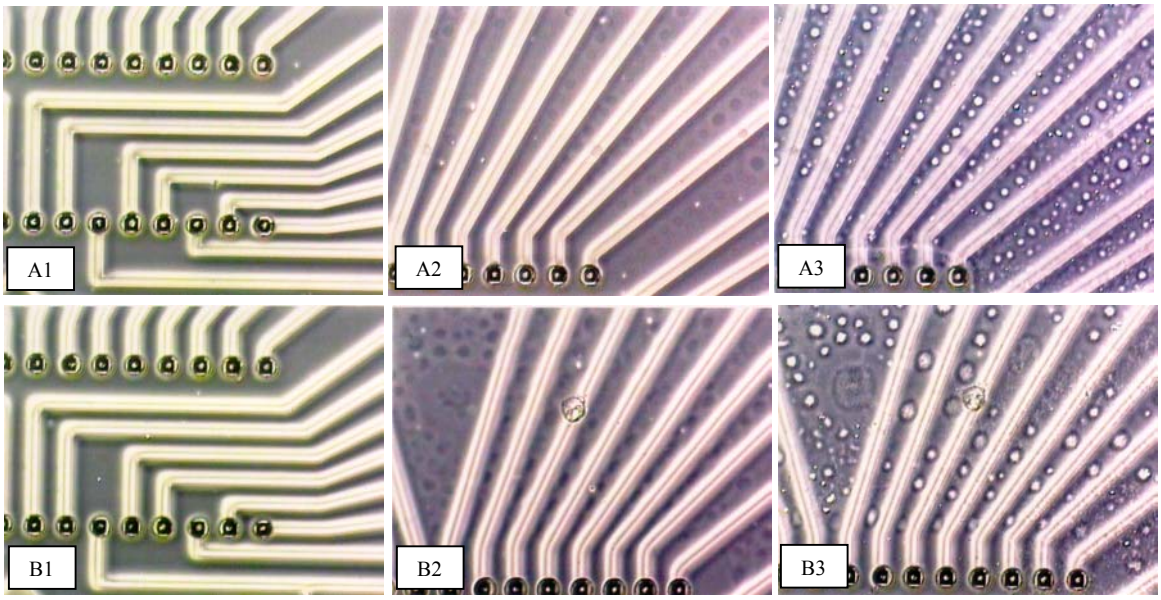

Figure 20: Progressive type IIB and IIC deterioration on two MMEPs (A:Y3C390 and B:Y3C392). Like all MMEPs tested in this experiment (n=6), these two examples displayed no deterioration prior to autoclaving (A1,B1). After autoclaving (A2,B2), both showed premature type IIB deterioration. Then, after soaking in Ringers medium for 48 hours, both MMEPs exhibited severe type IIB or mild type IIC deterioration. Pictures were taken using phase contrast microscopy.

C. Culture Solvents

The most injurious solvent demonstrated to cause type II (usually IIC) deterioration was bleach. Bleach (1-5%) was used as a decontaminant for cultures containing bacteria, yeast, and fungus. Prolonged exposure to bleach usually displayed severe signs of insulation breakdown over quartz regions as well as ITO conductors.

Biological media and saline were also harmful to the insulation. This was dependent on the condition of the insulation prior to exposure. Figure 20 provided

insight into the progress of type IIB and IIC deterioration. After soaking the MMEPs in Ringers medium for 48 hours, significant changes were noticed in the severity of the insulation degradation. These findings indicated that the premature blotches observed after autoclaving progressed to the mature forms found in type IIB degradation after soaking in Ringers. Eventually, this led to the more severe phenotype portrayed in type IIC breakdown .

D. MMEP Pre-Cleaning

Recent evidence of a batch specific insulation degradation showing type IIB profiles indicated over-exposure of the MMEPs to the cleaning agent, Contrad 70 (Fisher Scientific). Prior to insulation, the MMEPs soaked in Contrad 70 detergent. This alkaline detergent was shown to react with the hydrophobic quartz layer after prolonged exposure (>50 hours). After cleaning and insulation, all MMEPs in the batch exhibited premature type IIB deterioration that paralleled the phenotypes from reprocessed MMEPs exposed to KOH/EtOH. As a result, exposure to the Contrad detergent was minimized to one hour.

2.3.2.3 Probable Causes for Class III Degradation

Class III degradation exhibited two types of delamination. Delamination at the electrode tips (type IIIA, Figure 15A) occurred in conjunction with type IB deterioration and repeated cycles through culture. Delamination was also noted to originate at the electrode tips after ultrasonication. The possible causes for type IIIB were exposure to culture solvents (especially bleach) or a very thin layer of insulation (<2 μm, Figure 15C). Prolonged exposure to bleach (greater than 5 minutes, depending on the

concentration) was known to destroy the insulation layer. The phenotype of insulation degradation that occurred goes beyond classic type I and type II breakdown. The outer surface of the insulation blistered, and delamination (type IIIB, Figure 15B) took place. Delamination, which exposes the ITO, leads to signal attenuation or other alterations of the electrical properties of the conductors.

2.3.2.4 Probable Causes for Class IV Degradation

The reason for type IVB deterioration (Figure 17) was particulate contamination. Minute particles were deposited randomly on the soft polysiloxane resin before or during the curing process. However, minimizing exposure of the soft resin to air currents and pre-cleaning the glassware and curing oven prevented type IVB deterioration.

Over-flaming sometimes resulted in cracking of the polysiloxane insulation (Figure 16C). The cracked polysiloxane was not observed on new MMEPs, flamed only once, but was more common on older MMEPs after repeated flaming.

The "halo" effect (Figure 16D) usually took place on deinsulated conductors with ITO exposed, and not on conductors in which the insulation was still intact over the electrode (not deinsulated), or upstream from a cut electrode. Therefore, it was postulated the exposed deinsulated electrodes were transferring heat during flaming. Thus, the ITO-polysiloxane bonding properties changed, altering the light transmittance along the edge of the conductors. There was no evidence that this led to breakdown. The non-deinsulated electrodes did not exhibit the halo-like properties. Thin layers (<2-3 μm) of polysiloxane insulation also showed a general halo effect on all electrodes.

2.3.2.5 Other Probable Causes for Degradation

A. DC648 Polysiloxane Age

The least understood problem was the quality of the DC648. As time progressed, the viscosity of the DC648 decreased substantially (from approximately 100 cP to less than 30 cP). In the past, the insulation protocol required the DC648 to be spun at a velocity of 4,400 rpm. At this speed, a thinner layer of insulation was deposited when aged DC648 was used. In contrast, the thinner layer of insulation may be more penetrable and vulnerable to degradation. The cross-linking may be compromised. How aged DC648 contributed to insulation degradation was unknown, but in general, insulation degradation was more common. The DC648 was no longer manufactured by Dow Corning. Production ceased in 1995, and the shelf life was limited to 6-9 months (Table 1).

In the forced insulation deterioration experiments, fresh DC648 (unopened) and old DC648 (opened for approximately one year) were compared (Table 5). Both the new and old DC648 were manufactured in 1995 and had exceeded their shelf-life. The MMEPs insulated using the original source of stock DC648 exhibited no problems with the insulation before autoclaving. Only one of three MMEPs (Y3C380) insulated using the new stock of DC648 showed very mild type IIB deterioration associated with the quartz regions before autoclaving. This MMEP, Y3C380 was cured twice. After autoclaving, all controls and two of the three new DC648 MMEPs displayed mild deterioration of type IIB. Y3C375 (new DC648) was the exception, and showed no deterioration. In comparison, the insulation on the control MMEPs appeared thinner than

those insulated using fresh DC648. The fresh stock DC648 was slightly more viscous than the old stock DC648, and resulted in a thicker layer of insulation. Also, the cured new DC648 insulation layer appeared to have less problems and imperfections than the old DC648 layer.

B. Direct $UHPN_{2(g)}$ Application

From the forced insulation deterioration experiments, two of the three MMEPs insulated immediately after the direct application of ultra-high purity nitrogen gas ($UHPN_2$) over the matrix were void of deterioration before autoclaving (Table 5). The other MMEP, Y3C88, displayed type IIB deterioration. Again, after autoclaving, all three MMEPs deteriorated (type IIB). There were no lasting advantages to using the direct N_2 application treatment.

C. Insulation Thickness

The rate of polysiloxane degradation depended on insulation thickness. Thin layers of insulation exhibited accelerated rates of degradation for all classifications. Insulation layers thinner than 2 μm were more inclined to breakdown after one (or less) cycle through culture. The very thin layers were easily removed by scratching the surface with a fingernail or blunt edge. The thicker layers of polysiloxane, up to 5 μm, were shown to last at least three complete cycles in culture. They were much more resistant to the detrimental conditions that force insulation deterioration and breakdown. Therefore, it was necessary to observe the dependence the thickness of the insulation has on breakdown and deterioration.

Insulation Thickness

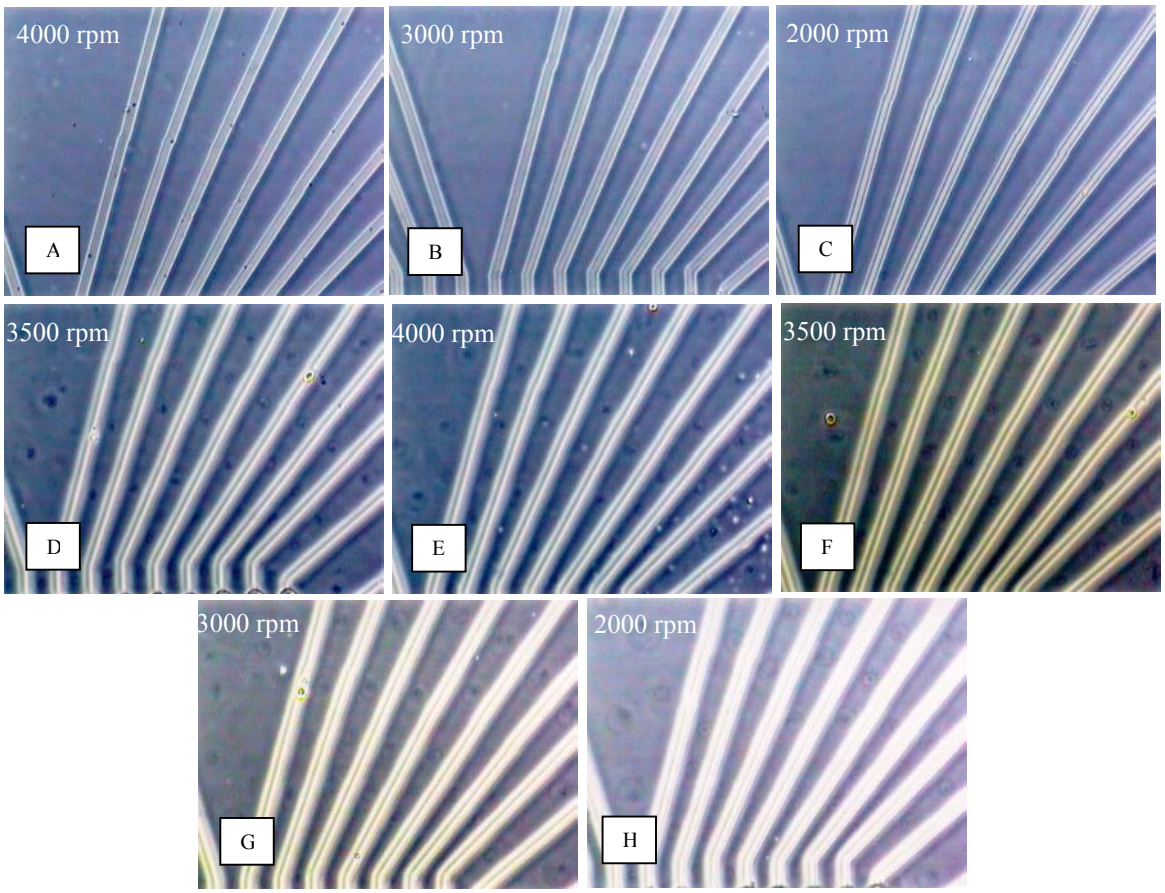

Figure 21: MMEPs were spun at indicated velocities during insulation: (A) 4000rpm (B) 3000rpm (C) 2000rpm (D) 3500rpm (E) 4000rpm (F) 3500rpm (G) 3000rpm and (H) 2000rpm. The pictures represent each MMEP after autoclaving where premature indications of type IIB deterioration were present in all cases. Pictures were taken using phase contrast microscopy.

An experiment was conducted to find the optimum rate of spinning to achieve a layer of thickness closer to 5 µm with the aged polysiloxane insulation. Four batches containing two MMEPs each were spun at various speeds. The unmodified spinner was used along with current methodology.

The insulation thickness of the MMEPs spun at speeds of 2,000 to 3,000 rpm using the aged (less viscous) DC648 was acceptable and the thickness ranged between 3 to 5 μm. At 4,000 rpm, the insulation was very thin (< 2 μm). The results with insulation deterioration appeared to be independent of the insulation thickness, only after autoclaving once. No degradation was exhibited before autoclaving. Nevertheless, after autoclaving the usual premature type IIB blotches appeared (Figure 21). The likely cause for deterioration was probably moisture contamination that occurred just prior to the spin application of polysiloxane. Exposure to flaming and biological media may be necessary to determine the effects of insulation thickness and rates of deterioration.

2.3.3 Method and Equipment Modifications

The improved insulation methods and equipment were (1) the spinner apparatus modifications, (2) the spin application of only a thin uniform monolayer of insulation, (3) the protection of the electrodes along the sides of the MMEP from insulation material, and (4) the application of 100% EtOH to the MMEP surface prior to insulating. The modified spinning apparatus is illustrated in Figure 22. A detailed description of the current insulation methods is provided in Appendix C.

2.3.3.1 Spinner Apparatus Modifications

The most significant equipment improvements that prevented H_2O contamination and type II deterioration (Figure 18) were the spinner modifications. The improvements made to the spinner apparatus included (1) covering the spinner well, (2) closing the neck of the spinner, and (3) redirecting the $N2_{(g)}$ up through the spinner drain (Figure 22). The strategy was to close the system and create an internal dry environment saturated with

The Modified Spinner Apparatus

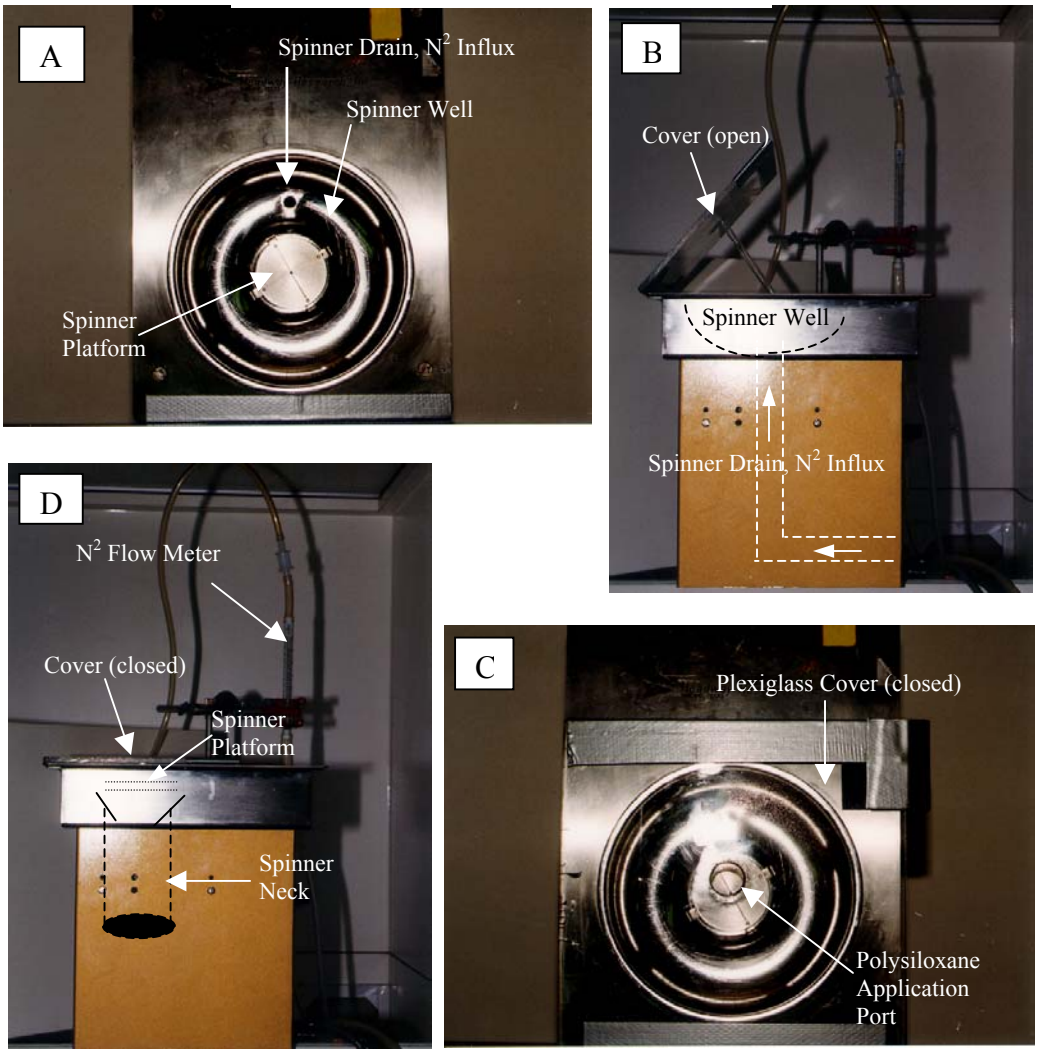

Figure 22: The top view and front view of the modified spinner apparatus with the spinner cover up (A and B) and down (C and D), respectively. Spinner apparatus features are indicated by a white arrow and labeled accordingly.

ultra-high purity (UHP) $N_{2(g)}$. A two-centimeter hole in the plexiglass cover was added to allow the deposition of the 100% EtOH and DC648 insulation.

A. Spinner Air Flow Tests

The spinner modifications resulted from the spinner airflow tests, which were designed to investigate the airflow dynamics of the spinner apparatus before and after modifications were made. Before the spinner modifications, UHP $N_{2(g)}$ was added to the spinner apparatus, streaming into the spinner well from above. We postulated that $N_{2(g)}$ might be escaping around the edges of the open well to the outside environment while spinning. At the same time, a vortex created an influx of humid air contaminating the surface of the spinning MMEP just prior to the application of the insulation. To visualize the airflow dynamics, crushed $CO_{2(s)}$ was added to water and placed throughout the base of the spinner well. The $CO_{2(g)}$ flow was examined.

The flow of the $CO_{2(g)}$ depended on two factors, spinner motion (4,000 rpm) or UHP $N_{2(g)}$ flow rate (8 L/min). With the rotor stationary and the nitrogen turned off, the $CO_{2(g)}$ ran towards the center of the spinner well down through the neck located under the platform and down through the drain at the bottom of the well. With the spinner rotating at 4,000 rpm, the $CO_{2(g)}$ flow was primarily pushed up and outside the spinner well. Once the rim of the spinner well was breached, the $CO_{2(g)}$ was directed out in a horizontal fashion. Residual $CO_{2(g)}$ flowed down through the spinner neck and drain. With only the UHP $N_{2(g)}$ gas streaming down into the bottom edge of the spinner well, the $CO_{2(g)}$ was forced up and outside the spinner well on the opposite side. With the rotor spinning and the nitrogen turned on, a vortex was formed that transported air to the MMEP surface. This was demonstrated with a small chunk of $CO_{2(s)}$ held about 3-5 cm above the MMEP. The flow was observed before and during spinning with the $N_{2(g)}$ present. Importantly,

the $CO_{2(g)}$ was forced downwards onto the surface of the spinning MMEP, and was not forced down when the MMEP was at rest. This suggested the quartz was exposed to contaminated air currents while spinning, and the UHP $N_{2(g)}$ was escaping to the outside environment. We believed this moisture contamination caused the type II deterioration.

Modifications were made to the spinner apparatus to prevent contamination, and the airflow dynamics were retested. The tests used crushed $CO_{2(s)}$ saturated with water placed in the bottom of the spinner well, with a block of $CO_{2(s)}$ traversing, but not blocking the hole in the plexiglass.

Without the spinner and UHP $N_{2(g)}$ activated, the $CO_{2(g)}$ flow was directed down the neck and drain of the modified spinner apparatus. At a constant flow rate of UHP $N_{2(g)}$ at 8 L/min, the $CO_{2(g)}$ was primarily directed up through the two-centimeter hole in the closed plexiglass cover. Some residual $CO_{2(g)}$ ran down the spinner neck. The same results were noticed in the presence of both variables, spin (2000 rpm) and UHP $N_{2(g)}$ (8 L/min). However, less $CO_{2(g)}$ seemed to escape through the hole in the plexiglass. Based on these results, it was apparent that the modifications to the spinner apparatus successfully minimized exposure of the MMEP surface to air contaminants. As a result, these modifications prevented type II deterioration.

2.3.3.2 Other Method and Equipment Modifications

The thicker hand-painted insulation layer (10-15 μm) was replaced with a monolayer of thin insulation (2-5 μm). This entailed the spin-application of over 1.0 mL of DC648, enough to completely cover the surface of the spinning MMEP.

After insulating a batch of MMEPs, the excess resin on each set of electrodes (32) along the edge of the MMEP had to be cleaned using cotton swabs with xylenes and 100% EtOH. It was very difficult to remove all the residual resin and obtain an equidistant, straight edge on either side of the MMEP. The taped-edge technique (TET) was created to eliminate the laborious task of resin removal and excess exposure to xylenes. With the TET, scotch tape was added to each side of the MMEP along the edge of the ITO conductors, just prior to the application of the DC648 polysiloxane resin. After the spin-application of the resin, the tape was removed and the MMEP required a brief cleaning with cotton swabs and 100% EtOH to remove any residual resin. Hence, the TET decreased the amount of time for cleaning the edge electrodes and exposure to xylenes.

To apply the tape along the edge conductors, the MMEP had to be removed from the spinner apparatus and away from the UHP $N_{2(g)}$ source. As a result, we believed this was an opportune time for the MMEP surface to be exposed to moisture contamination. Therefore, 100% EtOH was applied to remove this H_2O contamination. After applying the tape and returning the MMEP to the spinner, about 1-2 mL of 100% EtOH (obtained from the Biology stockroom) was added to the matrix of the MMEP. The excess was removed via spinning for ten seconds. Since the EtOH obtained from the university was believed to be contaminated (EtOH Comparison, Table 6), it was replaced by new 100% EtOH acquired from Sigma.

2.4 MMEP Reprocessing

2.4.1 Background

MMEP reprocessing, or refurbishing, is a method designed to reutilize old MMEPs that cannot be reused in culture for various reasons such as insulation degradation (poor optics), electrode breakdown (gold loss from ITO), and other problems that may hinder cell adhesion or cell electrophysiology and recording. Reprocessing is advantageous in that it is cheaper, more efficient, and uses less resources and raw materials. For instance, reprocessing does not require the materials and labor necessary for photoetching and sanding the MMEPs, as outlined in the MMEP fabrication protocol.

Unfortunately, the polysiloxane insulation applied to the reprocessed MMEPs deteriorated at accelerated rates compared with the polysiloxane insulation applied to new MMEPs. The class of insulation degradation observed most often on reprocessed MMEPs was Class II deterioration and breakdown associated with quartz regions. Therefore, the hypothesis was formulated that the poor adhesion resulted from a change in the quartz surface during reprocessing.

2.4.2 Reprocessing Methodology

The MMEP reprocessing protocol required two steps for stripping the polysiloxane insulation off the microelectrode plates. First, the MMEPs were placed upright into teflon holders inside a clean 250 mL beaker. The MMEP reprocessing solution was mixed from fresh 45% KOH and 100% EtOH at a ratio of 1.0 to 4.3. To strip the insulation, the MMEPs were completely submerged in the KOH/EtOH mixture

for 12 to 24 hours. The beakers were rinsed thoroughly under running water for five minutes. After rinsing, the stripping cycle was repeated one or two times using a fresh mixture of stripping solution for each cycle. Usually, two cycles were sufficient for removing the thin insulation (2-5μm) and three cycles for removing the hand-painted thick insulation (10-15μm). Sometimes, it was necessary to use ultrasonication for 3 to 5 minutes to eradicate any trace or residual polysiloxane that remained and to remove any gold remaining on the electrode tips. After the polysiloxane insulation had been completely removed from the surface of the microelectrode plate, the usual MMEP fabrication procedure was utilized (see pages 18-22).

2.4.3 Methods and Results

2.4.3.1 KOH

It is generally known that strong bases can react with quartz (Scoog et al., 1996). Hence, long periods under 45% KOH could either change the surface characteristics of the quartz or remove it entirely, exposing the soda-lime carrier glass underneath. It was also known that DC648 did not adhere well to the hydrophilic soda-lime surfaces (Dow Corning, personal communication). This experiment was designed to confirm this hypothesis.

Five new uninsulated MMEPs were completely submerged in the 45% KOH/ EtOH reprocessing solution and removed at sequential intervals. To test the hydrophobicity of the quartz layer, drops of UPH_2O were placed at various locations around the MMEP surface and observed. The results pictured in Figure 23 clearly indicated a change in the surface of the quartz from hydrophobic to hydrophilic as

Quartz Hydrophobicity Test

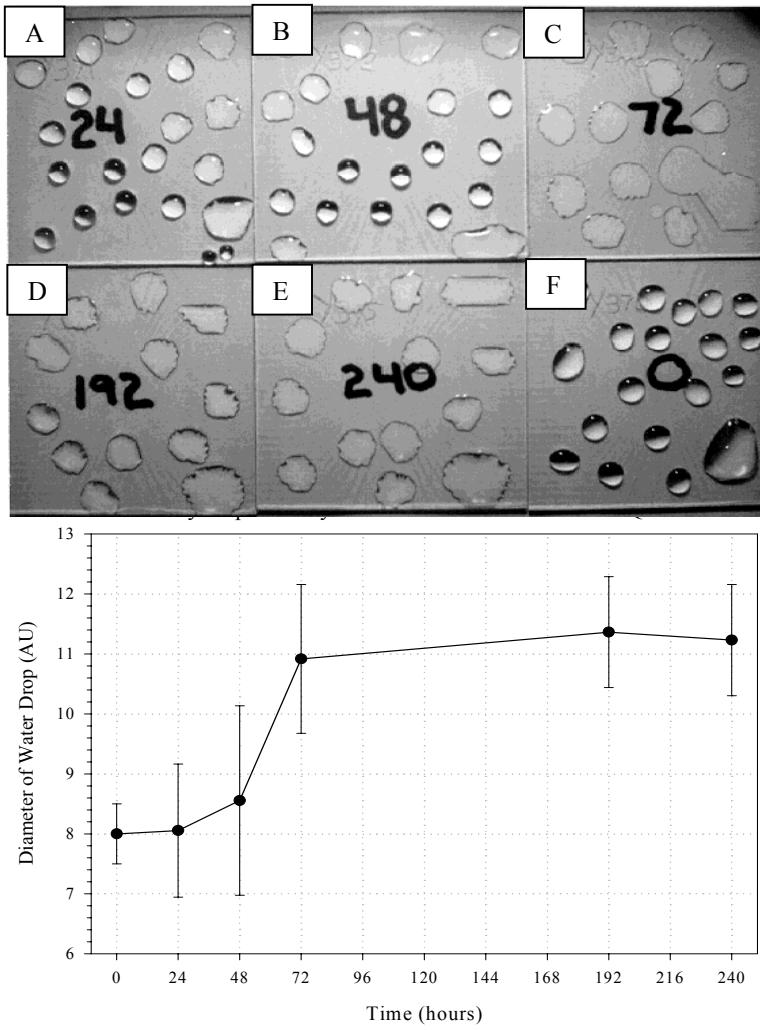

Figure 23: Results of the hydrophobicity test. (top) Water droplets were randomly placed on the exposed quartz surface. Except for the control (F), the MMEPs were pretreated with 45% KOH/EtOH reprocessing solution prior to testing. The number in the center of each MMEP indicates the number of hours the quartz was exposed to the reprocessing solution. (bottom) The diameter of the droplets were measured at each time interval to address surface hydrophobicity. The data represents the mean ± standard deviation at 0 (n=17), 24 (n=18), 48 (n=18), 72 (n=12), 192 (n=11), and 240 (n=13) hours. Data represented at 0 (control) and 24 hours are significantly different than at 192 and 240 hours (p<0.01; t test). The hydrophobicity of the quartz surface begins changing at 24 hours and loses hydrophobicity after 72 hours of 45% KOH/EtOH exposure.

a function of increasing time (0-240 hours) in the KOH/EtOH reprocessing solution. The control, which was not exposed to the reprocessing solution, exhibited hydrophobic surface properties. After 24 to 48 hours the quartz surface was beginning to show hydrophilic properties when random water drops were applied. At 72 hours and thereafter, all the MMEPs tested displayed hydrophilic surface properties. Note that contact angle measurements may have provided more quantifiable results. From these

observations, it was apparent that the KOH/EtOH solution was modifying or removing the quartz layer. The surface became more hydrophilic with exposure time to the reprocessing solution. Therefore, it was necessary to find a better stripping solution that would not affect or alter the surface of the quartz layer.

2.4.3.2 Xylene and Benzene

Combinations of four different solvents were tested to remove the cured polysiloxane insulation via reprocessing without damaging the quartz (Table 7). The solvents were xylene, benzene, ethylene dichloride (ED) and tetramethylguanidine (TMG). Four MMEPs with thick layers of insulation were subjected to solutions consisting of pure benzene, pure xylene, 50% benzene/EtOH, or 50% xylene/EtOH for allocated time intervals that mimic the regular reprocessing protocol (3x every 12-24 hours). The solutions were constantly agitated using an orbital shaker. The MMEPs were rinsed and observed after each interval.

In summary, neither of the two organic solvents showed the ability to remove the cured layer of polysiloxane insulation effectively. The only organic solvent that affected the thick layer of insulation was the xylene. Here, the edges of the thick layer of insulation began to fray and decompose slightly, and the surface seemed a little softer after saturation for 12 or more hours.

2.4.3.3 Ethylene Dichloride

The entire surface of a MMEP with thick insulation was covered with Ethylene dichloride (ED). The polysiloxane layer was allowed to dissolve until it was completely removed. After ten minutes, the excess ED solvent was discarded and the MMEP was

Summary of Reprocessing Solvents			
	Reprocessing Solvent	**Effects on Polysiloxane**	**Effects on Quartz**
1	45% KOH/EtOH	Complete (24-36 hrs)	Hydrophilic
2a	Xylene	Edge-flaking, Soft	Not Tested
2b	50% Xylene/EtOH	Ineffective	
3a	Benzene	Ineffective	Not Tested
3b	50% Benzene/EtOH	Ineffective	
4	Ethylene dichloride (ED)	Rapid, complete (10 min)	Not Tested
5a	Tetramethylguanidine (TMG)	Rapid, complete (<1 hr)	Not Tested
5b	70% TMG/EtOH	Rapid, complete (<5 hrs)	
5c	50% TMG/Acetone	Rapid ,complete (<3 hrs)	Hydrophobic
6	Liquid Nitrogen ($N_{(l)}$)	Thick layers only	Not Tested

Table 7: The results of using different reprocessing solutions to strip the polysiloxane insulation off MMEPs and their affects on the sputtered quartz layer. The effect on the quartz was determined using a hydrophobicity water droplet test.

rinsed with UPH_2O. The ED quickly dissolved the polysiloxane insulation, but mechanical scrubbing with cotton swabs was necessary to remove any residual insulation left behind by the volatile ED solvent. The ED also removed a majority of the electrodeposited gold. However, ED is highly toxic and was not selected as a primary solvent for reprocessing.

2.4.3.4 Tetramethylguanidine

Tetramethylguanidine (TMG) was tested on a MMEP containing a thick layer of insulation. After the insulation was completely removed (approximately one hour), the TMG was removed and rinsed with UPH_2O. The stable TMG completely dissolved the polysiloxane insulation. There was no residual insulation.

Various dilutions were examined to reduce the cost of TMG cleaning. Individual MMEPs with thin layers of insulation were submerged in a series of dilutions for both

TMG/EtOH and TMG/Acetone ranging from 90% TMG to 10% TMG. Each MMEP was allowed to soak in the reprocessing solution a minimum of five hours, while agitated with a mixer. Then, they were removed from the reprocessing solution and rinsed for 20 seconds with UPH_2O and observed using high magnification phase contrast microscopy.

At concentrations equal to or greater than 70% TMG/EtOH, all insulation was removed. At concentrations below 70% TMG/EtOH, residual polysiloxane insulation material remained with decreasing TMG concentration, especially around the electrodes. The same results were observed with concentrations below 50% TMG in acetone. Concentrations equal to or greater than 50% TMG (in acetone) resulted in the complete removal of all insulation. At 50% TMG/Acetone, the entire layer of insulation was stripped within two to three hours. TMG had no affect on the gold-plated ITO electrodes. In addition, all residual polysiloxane that remained after exposure to low concentrations of TMG in either EtOH or acetone could be removed using ultrasonication for about five minutes. However, five minutes in the ultrasonicator also removed the gold from a majority of the gold-plated ITO electrodes (especially from older gold-plated MMEPs). Therefore, to effectively strip the polysiloxane off the MMEPs for reprocessing, without ultrasonication, the 50% TMG/Acetone (1:1) solution was selected. The equivalent for EtOH was 70% TMG.

After the appropriate dilution of tetramethylguanidine (TMG) in acetone was determined, the TMG was tested on the quartz to determine if the solvent altered the hydrophobicity of the quartz surface. A MMEP with no insulation and the quartz completely exposed was submerged in 50% TMG/Acetone for time intervals of 1,2,12,

and 24 hours. At the end of each time interval the MMEP was removed, rinsed, and a hydrophobicity test was performed with a random distribution of water drops placed on the surface of the quartz on both the exposed MMEP and a control MMEP. At each time interval, the results paralleled that of the control, in that no changes were observed. The water drops maintained the beaded shape shown in the control of Figure 23F. Thus, TMG did not alter the hydrophobicity of the quartz surface.

2.4.3.5 Liquid Nitrogen

Attempts to remove the insulation with liquid nitrogen ($N_{(l)}$) was unsuccessful. Two insulated MMEPs that required reprocessing were randomly selected. One MMEP had a thick layer of insulation and the other a thin layer. Each MMEP was completely submerged in $N_{(l)}$ until the temperatures equilibrated (about 10 seconds), and was transferred to a beaker containing warm tap water. This process was repeated several times until no more changes were observed with the polysiloxane insulation layers on each MMEP tested.

The MMEP containing the thin layer (3-5 μm) of insulation showed no significant insulation removal after four cycles in $N_{(l)}$ and water . Although the insulation layer cracked in many places, it maintained its integrity and adhesion to the quartz layer. On the MMEP with the thick layer of insulation (10-15 μm), the thick layer cracked and peeled off after the first four to five cycles, leaving only the thinner layer remaining. The thinner layer (<2 μm) underneath the thick layer was not removed. The cracking was not as defined with the thinner layer but was noticeable after two more cycles. Hence, the $N_{(l)}$ was not a very good means of stripping thin layers of insulation.

2.5 Alternative Insulations

2.5.1 Introduction

DC648 was discontinued in 1995 by Dow Corning. No other sources of DC648 polysiloxane have been found, and the CNNS is now low on supply of DC648. Therefore, it is imperative to begin testing alternative insulations. The alternative insulation needs to fulfill the criteria listed in section 2.1.1 (Insulation Criteria). In addition, the replacement insulation should allow application and manipulation using current methodology. Two alternative insulations have been examined so far: (1) HIPEC R-6101 Polysiloxane Semiconductor Protective Coating and (2) Pyralin Photodefinable Polyimide Resin.

2.5.2 HIPEC R-6101 Semiconductor Protective Coating

HIPEC R-6101 polysiloxane is a one-component, silicone elastomer. The properties and specifications for HIPEC R-6101 are listed in Table 8. In general, the HIPEC R-6101 features include high purity, excellent self-priming adhesion to common electronic device and circuit substrates with superior moisture resistance, flexibility at high and low temperatures, excellent electrical properties over a wide operating temperature range, protection from moisture, dirt, and other atmospheric contaminants, and light transmission. Unlike DC648 polysiloxane, which is a silicone resin, HIPEC R-6101 is a silicone elastomer. HIPEC R-6101 is highly cross-linked with a greater tensile strength than DC648. The cure is achieved via an addition reaction with the application of heat. For the application of insulating microelectrode plates, the viscous HIPEC R-

HIPEC R-6101 - Semiconductor Junction Coating			
Typical Properties		**Product Specifications**	
Physical		*Physical*	
Appearance	Clear	Color, APHA. maximum	20
Flash Point, ºF	230	Viscosity at 77º F (25º C), cP	4000-7800
Viscosity. immediately after curing agent. cP	N/A	Tensile Strength, psi	230
Mixing Ratio. base/curing agent. parts by weight	N/A	Specific Gravity at 77º F (25º C)	0.99 to 1.09
Durometer Hardness, Shore A. minimum	30 when cured 1 hr at 70ºC and 2 hrs at 150ºC	Solids Content. after 3 hrs at 275º F (135º C). percent minimum	No Solvent
Electrical			
Dielectric Constant, at 10^2 Hz 10^5 Hz	2.76 2.76	Solvent	None
Dissipation Factor, at 10^2 Hz 10^5 Hz	0.0005 <0.0002	Na, ppm maximum K, ppm maximum	<2 <2
Dielectric. Strength, volts/mil	475	Cl, ppm maximum	<10
Volume Resistivity, ohm-cm x 10^{15}	1.4	Other metals, ppm maximum	Not Tested
		Shelf Life at 77º F (25º C), months	9

Table 8: HIPEC R-6101 Semiconductor Protective Coating (Dow Corning Corp.) properties and specifications.

6101 was diluted with HIPEC Q2-1345. HIPEC Q2-1345 Diluent is a non-reactive, volatile silicone fluid that can be used to lower the viscosity and reduce the thickness of HIPEC Silicone Semiconductor Protective Coatings.

2.5.3 Methods and Results

Two clean MMEPs were insulated using current methods. The viscous HIPEC R-6101 was diluted 25% with Q2-1345 Diluent. The regular curing cycle was changed to the recommended time of two hours at 150ºC. Following the cure, the MMEPs were fabricated according to protocol.

Qualitative characteristics of the HIPEC R-6101 insulation paralleled DC648. The insulation layer was approximately 5 μm thick, smooth and uniform. The HIPEC R-6101 polysiloxane insulation layer appeared to have excellent adhesion to the quartz surface. There were no signs of insulation deterioration. Light transmission was excellent. DC648 polysiloxane controls were insulated in parallel (Table 9).

Unfortunately, a problem with the laser deinsulation was encountered. The deinsulation did not produce the typical craters created when DC648 was deinsulated (Figure 24). Instead, the vaporization of the ITO was contained by the insulation, and deinsulation craters rarely formed. In most cases, a phase bright bubble instantaneously appeared at the origin of the laser focus upon discharge, and spread out in all directions before it dissipated. To verify this, four of the electrode tips were covered with water and deinsulated under observation using phase contrast microscopy (20x). Again, the ITO vaporization was contained and no crater lids were expelled into the water medium. In addition, the laser focus was manipulated and the power was increased, but the results were similar. At full power, about 12% of the electrodes appeared to deinsulate leaving behind an exposed ITO electrode tip.

HIPEC R-6101 Deinsulation Results (Y3C407)

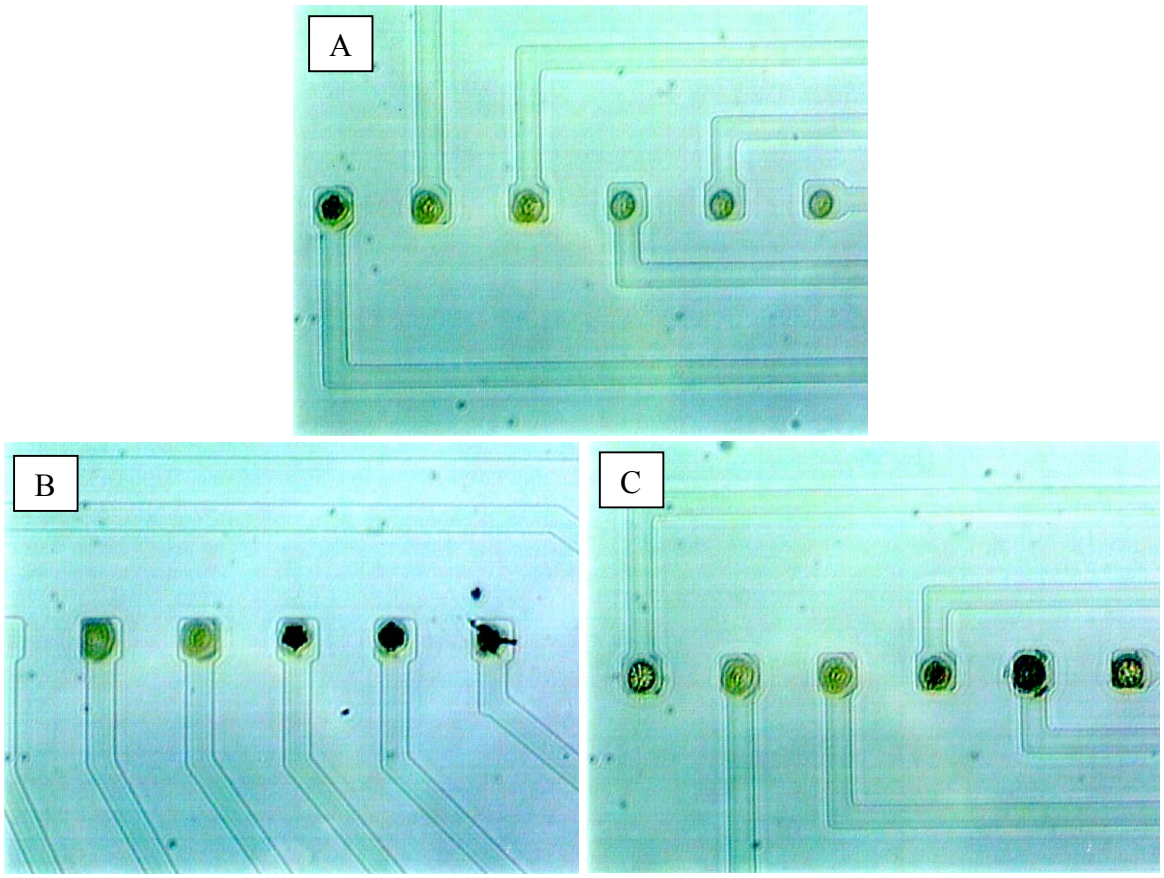

Figure 24: The deinsulation results (Y3C407) using with the new (75%) HIPEC R-6101 polysiloxane elastomer. In A, the insulated ITO electrode tips were deinsulated at 60% laser power. B and C were deinsulated at 100% laser power. The black appearing craters are thought to represent insulation breakthrough.

Nevertheless, the craters were not rounded, but were irregular in shape. Thus, the HIPEC R-6101 elastomer was either too strong or too elastic to deinsulate using the laser method.

HIPEC R-6101 Experimental Summary						
	MMEP #	Insulation Type	Dilution %	Spinner RPM	Thickness (µm)	Craters Deinsulated % of Total
1	Y3C408	DC648 Control	0	2000	4-5	100
2	Y3C409	HIPEC R-6101	25	3500	4-5	12
3	Y3C410	HIPEC R-6101	25	4000	3-4	15
4	Y3C411	HIPEC R-6101	25	4500	2-3	20
5	Y3C412	DC648 Control	0	2000	4-5	100
6	Y3C414	DC648 Control	0	2000	4-5	100
7	Y3C415	HIPEC R-6101	50	4000	<2	65
8	Y3C416	HIPEC R-6101	50	4000	<2	65
9	Y3C417	DC648 Control	0	2000	4-5	100

Table 9: The parameters and results for the HIPEC-R6101 experiments. All MMEPs were insulated in sequential order using conventional methods. HIPEC R-6101 was diluted 25% or 50% with HIPEC Q2-1345 Diluent. Y3C408, Y3C412, Y3C414, and Y3C417 controls were insulated with DC648 polysiloxane resin.

A flaming test showed that surface activation on HIPEC R-6101was similar to that seen on DC648. It was evident that the HIPEC R-6101, like DC648, was fully capable of patterned surface modifications for cell-substrate adhesion.

To improve the laser deinsulation of HIPEC R-6101, three protocol modifications were attempted: (1) longer curing to maximize cross-linking and possibly increase "brittleness" of the substance, (2) higher spinner rates to reduce the thickness of the insulation layer, and (3) reduction of the viscosity of HR to further reduce the thickness of the insulation layer. All MMEPs were insulated and cured using current methodology. The experimental parameters outlined in Table 9.

Observations of the HIPEC R-6101 and DC648 polysiloxane insulation layers using phase contrast microscopy showed no phenotypes of deterioration. The thickness of the HIPEC R-6101 (75%) approached 2 µm as the spin rate was increased to 4500

HIPEC R-6101 Deinsulation Results (Y3C415)

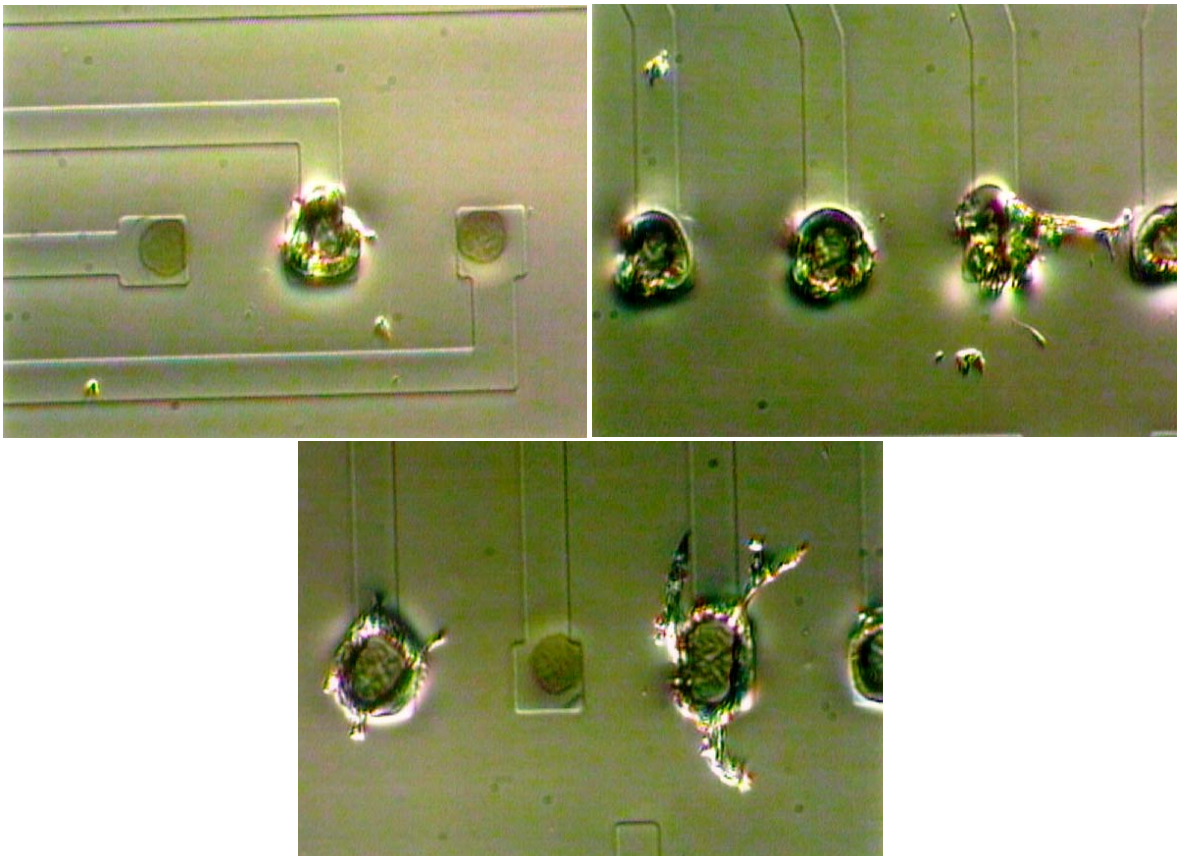

Figure 25: Deinsulation results (Y3C415) using the diluted (50%) HIPEC R-6101 polysiloxane elastomer. The insulated ITO electrode tips were deinsulated at 100% laser power. This MMEP was subjected to autoclaving to force insulation deterioration prior to photography (Hoffman modulation microscopy).

rpm. Similar deinsulation results were observed with the HIPEC R-6101 as those in the previous experiment. The MMEPs insulated at a higher spinner rate resulting in a thinner insulation layer (deinsulated at 100% laser power), produced about 18-20% exposed ITO electrode tips. The insulation layers of the two MMEPs insulated with the less viscous 50% HIPEC R-6101 appeared very thin (<2 μm). Moreover, about 65% of the laser

deinsulated electrode tips produced deinsulation craters when deinsulated at full power (100%) (Figure 25). The craters were more rounded than in previous deinsulation attempts. The deinsulated ITO electrode tips that formed craters appeared to contain regions of exposed ITO within the crater. The longer cure at higher temperatures did not seem to have an effect on the brittleness of the insulation layer. In all cases, control MMEPs insulated with DC648 exhibited the usual deinsulation profile. In summary, the results suggested the cured HIPEC R-6101 elastomer was still too elastic or too strong to deinsulate.

To determine if thin layers (<2μm) of HIPEC R-6101 would exhibit classic signs of DC648 polysiloxane insulation degradation, the four MMEPs listed in Table 9 (6-9) were autoclaved. No degradation was observed with the MMEPs insulated with the dilute HIPEC R-6101 and DC648 controls.

2.5.4 Pyralin Photodefinable Polyimide Resin

A different type of polymer commonly used to insulate microelectronics is polyimide. In general, polyimides are a very interesting group of strong, heat and chemical resistant polymers. Polyimides usually take one of two forms as shown in Figure 26. The first form is a linear structure where the atoms of the imide group form a linear chain. The second is a heterocyclic structure where the imide group is part of a cyclic unit in the polymer chain. In fact, it is the aromatic heterocyclic polyimide polymers that have such incredible mechanical and thermal properties. These properties come from strong intermolecular forces between polymer chains. The polymer chains stack and allow the carbonyls of the acceptor on one chain to interact with the nitrogens

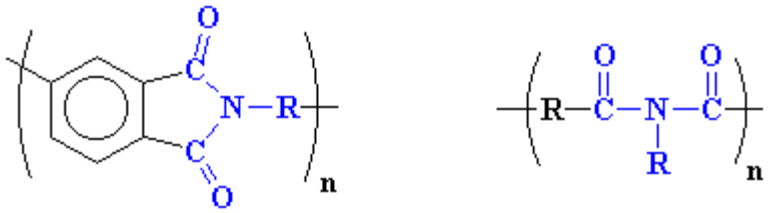

Figure 26: The two forms of polyimide. With the linear polyimide (right), the atoms of the imide are part of a linear chain. The heterocyclic polyimide (left) is part of a cyclic unit in the polymer chain. The aromatic heterocyclic polyimides are typical of most commercial polyimides.

of the donor on adjacent chains (Figure 27). This charge transfer complex holds the chains together very tightly, with no freedom to move. These strong intermolecular forces between the polymer chains are why polyimides are responsible for the strength and durability of polyimide. Polyimide is hydrophilic, transparent and has a yellow tint.

2.5.5 Methods and Results

The Pyralin Photodefinable Polyimide Resin was purchased from DuPont Company (Wilmington, DE). The primary components of this resin were N-methyl-2-pyrollidone and tetraethyl glycol diacrylate. This polyimide was applied to insulate the MMEPs using the same current polysiloxane insulation methods. The material was light sensitive and required handling under proper illumination. The MMEPs were spun at the recommended range of 3000 to 3600 rpm. After curing, the electrode tips were deinsulated and the exposed ITO electrodes were gold plated.

The results were both promising and disappointing. The hydrophilic polyimide retracted from the edges of the MMEP after spinning. Apparently, the quartz surface was

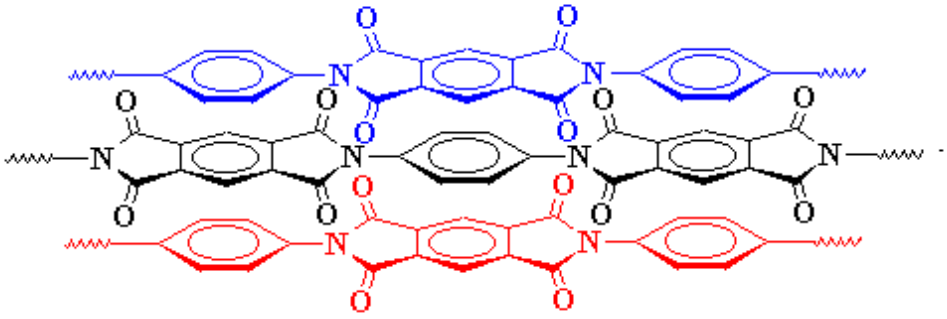

Figure 27: The three polyimide chains stack in this arrangement allowing the carbonyls of the acceptor on one chain to interact with the nitrogens of the donor on adjacent chains.

too hydrophobic for the hydrophilic liquid resin, and caused the resin to retract and bead prior to curing. The TET (taped-edge technique) utilized for achieving a straight edge along the edge ITO conductors during polysiloxane insulation did not work. The scotch tape dissolved when it made contact with the polyimide resin. Moreover, the entire hydrophilic cured polyimide surface would act as a substrate for cell adhesion. Thus, patterned cell adhesion would be difficult to manage, but flaming would be unnecessary. On the other hand, the electrode tips were laser deinsulated and did produce craters with exposed ITO electrode tips, which were then gold electroplated. The polyimide insulation layer exhibited no signs of deterioration at the quartz surface.

In summary, the use of Pyralin Photodefinable Polyimide Resin showed potential as an alternative insulation to polysiloxane. However, other polyimides need to be tested. Photoetched MMEPs that lack the sputtered quartz layer, with only the hydrophilic soda-lime glass exposed, may provide a better substrate for the hydrophilic polyimide resin.

CHAPTER 3

GOLD ELECTROPLATING

3.1 Introduction

3.1.1 Electroplating Criteria

The electrical characteristics of gold-plated indium-tin-oxide ($SnIn_2O_3$, ITO) micro-electrodes for the extracellular recording or stimulating of neural network activity are essential for recording. For the multimicroelectrode plates (MMEPs) fabricated at the Center for Network Neuroscience, these electrical characteristics have been thoroughly examined and reported (Gross et al., 1985, Kesselring and Howard, 1986). The primary function for gold electroplating the exposed laser-deinsulated ITO electrodes is to lower the impedance. It has been shown by Gross et al. (1985) that laser-deinsulated recording craters that expose 100 μm^2 of ITO yield impedances of 8-10 MΩ at 1 kHz, and that conventional gold plating of the craters reduces these impedances to below 3MΩ. They also demonstrated substantial differences between the ITO and gold interface impedances (1130 $M\Omega\mu m^2$ and 255 $M\Omega\mu m^2$ respectively). The approximate values for interface capacitances were 0.62 pF for gold and 0.14 pF for ITO, and imply that gold-plated ITO is more efficient than bare ITO in signal acquisition.

In addition to the electrical characteristics of gold-plated ITO, there are other significant criteria to consider. Good adhesion that results from the electrolytic

deposition of the gold to the ITO electrodes is important. Photoetched ITO conductors provide transparent microelectrode patterns that do not interfere with the optical analysis of cultured monolayer networks. Other photoetched microelectrode conductors (conventionally gold on a thin layer of titanium, tungsten, or copper to improve adhesion to glass) interfere with microscopy because of the low light transmission of these materials (Gross et al. 1985). Deinsulation with a near UV laser is a convenient procedure to expose the electrodes for gold electroplating. In short, all deinsulations are performed with single 12 ns laser pulses at 337 nm and at an energy density of approximately 2 $\mu J/\mu m^2$ (Gross et al., 1985). The ITO electrodes in the laser focus were exposed via single shot by local evaporation of small quantities of ITO causing of rupture of the polysiloxane resin and removal of a relatively circular region of insulation above the conductor, thus exposing the ITO electrode tips for gold electroplating. In addition, the adhesion of ITO to soda lime glass or quartz is excellent and provides a tough, stable conductor pattern.

3.1.2 Gold Electroplating Problems

A majority of the problems related to gold electroplating concerns poor gold-ITO adhesion. Entire colloidal deposits of the gold become dislodged from the ITO electrode, leaving behind trace amounts that border around the rim of the laser-ITO origin of contact. This is observed using high magnification phase contrast microscopy (Figure 28). The gold deposits at various points on the ITO and subsequently stacks until the gold contacts any neighboring gold deposits, and fuses together (Figure 29). Therefore, the gold deposits appear as large granules acquiring the dimensions similar to

Gold Loss from ITO Electrodes

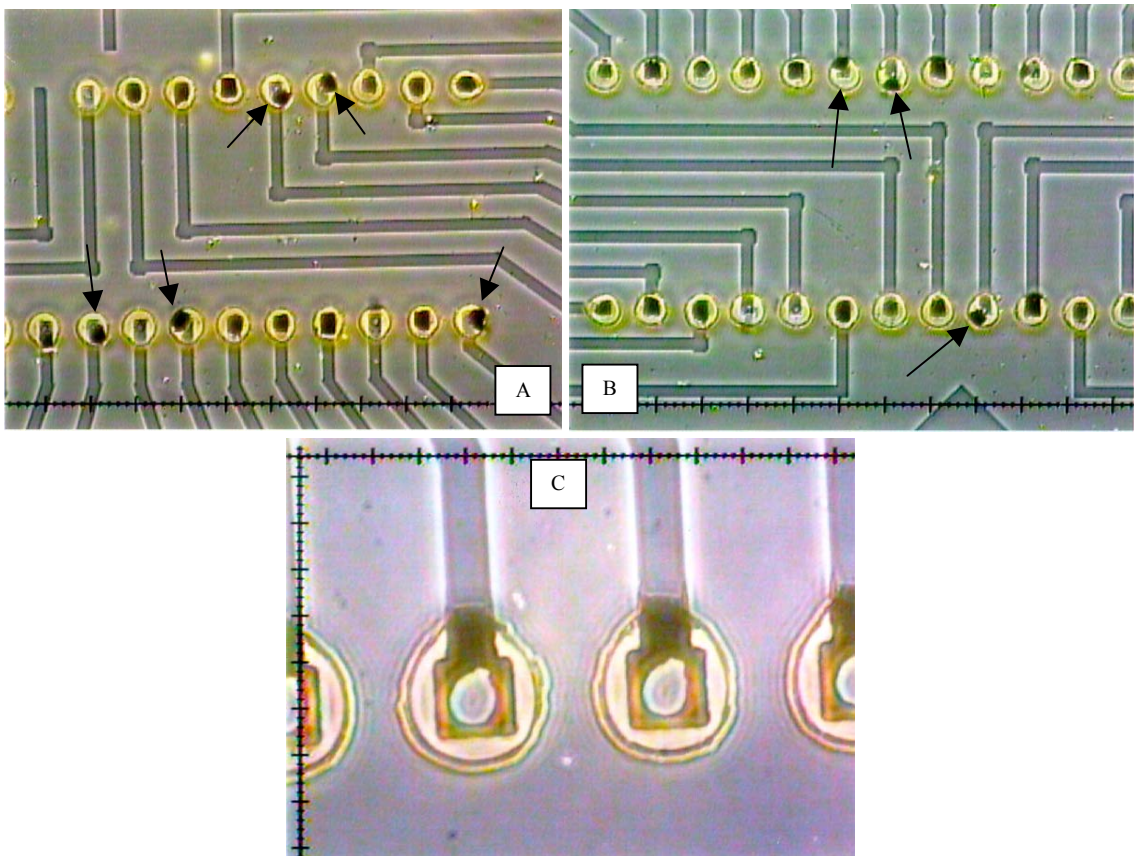

Figure 28: Common problems encountered with poor gold adhesion resulting in gold loss when old electroplating procedures where used. The arrows in A and B (Y3B design) show gold loss via dislodging completely from the ITO electrode after autoclaving. C shows an ideal layer of gold with excellent adhesion electrodeposited using the modified procedure. The gold was not removed after 5 min. ultrasonication.

cauliflower. Hence, the actual contact between the gold and ITO electrode is minimal, and the adhesion weak. Another typical problem examined with poor gold adhesion has a similar phenotype. The gold appears to randomly flake off the surface of the ITO electrode in patches, which vary in size. This problem occurs when the electrode is plated at low current (less than 0.50 μA under current plating methods), suggesting poor

EM of Gold-plated ITO Electrodes

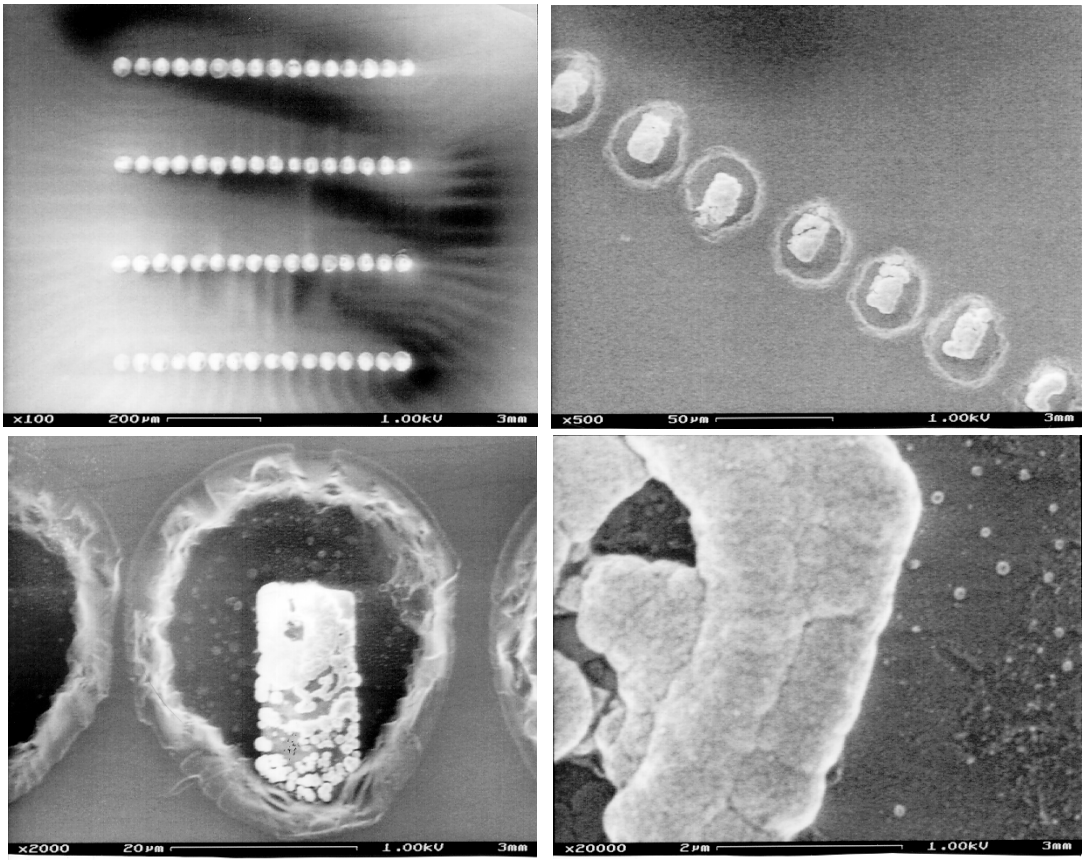

Figure 29: A series of gold-plated ITO electron micrographs of a Y3A MMEP design at a magnification 100x, 500x, 2000x, and 20000x. The gold was electrolytically deposited using PGC electroplating solution and previous methods. (CNNS Archives)

bonding between the gold and ITO. The flaking is more predominant with thinner layers of deposited gold. In other instances, tiny granules of gold are missing throughout the entire gold-ITO surface, and the colloidal deposition looks thinner and powdery. The gold loss is also observed to occur every time the MMEP cycles through culture, until only residual quantities remain. Metallic deposits that appear powdery or flaky are likely

to be less pure and less adherent than those with a smooth surface and bright metallic luster (Hargis, 1988). In addition, any conformation of hydrogen gas at the electrode (cathode) often prevents the gold electrolyte from adhering properly. Hydrogen can lead to holes and pores in the deposit and give rise to powdery deposits, and hydrogen absorption by the metal being plated can lead to embrittlement (Palin 1969).

Sometimes, when the gold wire anode is introduced into the electroplating solution, the evolution of gasses occur at most of the ITO cathodes. This problem takes place instantaneously during electroplating when the current is too high (>1.5 μA for Y3C (0.0144 mm^2) and >3.0 μA for Y4A (0.0452 mm^2). At a constant applied potential, the current decreases with time. Therefore, the current density is high enough at first to create electrolysis at the inert ITO cathode (cathodic overpotential) and results in the evolution (reduction) of hydrogen gas (Hargis, 1988).

The electrolysis is a type of concentration polarization, which is termed kinetic polarization (Scoog et al., 1996). Here, the concentration polarization occurs when the rate of reduction at the surface of the inert ITO cathodes is faster than the rate at which fresh reactants (gold electrolyte) can be supplied to or products (cyanide) removed from the surface. Specifically, in kinetic polarization, the rate of electron transfer at the cathode rather than the rate of mass transfer governs the current, and the product is usually $H_{2(g)}$. The experimental variables that influence the degree of concentration polarization are reactant concentration, total electrolyte concentration, mechanical agitation, and electrode size (Scoog et al., 1996). Because kinetic polarization occurs at the cathode and electrolysis of H^+ to $H_{2(g)}$ results, gas pockets form in many of the

MMEP Gold Electroplating Variables		
UV Laser Deinsulation	*Acid Striking*	*Environmental Factors*
1. UV Focal Characteristics	1. Type of Acid	1. Atmospheric Oxidation
a. Placement	a. Strength	2. Temperature
b. Surface area	b. Concentration	3. Humidity
c. Depth of focal plane	2. Duration of Strike	
d. Objective power		*Electroplating Equipment*
e. Interphase optics	*Gold Electroplating Solution*	1. Pulse Generator
2. UV Laser Power	1. Solution contents	a. Voltage/current (density)
3. UV Induced ITO Oxidation	2. Gold Concentration	b. Cycle spacing/width
4. Residual Polysiloxane	3. pH	2. Cathode
5. Electrode Surface Area	4. Temperature	3. Zebra Connectors
	5. Age	4. Heat Lamp

Table 10: All MMEP gold electroplating variables that may influence gold deposition and adhesion of the gold to the indium tin oxide (ITO) electrodes during fabrication.

deinsulation craters and prevents any further electrolytic deposition of gold at those ITO electrodes. Kinetic polarization at the gold wire anode has not been observed.

3.1.3 Gold Electroplating Variables

All the variables that may influence the deposition and adhesion of the gold to the ITO are included in Table 10. The variables are tabulated into the categories of (1) UV laser deinsulation, (2) acid striking, (3) gold electroplating solution, (4) environmental factors, and (5) electroplating equipment.

The deposition and adhesion of the gold depends on any combination of the variables listed in Table 10. The contents of the gold electroplating solution and the electroplating parameters primarily dictate the characteristics associated with gold deposition. Some of the most significant electroplating parameters are voltage and current. These variables influenced the deposition of gold on the ITO electrodes , as well as the rate of electrolysis at the surface of the electrodes. The adhesion depends on the

surface conditions of the ITO and the electroplating parameters. The surface morphology of each ITO electrode is slightly different after laser deinsulation. The interphase optics of the laser and the focal point, concentration, and placement of the UV photons determine the different morphologies observed with the ITO surface (such as surface area, UV induced oxidation, and residual insulation), which may affect gold adhesion.

3.2 Materials and Methods

3.2.1 Equipment and Materials

The Pure Gold SG-10 potassium gold cyanide (PGC) electroplating solution (8.2 g Au^{2+}/L) was acquired from Transene Co., Inc., Rowly, Massachusetts. Hydrochloric acid (12 N) was purchased from EM Industries, Gibbstown, NJ. An Olympus CK2 light microscope was used to observe the gold electroplating process. After electroplating, the quality control evaluations were performed using a Micromaster light microscope (Fisher Scientific). A Global Specialties 400P pulse generator was used to generate the DC current pulses for electroplating. The pulses were monitored with a Tektronix 2205 20 MHz Oscilloscope. The anode wire (Premion 99.999% pure gold, 1.0mm diameter) was obtained from Alfa Aesar. The Dyna-Lume 3151-6 heat lamp was acquired from Cole-Parmer.

3.2.2 Previous Gold Electroplating Methods

The previous gold electroplating methods have been mentioned elsewhere (Gross et al., 1985). In summary, the exposed laser-deinsulated electrodes were subjected to a 30 seconds acid strike using 3.7%HCl (1.6 N). The electrolytic deposition of the gold took place simultaneously on all 64 electrodes. This was performed using a DC current at 1.5 μA for approximately 30 seconds with the SG-10 electroplating solution. The electroplating apparatus consisted of a base plate to support the MMEP, zebra connectors to contact the edge electrodes, and a heavy bronze block connected to the current source. The bronze block contained a one-inch diameter cylindrical shaft through the center from

top to bottom, in which a 24k gold wire anode was suspended in the PGC electroplating solution saturating the ITO cathodes.

3.2.3 Quality Control

To better understand gold adhesion with the ITO electrodes, several quality control standards were created. The gold electroplating quality control measures are discussed in Appendix B. They consist of the (1) MMEP Deinsulation and Gold Plating Records, (2) MMEP Pre-culture Evaluation and MMEP Feedback Evaluations, and (3) MMEP Sonication. These quality control measures are designed to furnish valuable feedback and monitor the status of the gold adhesion to the electrodes. Detailed notes on the variables that exist when each MMEP is plated, coupled with feedback on the gold deposition and adhesion, are valuable tools that can help troubleshoot most of the problems encountered during gold electroplating. Thus, improvements may be made to the current methodology.

3.3 Results and Discussion

3.3.1 Citrate Potassium Gold Cyanide (CPGC) Electroplating Solution

The most notable improvement for the electrolytic deposition of gold onto the ITO electrodes was the modified electroplating solution. The old electroplating solution was potassium gold cyanide (PGC). Briefly, the PGC solution (Pure Gold SG-10, Transene Co.) deposited pure gold (99.99%) producing plate characteristics with center cubic structure and Rockwell hardness of 24 (15T scale). The concentration of the gold in PGC was about 8.2 g/L (Transene Co., Technical Services). The modified electroplating solution currently used to gold plate the ITO electrodes was a citrate potassium gold cyanide (CPGC) solution. The CPGC (3.1 g Au^{2+}/L) electroplating solution consisted of PGC diluted in UPH_2O, sodium citrate (50 g/L), and citric acid (50 g/L) at a pH of 4.5 to 4.7.

The first attempt to improve gold-plating characteristic was to dilute the PGC to 4.2 g Au^{2+}/L and slow the rate of deposition by reducing the electrolyte migration to and deposition at the ITO cathodes. Unfortunately, the morphology of the colloidal deposition of gold remained the same as before. The deposition took on a cauliflower appearance in which there was very little contact of the gold with the ITO. The gold appeared to stack and branch until it fused with adjacent gold structures.

The second effort involved modifying the PGC plating solution by the addition of citric acid and sodium citrate. It was reported by Rajagopal et al. (1992) that gold deposits on stainless steel produced from citrate baths under appropriate conditions are fine-grained and pore-free at thicknesses greater than 3 μm. Similar results were

published about gold plating on stainless steel for space applications using a citrate bath (Sharma et al., 1990). Here, the gold electroplating solution contained citric acid (45-55 g/L) and sodium citrate (45-55 g/L).

A. CPGC vs. PGC Electroplating Solutions

The use of citric acid and sodium citrate (both 50.0 g/L) in the former dilute PGC (3.1 g Au^{2+}/L) solution, yielding the new CPGC solution, provided a much finer electrolytic deposition of gold, with improved adhesion. Figure 30 lists the results of a MMEP sonication test using the PGC electroplating solution applied using DC (n=5) , and CPGC applied using pulsed DC methods (n=10). The five MMEPs plated with PGC lost most of their gold (18, 47, 88, 98, 100% gold loss) within the first thirty seconds of sonication. The adhesion of the gold was poor. Seven of the ten MMEPs plated with CPGC did not lose any gold, and the other three lost 2, 32 and 48%. These findings showed a significant improvement with the gold adhesion to the ITO when the CPGC electroplating solution and pulsed DC currents were used.

The characteristics of the gold deposits using CPGC electroplating solution were fine, not granular, with a smooth surface and bright metallic luster. The applied voltage necessary to drive the electrolytic deposition of gold at equal rates was more than twice the amount for CPGC (2.1V) than PGC (0.8V). The deposits were thin and the thickness was easier to maintain during plating. It appeared there was more contact between the deposited gold to the ITO surface. The bonding and adhesion of the gold to the ITO improved as well. The problem of gold dislodging from the electrodes, typically seen with the MMEPs plated using the PGC solution (Figure 28) was solved.

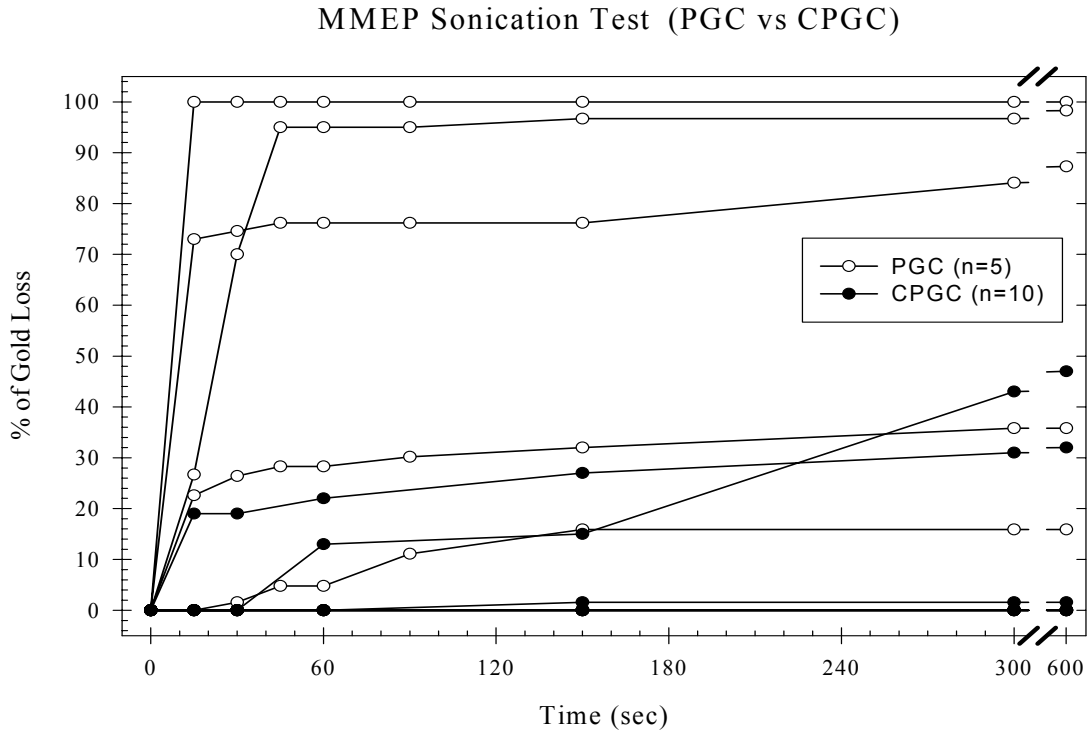

Figure 30: Sonication results of MMEPs electroplated using the PGC (n=5) and CPGC (n=10) solutions. The PGC was applied using DC (old methodology) and the CPGC was deposited using pulsed DC (improved methods). They were subjected to ultra-high frequency sonication for a total of 10 minutes, and observed a the given intervals. A majority of the PGC plated MMEPs lost significant amounts of gold within the first 30 seconds. The CPGC plated MMEPs maintained their gold. Note 7 of the 10 MMEPs electroplated with the CPGC solution did not lose any gold after sonication. In addition, all CPGC electroplated MMEPs had cycled through culture at least once.

B. CPGC pH and Age

The only other minor problems, previously discussed, were flaking and powder-like deposits. These may result from improper plating parameters and impurities present in the electrolytic solution. Using the improved equipment and methods, several

variables were qualitatively tested via ultrasonication. The results (not shown) of testing the age, fresh versus 90 days, of the CPGC solution indicated no significant difference in adhesion and deposition. The gold deposition and adhesion was also tested at various pH's of the gold electroplating solution. The pH values tested were approximately 1.9, 2.5, 3.5 and 4.5. The native pH of CPGC was 4.5 to 4.7. After sonication, the best adhesion was observed at higher pH when the plating current was held constant. At lower pH values, especially 1.9, the deposition was powdery and adhesion poor.

Theoretically, an increase in the hydrogen ion concentration alters the discharge potential at the cathode and may lead to co-deposition of gold and hydrogen simultaneously. The cathode is said to be depolarized by the hydrogen ions under these conditions (Scoog et al., 1996). The low pH also affects the nature of the complex ion (gold cation with cyanide anion) and the degree of hydration of the simple ion, and this in turn may affect the nature of the deposit (Palin, 1969). Therefore, because of the low pH, these two rationales suggested that the evolution of hydrogen gas at the ITO cathodes may impede gold deposition. On the other hand, it is mentioned that cyanide baths must be alkaline because most of the complex ions are stable and do not easily dissociate in acid solution. The cathode process is the deposition of the metal from the complex ion, which is usually formed in solution, followed by the liberation of cyanide (Palin, 1969). Perhaps an electroplating solution with a higher pH should be investigated.

C. CPGC Temperature

Increasing the temperature of the CPGC not only assisted with the removal of the trapped air pockets in the craters, but it also aided the electroplating process. The warm

CPGC solution, coupled with the use of a heat lamp, resulted in better adhesion of the gold when tested using ultrasonication. The effect was much greater than expected. Apparently, the thermal convection increases the rate at which ions were transported to and from the electrode, which resulted in a decrease of concentration polarization and better deposition and adhesion strength.

3.3.2 DC vs. Pulsed Currents

Just after the CPGC electroplating solution was incorporated into the protocol, the constant DC source was changed to a pulsing method of application. At the time, it was believed that the constant applied potential, when compared with pulsed methodology, caused accelerated rates of gold deposition that yielded typical characteristics to those observed when using the PGC electroplating solution (minimal gold-ITO contact, gold stacking, etc…). A pulse generator (50/50 on/off cycle at 500 ms) coupled to an oscilloscope, to monitor the voltage, replaced the existing DC source (9V battery). With the application of a pulsed DC supply, the gold deposition improved (Figure 30).

The best electrolytic deposition and adhesion of gold to the ITO electrodes occurred at an applied voltage that initially produced electrolysis. Using the current electroplating methods, at a constant applied potential, the electrolytically pulsed deposition of gold began at high plating currents between 2.5 and 4.0 μA (for MMEP 3C and 4A designs). After 4-5 cycles (4-5 seconds), the plating current decreased and leveled off to approximately 0.50 to 1.50 μA, and was observed to be dependent on the total surface area of the cathodes. MMEPs with less than 64 exposed ITO electrodes, and consequently less surface area, tended to plate at lower currents when the voltage was

held constant. At 2.5 to 4.0 μA plating current (MMEPs 3C and 4A, respectively) , electrolysis producing hydrogen gas was observed at some of the ITO cathodes, but only for the first 1-2 seconds. It was under these circumstances that the gold was shown to have the best adhesion.

This was tested using ultrasonication and studied using feedback from the MMEP evaluation database coupled with the gold plating records (Figure 38). Less than 2% of the 3C's (n=100) lost gold after a single cycle through culture, under these electroplating conditions.

3.3.3 Gold Wire Anode

It was noticed that the applied voltage in the electrolytic cell varied, and depended on the surface of the 24k gold wire anode. Cleaning the gold wire anode using sandpaper or a strong acid produced electrolysis at the ITO cathodes when MMEPs were electroplated. Furthermore, the plating occurred much faster which required a decrease in the applied voltage.

Apparently, the sanding or acid cleaning removed oxides and other impurities on the surface of the anode, which interfered with electroplating. Also, after 5-10 MMEPs had been plated, an increase in the applied voltage was required to maintain the same rates of gold deposition onto the ITO electrodes. To correct these problems, a pure gold (99.999%) wire anode was put to use. The variations in the applied voltages were no longer noticed.

3.3.4 Laser Deinsulation

The morphological characteristics of the gold on the plated ITO electrodes were governed by the UV laser deinsulation. The local evaporation resulted in the removal of small quantities of ITO during the deinsulation step, which appeared to generate different surface properties of the affected areas, such as surface roughness. Laser deinsulation may also cause oxidation of the ITO and a concomitant local increase in the resistivity. After laser deinsulation, the areas directly contacted by the photons appeared darker (light transmission was reduced). Crater dimensions were directly proportional to the laser power (concentration of photons) and laser focus diameter (total surface area).

The morphological characteristics of the electrodeposited gold vary per electrode and MMEP because the laser focus was slightly different in each case, resulting in the common effects already described. The pattern of gold deposition usually followed the best adhesion in those ITO regions that made direct contact with the laser photons, resulting in the possible formation of metal oxides. This was observed quite often after ultrasonication and removal of the majority of electrolytically deposited gold, in which the remaining residual gold appeared to bond tightly in these regions. It was also seen initially during gold plating when these regions plated first. Increasing laser power and vaporizing more ITO usually resulted in better adhesion of the gold to the electrodes. Unfortunately, with too much power, a conical hole was created that penetrated through the ITO conductor, leaving behind an electrode that looked like a donut. As a result, the surface area of the electrode was decreased and the electrical characteristics of the electrode were changed. With not enough power (or a low photon concentration), the

vaporization of the ITO was not enough to break the cross-linked polysiloxane, thus, not exposing the ITO electrode for plating. Low power deinsulations also leave residual traces of insulation over small regions of the ITO electrodes.

A. High (20x) vs. Low (10x) Power

Deinsulation with a high (20x) versus low (10x) power objective resulted with better gold adhesion. This was demonstrated on two MMEPs: Y613 and Y637. On each MMEP, rows 1 and 3 were deinsulated using the low (10x) power objective, and 2 and 4 with the high (20x) power objective. The MMEPs were gold-plated using standard methods (PGC/DC) and sonicated at 10 minutes intervals. The results summarized in Figure 31 indicate better adhesion of the gold on the electrode deinsulated at high (20) power. Gold loss ranged from 0-33%. At low (10x) power, the gold loss was 48-68%. However, the craters were more irregular at high power deinsulation.

3.3.5 Cathode Cleaning

Preconditioning of the electrodes via acid striking was another variable that may affect gold deposition and adhesion. Theoretically, the acid strike was advantageous in that it removed metal oxides from the electrodes and allowed for a local increase in current density. However, acid striking the ITO electrodes did not show any significant changes with gold deposition and adhesion. Previous electroplating methods required acid striking for one minute using 3.7% HCl. Current methods used 9.5% HCl for 2-3 minutes. Microscopic analysis of the ITO electrodes before, during and after acid striking exhibited no observable changes. Two MMEPs were fabricated in parallel and subjected to ultra-high frequency sonication. One MMEP was not acid struck and the

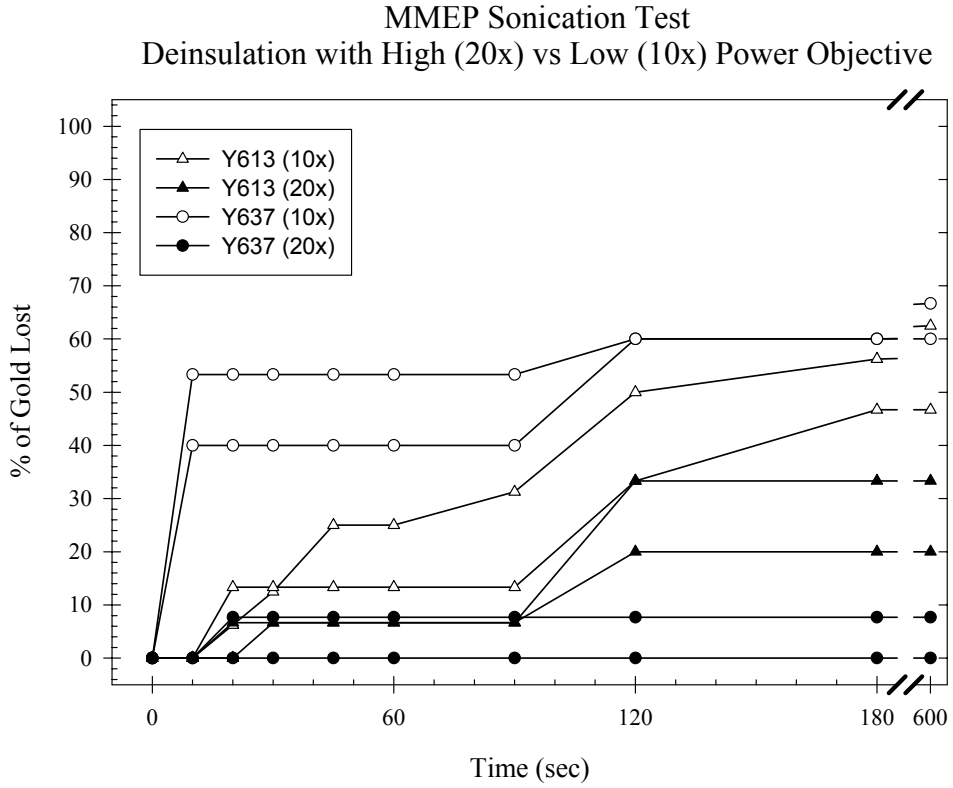

Figure 31: Sonication results of the gold electroplated MMEPs Y613 and Y637 using PGC/DC. Rows 1 and 3, and rows 2 and 4 were deinsulated at low (10x) and high (20x) power, respectively, on each MMEP They were subjected to ultra-high frequency sonication for a total of 10 minutes, and observed a the given intervals. The gold adhesion was better on those electrodes deinsulated at high (20x) power (black symbols).

other was preconditioned in 9.5% HCl for ten minutes, yet both MMEPs resulted in the loss of similar amounts of gold (results not shown). This suggested that under current acid striking conditions, the pre-conditioning may not significantly affect gold adhesion.

3.3.6 Current Gold Electroplating Protocol

The current gold electroplating techniques have been modified from previous methods. In short, all (64) laser-deinsulated and exposed electrodes were electroplated simultaneously using the citrate potassium gold cyanide (CPGC) solution. (1) Roughly 1.0 mL CPGC electroplating solution was added to cover the exposed ITO cathodes. (2) The compressed sandwich arrangement was assembled consisting of a non-conducting base plate, the deinsulated MMEP, zebra conductors that span the edge electrodes on the MMEP, and a conducting top plate connected directly to the pulse generator. (3) The gold wire anode was lowered into the CPGC electroplating solution. The pulse generator supplied approximately 2100 mV at about 1.0 μA for roughly two minutes (MMEP 3C). The gold electroplating apparatus and sandwich assembly is pictured in Figure 32. Technical detail for the current gold electroplating methods is presented in Appendix D.

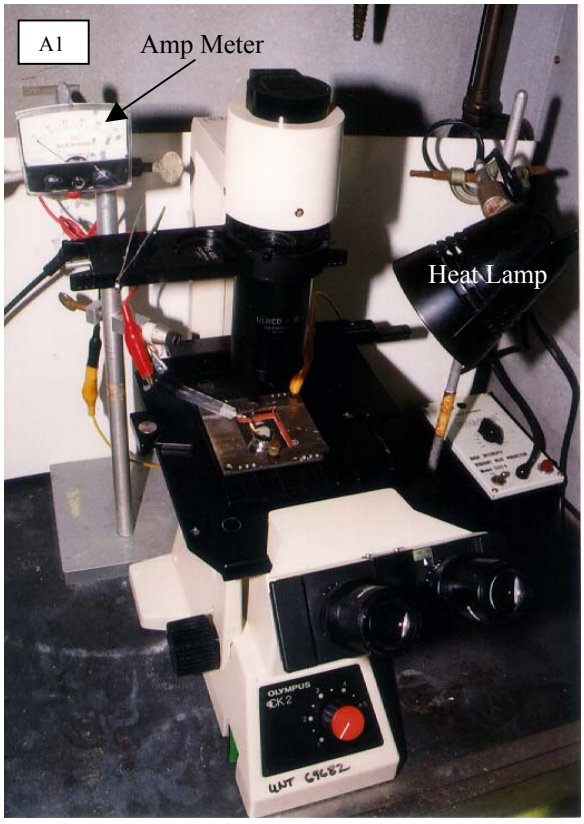

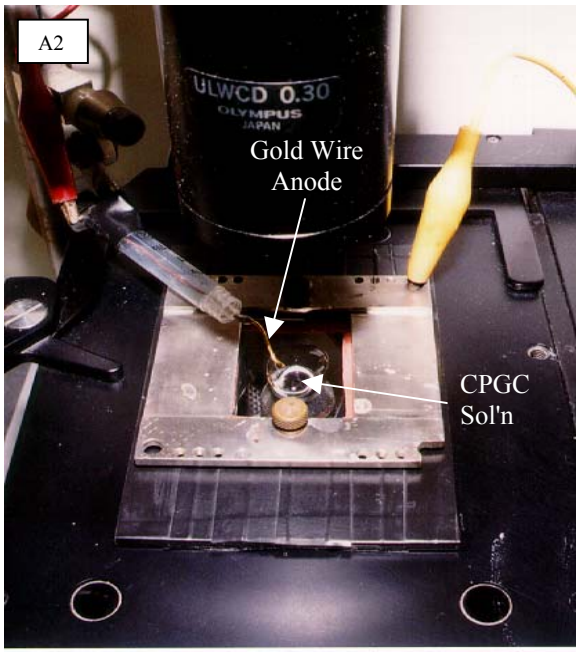

Gold Electroplating Apparatus and Sandwich Assembly

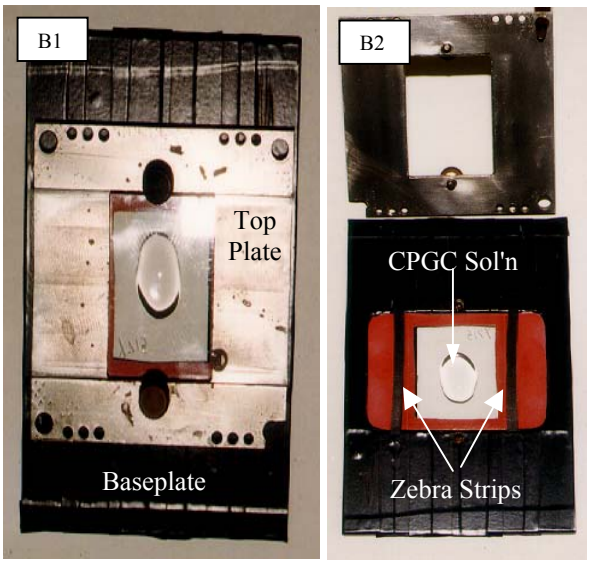

Figure 32: The gold electroplating apparatus (A1,A2) and MMEP sandwich assembly (B1,B2) used for gold plating the MMEPs. Pictures A1 and A2 represent the electrolytic cell used to deposit the gold onto the ITO electrodes. The MMEP sandwich assembly rests on the microscope platform (Olympus) and the gold wire anode is lowered into the electroplating solution (CPGC) as shown. Not shown is the oscilloscope (Tektronix) and pulse generator (Global Specialties Corp.) used to monitor and supply the DC current. The MMEP sandwich assembly, B1 and B2, is composed of the non-conducting base plate (black), a rubber pillow (orange), the MMEP, zebra contacts, and conducting top plate (silver). B1 shows the assembled sandwich, and B2 the unassembled sandwich with MMEP, zebra strips, rubber pillow, and electroplating solution intact.

CHAPTER 4

CONCLUSION

4.1 Polysiloxane Insulation

The leading cause of class II polysiloxane insulation degradation associated with quartz regions was moisture contamination. At the critical time just before the spin-application of polysiloxane, a vortex of humid air currents led to moisture condensation on the MMEP surface. As a result, most MMEPs exhibited type IIB deterioration, which increased in severity following exposure to routine culture procedures (autoclaving and biological media). To prevent moisture contamination, modifications were made to the spinner apparatus. These modifications closed the system, prevented the vortex and provided humidity control. Subsequent to the spinner modifications, less than 5% of all MMEPs insulated exhibited type IIB deterioration after five cycles through culture, and type IIC breakdown was never observed.

The causes for class I insulation deterioration on the ITO conductors were correlated with repeated cycles through culture. Hence, increased exposure to flaming and culture solvents was directly proportional to the incidence and severity of type IA and IB deterioration. However, the causes for class I degradation requires further investigation.

Other significant method and equipment modifications were made to improve fabrication quality. (1) To further control moisture contamination, 100% EtOH was

applied to the MMEP surface just prior to the application of polysiloxane insulation. (2) The thicker hand-painted insulation layer was replaced with the spin-application of a monolayer of thin insulation. (3) The taped-edge technique (TET) protected the two sets of 32-electrode contacts along each side of the MMEP from the insulation material.

4.2 MMEP Reprocessing

Reprocessed MMEPs exposed to KOH usually exhibited accelerated rates of class II deterioration associated with quartz regions. Greater than 24 hours of quartz exposure to 45% KOH/EtOH reprocessing solution was shown to change the hydrophobic surface characteristics of the quartz barrier layer, probably exposing the hydrophilic soda-lime glass carrier underneath. Therefore, the 45% KOH/EtOH reprocessing solution was replaced with tetramethylguanidine/acetone. The tetramethylguanidine rapidly dissolved the polysiloxane insulation layer without damaging the quartz.

4.3 Alternative Insulations

Neither of the two alternative insulations tested, HIPEC R-6101 polysiloxane and Pyralin Photodefinable polyimide resin, completely fulfilled the criteria necessary for MMEP insulations. The HIPEC R-6101 elastomer was satisfactory, but was either too elastic or strong to deinsulate using the laser method. Further investigations are necessary to improve laser deinsulation of HIPEC R-6101 insulated MMEPs. Other alternative insulations should be explored.

4.4 Gold Electroplating

The most significant contributions to improve gold deposition and adhesion strength to the ITO electrodes were the utilization of a new citrate potassium gold cyanide (CPGC) solution and the electrolytic deposition using a pulsed DC method. The pulsed gold deposition using CPGC prevented gold loss. Less than 2% of all MMEPs electroplated using this method lost gold at one or two electrodes, after five cycles through culture. Gold loss via MMEP sonication (a valuable quality control measure which uses ultra-high frequency vibration to remove the gold) was almost entirely prevented using the new methodology. Other gold electroplating method and equipment modifications include improving the gold wire anode and the assembly for electroplating the MMEP.

APPENDIX A

POLYSILOXANE INSULATION QUALITY CONTROL

APPENDIX A

POLYSILOXANE INSULATION QUALITY CONTROL

A.1 MMEP Insulation and Curing Records

The first quality control measure is the MMEP Insulation and Curing Records (Figure 33). In general, the form is designed to document all variables, techniques, and notes that apply during the insulation and curing of any particular batch of MMEPs. Every batch of MMEPs insulated and cured is recorded and archived in chronological order primarily by date, and subsequently by MMEP number. Here, a batch usually consists of fifteen MMEPs arranged in sequential order. The experimental parameters (in the MMEP fabrication clean room) include relative humidity and temperature , N_2 flow rate, spinner rpm, and time both before and after the insulation process. Polysiloxane data such as the date the DC648 stock was opened, the type of insulation layer applied (thin versus thick), the temperature of the insulation when it is applied, and other notes pertaining to insulation pre-conditioning are reported. All information on the various techniques used plus modifications to the equipment is documented. Information on the quantity of 100% EtOH and the spin duration, before and after the DC648 application, is also noted. Also, any post-cleaning change to the MMEPs, prior to spinning, is included. After insulating the MMEP's, qualitative observations of the fresh insulation, plus detailed cleaning and curing records are recorded.

All the information documented in the MMEP Insulation and Curing Records provides valuable feedback when required. Any MMEP that exhibits a sign or marker of deterioration can be back tracked beginning with these records. Close examination of the

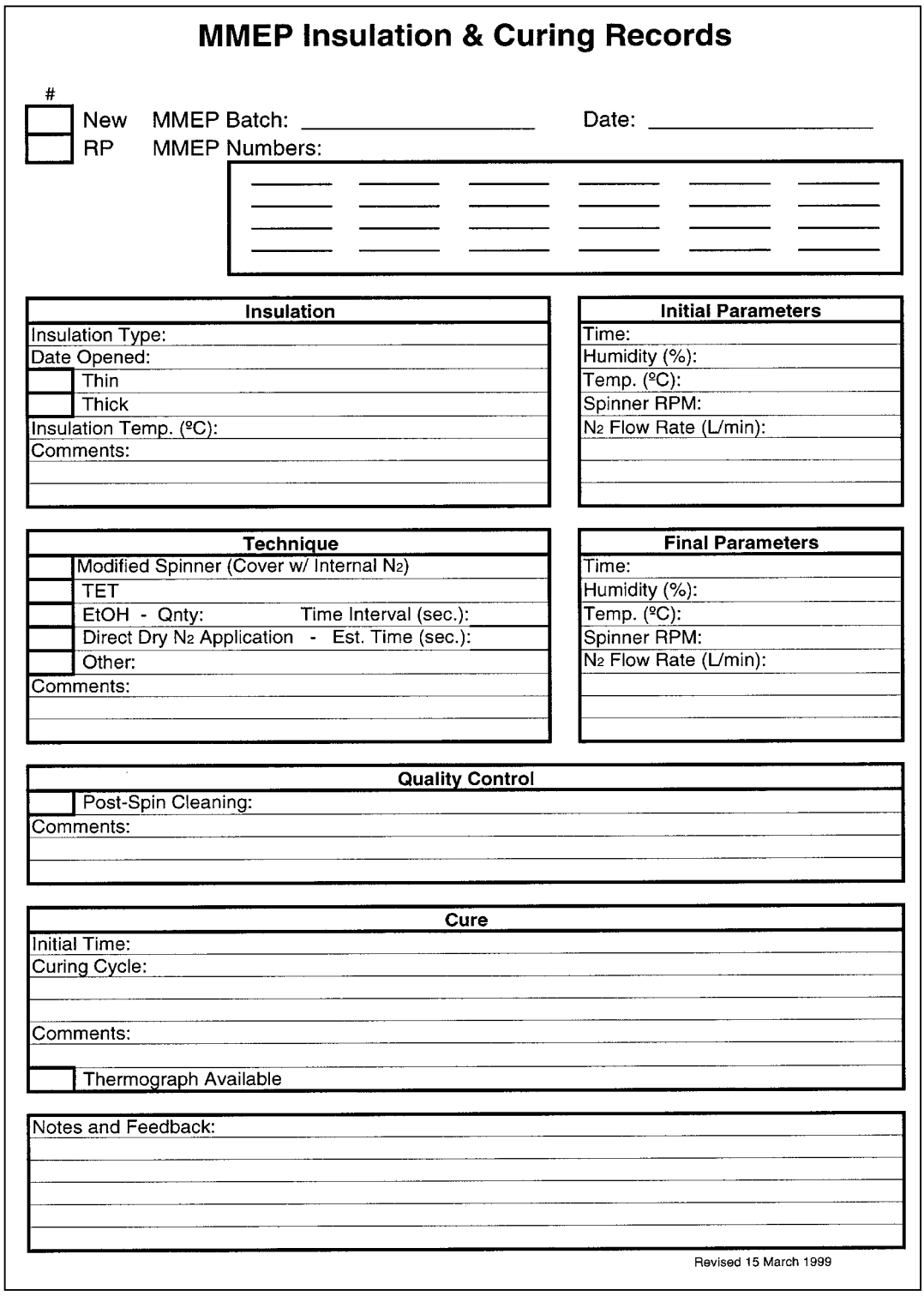

MMEP Insulation & Curing Records

☐ New MMEP Batch: _____ Date: _____
☐ RP MMEP Numbers:

Insulation
Insulation Type:
Date Opened:
☐ Thin
☐ Thick
Insulation Temp. (ºC):
Comments:

Initial Parameters
Time:
Humidity (%):
Temp. (ºC):
Spinner RPM:
N_2 Flow Rate (L/min):

Technique
☐ Modified Spinner (Cover w/ Internal N_2)
☐ TET
☐ EtOH - Qnty: Time Interval (sec.):
☐ Direct Dry N_2 Application - Est. Time (sec.):
☐ Other:
Comments:

Final Parameters
Time:
Humidity (%):
Temp. (ºC):
Spinner RPM:
N_2 Flow Rate (L/min):

Quality Control
☐ Post-Spin Cleaning:
Comments:

Cure
Initial Time:
Curing Cycle:
Comments:
☐ Thermograph Available

Notes and Feedback:

Revised 15 March 1999

Figure 33: The MMEP insulation and curing quality control form is used to record technical parameters and major variables associated with insulating and curing a batch of new or reprocessed MMEPs.

variables and techniques used to insulate and cure a particular MMEP yields insight into the causes of insulation deterioration and breakdown.

A.2 MMEP Pre-Culture Evaluations and MMEP Feedback Evaluations

The next two quality control measures employed are the MMEP Pre-culture Evaluations (Figure 34) and the MMEP Feedback Evaluations. Both forms are very similar. This data sheet is designed to record all observations on individual MMEPs pertaining to insulation deterioration and electroplating quality as a function of wear and tear via cycling through cultures. Every new MMEP that is fabricated for culture (or client) use for the first time and every reused MMEP that has cycled through culture at least once is logged into the MMEP Pre-culture Evaluations. The MMEP Feedback Evaluations are aimed at deriving similar information. These forms are utilized to evaluate all MMEPs returned from various clients after use for reprocessing.

A comprehensive MMEP Pre-Culture Evaluation Database has been created to archive all pre-culture and feedback evaluations. There are more than 1600 individual MMEP evaluations or entries in the database from more than 400 different MMEPs. Each entry assesses a subjective qualitative analysis on the class and severity of any deterioration or breakdown observed with the polysiloxane insulation. Also, a ratio of the number of electrodes gold plated versus the number deinsulated and an analysis on adhesion is conducted. This will be discussed in the following chapter. Therefore, the database allows an overall quality control assessment for both insulation deterioration and gold adhesion. The MMEP Pre-culture Evaluation Database sorts all MMEPs individually by their unique identifier. Since any single MMEP may have multiple entries in the database, they are ordered chronologically by the evaluation date. Without

MMEP Pre-Culture Evaluations

Evaluator:_____ Date:_____

	MMEP#	Insulation			Gold Adhesion			Destination
		Det. Type	º Severity	Comments	# GP	# DeIns	Comments	
1								
2								
3								
4								
5								
6								
7								
8								
9								
10								
11								
12								
13								
14								
15								
16								
17								
18								
19								
20								
21								
22								
23								
24								
25								

Figure 34: The MMEP pre-culture evaluations form is used to document all new and used MMEPs before each use in culture. The MMEP evaluations are entered into a comprehensive MMEP Pre-Culture Evaluation Database.

exception, each and every MMEP is evaluated and eventually destined for reuse (culture), additional gold plating and reuse, or reprocessing.

There are some excellent advantages the database provides. Most importantly, we can monitor the progress as degradation occurs as a function of time or cycles through culture (Figure 18). The mechanism on how the various phenotypes of deterioration or breakdown are better understood. Any special conditions the MMEPs are exposed to during culturing are often linked to any damage associated with the insulation. Another advantage of the database involves the identification and back tracking of poorly insulated MMEPs, or those showing problems with the insulation. Because the MMEPs are listed alphabetically, it is easy to back track a particular MMEP via the MMEP Insulation and Curing Records. If necessary, the variables and techniques used for the MMEP in question may be further investigated. In conjunction, other MMEPs insulated in the same batch, may be retrieved from the database and compared. Hence, using the database and insulation records together, the types of insulation deterioration observed may possibly be linked to specific variables during fabrication and provide insight into the causes of deterioration. The database also allows for a statistical analysis on the various types and classes of deterioration. The evaluation database may be cross-referenced with additional culture databases when special circumstances apply.

A.3 Post-Insulation Quality Control Assessment Protocol, Checklist, and Datasheet

The third and major quality control measure is the Post-Insulation Quality Control Assessment. The goal is to test the integrity of the insulation on new MMEPs using severe insults which accelerate the effects of normal culturing exposure to force

insulation degradation. The protocol currently used is represented in Figures 35. Take note that some of the steps in the original culture protocol have been omitted from this protocol to expedite the assessment. Only those culture methods that are believed to contribute significantly to insulation deterioration and breakdown have been put to use. Briefly, one complete cycle in the assessment protocol begins with autoclaving, is followed by flaming and soaking in saline (or Ringers), and ends with typical reuse methodology (decontamination in 70%EtOH or 1% bleach and soak in DIH_2O). The cycle may then be repeated as necessary.

To keep track of all the variables and parameters during each individual step of the assessment protocol, a checklist has been developed. This is termed the Post-Insulation Quality Control Assessment Checklist (Figure 36). Per cycle, the checklist includes criteria such as autoclave location, time and temperature, the drying oven time and temperature, the number of times the matrix and feeder area are flamed, the type of saline (soak) solution and incubation time and temperature, and the type of solutions and time the MMEPs are used for reuse. The Post-Insulation Quality Control Assessment Data Sheet (Figure 37) has been drafted to coincide with the checklist. Before and at the end of all four steps in the protocol, as outlined in the protocol and checklist, the investigator is required to observe each MMEP for any signs of deterioration and breakdown with the insulation using high-magnification phase microscopy. For each MMEP per cycle, the data sheet is used to record the class, type and severity, if any, of insulation degradation.

Ideally, a MMEP from any batch that has just been insulated can be immediately subjected to the Post-Insulation Quality Control Assessment to determine if there are any

Post-Insulation Quality Control Assessment Protocol

The following protocol will be used for the quality control assessment of insulation adhesion, breakdown and deterioration. The goal is to test the integrity of the insulation using accelerated culture methods to force insulation degradation. The feedback provided should aid in the identification of insulation breakdown, optimization of MMEP insulation, and to classify and link insulation deterioration with causal relationships, either related to MMEP fabrication and/or culture procedures. Prior to testing, all MMEP's tested should be both insulated and deinsulated. Gold plating is not necessary.

Protocol

1. Autoclave
   a. Place MMEPs on a clean, low fiber residue filter paper in a large glass petri dish.
   b. Autoclave MMEPs at 120°C for 20-25 minutes.
   c. Oven dry MMEPs at 56°C for one hour.
   d. Observe MMEPs for insulation deterioration.

2. Flame
   a Place MMEPs in sterile 135mm plastic petri dishes (Fisher 95x15mm).
   b. Using the stereo microscope within the laminar flow hood, position the sterile MMEP mask so that the small hole is centered over the matrix area.
   c. Direct the microtorch flame at both the matrix and feeding area and hold for 0.5 to 1.0 second. Wait 5 seconds to allow heat dissipation. Repeat 1 to 3 times for both the matrix and feeding area.
   d. Allow MMEP to cool for approximately 20 seconds.
   e. Observe MMEPs for insulation deterioration.

3. Soak
   a. Place MMEPs in teflon holders inside 200ml beaker.
   b. Completely submerge the MMEPs in 1.0% saline or Ringers solution.
   c. Seal and cover beaker with parafilm and petri lid.
   d. Allow MMEPs to incubate at 37°C for a minimum of 48 hours.
   e. Rinse beakers in DIH_2O.
   f. Observe MMEPs for insulation deterioration.

Ringer's
5mM KCL
124mM NaCl
45mM$NaHCO_3$
2.4mM $CaCl_2$
1.3mM $MgSO_4$
10mM Glucose
1.2mM KH_2PO_4

4. ReUse
   a. With MMEPs still in the beakers, submerge the MMEPs in 70% EtOH for approximately 1 minute. Rinse thoroughly with DIH_2O.
   b. Submerge the MMEPs in 5% bleach for no more than 1 minute. Rinse thoroughly with DIH_2O.
   c. Soak the MMEPs in DIH2O for a minimum of 12 hours.
   d. Observe MMEPs for insulation deterioration.

5. Repeat steps 1-4 as necessary.

Revised 4 February 1999

Figure 35: The post-insulation quality control assessment protocol is designed to force insulation deterioration and breakdown at accelerated rates, while emulating standard culture practice. The protocol includes major factors proven to contribute to polysiloxane insulation degradation.

Post-Insulation Quality Control Assessment Checklist

Batch ID: _____ **Investigator:** _____

Cycle #

1. Autoclave

- ❑ Place MMEPs on a clean, low fiber residue filter paper in a large glass petri dish.
- ❑ Autoclave MMEPs at 120°C for 20-25 minutes.

Autoclave Location: _____
Autoclave Time: _____min
Total Time (approx.) in the Autoclave: _____hrs

- ❑ Oven dry MMEPs at 56°C for one hour.

Drying Time: _____min
Oven Temperature: _____°C

- ❑ Observe MMEPs for insulation deterioration.

_____
_____
_____

2. Flame

- ❑ Place MMEPs in sterile 135mm plastic petri dishes (Fisher 95x15mm).
- ❑ Using the stereo microscope within the laminar flow hood, position the sterile MMEP mask so that the small hole is centered over the matrix area.
- ❑ Direct the microtorch flame at both the matrix and feeding area and hold for 0.5 to 1.0 second. Wait 5 seconds to allow heat dissipation. Repeat 1 to 3 times for both the matrix and feeding area.

No. of Matrix Flames: _____
No. of Feeder Flames: _____

- ❑ Allow MMEP to cool for approximately 20 seconds, and remove the mask.
- ❑ Observe MMEPs for insulation deterioration.

_____
_____
_____

3. Soak

- ❑ Place MMEPs in teflon holders inside 200ml beaker.
- ❑ Completely submerge the MMEPs in 1.0% saline or Ringers solution.

Type of Solution: _____

- ❑ Seal and cover beaker with parafilm and petri lid.
- ❑ Allow MMEPs to incubate at 37°C for a minimum of 48 hours.

Incubation Time (approx.): _____hrs
Incubator Temperature: _____°C

- ❑ Rinse beakers in H_2O.

Rinsing Time: _____min

- ❑ Observe MMEPs for insulation deterioration.

_____
_____
_____

Ringer's
5mM KCL
124mM NaCl
45mMNaHCO$_3$
2.4mM CaCl$_2$
1.3mM MgSO$_4$
10mM Glucose
1.2mM KH$_2$PO$_4$

4. ReUse

- ❑ With MMEPs still in the beakers, submerge the MMEPs in 70% EtOH for approximately 1 minute. Rinse thoroughly with DIH_2O.

Time: _____sec

- ❑ Submerge the MMEPs in 5% bleach for no more than 1 minute. Rinse thoroughly with DIH_2O.

Time: _____sec

- ❑ Soak the MMEPs in DIH2O for a minimum of 12 hours.

Soaking Time(approx.): _____hrs

- ❑ Observe MMEPs for insulation deterioration.

_____
_____
_____

5. Repeat steps 1-4 as necessary.

Revised 19 February 1999

Figure 36: The post-insulation quality control assessment checklist is intended to keep track of which method and significant parameters are used.

Post-Insulation Quality Control Assessment
Data Sheet

Batch ID: _____ **Date:** _____

MMEP#	Treatment	Insulation Deterioration Observation & Classification			
		Cycle 1	Date	Cycle 2	Date
	Before				
	Autoclave				
	Flame				
	Soak				
(1)	ReUse				

Comments:

MMEP#	Treatment	Insulation Deterioration Observation & Classification			
		Cycle 1	Date	Cycle 2	Date
	Before				
	Autoclave				
	Flame				
	Soak				
(2)	ReUse				

Comments:

MMEP#	Treatment	Insulation Deterioration Observation & Classification			
		Cycle 1	Date	Cycle 2	Date
	Before				
	Autoclave				
	Flame				
	Soak				
(3)	ReUse				

Comments:

Revised 15 February 1999

Figure 37: The post-insulation quality control assessment data sheet is used to record information on insulation deterioration and breakdown for each MMEP tested. Qualitative observations are conducted using high-contrast phase microscopy after each major step in the protocol.

problems associated with the insulation, and moreover, which method in the protocol caused a particular type of deterioration. Coupled with the MMEP Insulation and Curing Records parameters recorded during the insulation of that batch of MMEPs, causes that lead to insulation degradation may be determined. Consequently, better techniques may be devised to correct the problem and optimize MMEP insulation.

APPENDIX B

GOLD ELECTROPLATING QUALITY CONTROL

APPENDIX B

GOLD ELECTROPLATING QUALITY CONTROL

B.1 MMEP Deinsulation and Gold Plating Records

The MMEP Deinsulation and Gold Plating Records are the most critical gold electroplating quality control measures in use. In general, this form is designed to keep records of a majority of the gold electroplating variables for each MMEP in any particular batch of MMEPs that is gold plated. A representation of the MMEP Deinsulation and Gold Plating Records is given in Figure 38. All the MMEPs in a batch (usually 15 MMEPs) are recorded in sequence. Moreover, every batch deinsulated and gold plated is archived in order by MMEP type, date, and MMEP number.

The deinsulation parameters include a ratio of the total number of gold plated electrodes to the total number of deinsulated electrodes, plus any observations with the ITO conductors or insulation immediately around the matrix. The gold electroplating parameters consist of the voltage, current, plating time, plating density (qualitative assessment), and feedback on the deinsulation quality by observing the pattern of the plated gold on the ITO electrode. The electrodes that fail to electroplate are listed. Information on the gold electroplating solution is recorded. This includes type, age, pH, temperature, and other applicable comments. Pulse generator and oscilloscope settings are noted. The parameters of any other equipment used for gold plating, such as a heat lamp, are logged on the form. Qualitative observations on gold deposition, appearance and bonding are also documented. When necessary, records of the laser deinsulation equipment settings and modifications are included.

MMEP DeInsulation & GoldPlating Record

MMEP Batch Identification: _____

Date DeInsulated: _____
Date Gold Plated: _____

	MMEP#	# GP'd	# DI'd	Cut & Damaged Electrodes	Insulation Notes	Acid Strike (min.)	Voltage (mV)	Current (uA)	Time (min)	Density	Non-GP'ed Electrodes	Additional Notes	Destination
1													
2													
3													
4													
5													
6													
7													
8													
9													
10													
11													
12													
13													
14													
15													

GP Solution Notes:
a. Type:
b. Date:
c. Age:
d. pH:
e. Temp:

GP Apparatus Notes:
a. Pulse Gen. Settings:
b. Oscilloscope Settings:
c. Heat Lamp Setting:

GP Adhesion Notes:
a. Appearance:
b. Bonding:

Other Notes:

Figure 38: The MMEP deinsulation and gold electroplating form is designed to document all methods, equipment parameters, variables and observations that concern the laser deinsulation and electrolytic deposition of gold on the ITO electrodes.

The deinsulation and gold plating observations note any problems associated with the insulation or mistakes made during the deinsulation. These notes ultimately help decide the fate and destination of each MMEP (trash, local use or client). They also provide valuable feedback and statistics for any problems that may arise during MMEP photoetching or fabrication. In addition, all documented variables and equipment settings used for any particular MMEP or batch of MMEPs is easily referenced. This is a beneficial tool that allows the variables to be linked to any problems associated with poor gold adhesion.

B.2 MMEP Pre-Culture Evaluations and MMEP Feedback Evaluations

The MMEP Pre-Culture Evaluations (Figure 34) and the MMEP Feedback Evaluations are discussed in detail in Appendix A.2. Therefore, the focus of these two quality control measures in this discussion primarily concerns gold plating. In review, these forms are designed to document all observations on individual MMEPs that pertain to insulation breakdown and gold electroplating quality after each use or cycle in cell culture (pre-culture evaluations) or after several uses from various clients (feedback evaluations). The evaluation of each MMEP is entered into the comprehensive MMEP Pre-Culture Evaluation Database. For each MMEP entry, an analysis on gold adhesion plus the ratio of gold plated electrodes to deinsulated electrodes is conducted.

In reference to gold plating, the database is very useful. Since the MMEPs are tabulated chronologically by MMEP number and then date, it is easy to monitor gold adhesion on any particular MMEP as a function of time. In other words, basic wear and tear resulting from repeated cycling through culture indicates the quality of the gold deposition and adhesion to the ITO electrodes as time progresses. On any individual

MMEP with multiple listings in the database, reviewing the ratio of gold plated to deinsulated electrodes helps to monitor the progressive loss of gold through time. The characteristics of how the gold is lost from the ITO electrodes are also investigated. Furthermore, MMEPs deinsulated and electroplated from the same batch are closely associated in the database, and very simple to compare. Once a problem has been recognized with an individual MMEP or a batch of MMEPs, the database may be linked to the MMEP Deinsulation and Gold Plating Records. After close examination of the variables and parameters via back tracking, causes to the problems may be discovered and corrected.

B.3 MMEP Sonication

MMEP ultra-sonication is an effective quality control test for gold-ITO adhesion. MMEP sonication entails ultra-high frequency sonication to displace or dislodge the gold plating from the ITO electrodes. Briefly, the MMEPs are placed upright into teflon holders inside a 250 mL beaker. Ultra pure water is added to the beaker until the MMEPs are completely covered, and the beaker is placed in the sonicator reservoir. UPH_2O is added to the reservoir until the level equals that in the beaker. Ultra-high frequency sonication is carried out at various time intervals in an ultra-sonicator (Fisher Scientific). After every time interval, each MMEP is removed and observed using light microscopy. The ratio of the number of gold plated to deinsulated electrodes is assessed.

The ultra-high frequency sonication of gold plated MMEPs has several benefits. First, the sonication provides both a qualitative and quantitative means of quality control for assessing gold adhesion and electroplating methodology. The observations of the MMEPs during sonication yield insight into the mechanisms of how the gold is removed,

whether the gold may be flaking off in patches or entirely dislodging from the ITO. Traces of the remaining residual gold are indicative of the regions of good gold-ITO contact and adhesion. This feedback is essential for determining the best plating parameters to utilize, such as the applied voltage, current and duration. It also renders useful information about optimizing plating procedures necessary to achieve the best gold-ITO adhesion and durability, like the plating density and thickness of the gold. The MMEP ultra-sonication test is quantitative in that a simple statistical analysis or graphical representation of the adhesion data yields comprehensive results given for that particular MMEP or batch of MMEPs. The data is graphed as the percentage of gold loss as a function of sonication time. Examples of the sonication graphs are represented in Figures 30 and 31. Furthermore, MMEP sonication is a rapid means of testing gold adhesion, and requires few resources (materials, labor, etc…).

APPENDIX C

CURRENT INSULATION TECHNICAL DETAIL

Ultra-pure compressed nitrogen was turned on at a flow rate of about 5 L/min for twenty minutes to purge and dry the spinning apparatus. Meanwhile, an aliquot of 15-20 mL of DC648 was obtained from a desiccated stock DC648 and placed into a clean, ultra-pure nitrogen purged glass vial. The aliquot was allowed to equilibrate to room temperature for fifteen minutes. A batch of fifteen pre-cleaned MMEPs was submerged in fresh 100% EtOH. Here, the MMEPs were sequentially arranged by MEPP number in grooved teflon holders, each in an upright position. After completing the preparation prior to the spin application, all important variables and notes were recorded into the MMEP Insulation and Curing Records (Appendix A). Just prior to spinning, a single MMEP was removed from the 100% EtOH. A majority of the EtOH was allowed to drain off the upright MMEP. The lid to the spinning apparatus, containing 100% dry nitrogen, was lifted and the EtOH saturated MMEP was placed on the spinner platform. The lid was closed and the MMEP was spun at 2000-2500 rpm for up to thirty seconds to remove excess 100% EtOH. The lid was reopened, the MMEP carefully removed, and closed again. Without delay while working quickly over the insulation application port, the left and right amplifier contact strips were covered with Scotch brand tape. The excess tape was quickly torn away, the lid raised, and the MMEP returned to the spinner platform. After the lid was shut, roughly 1 mL of pure denatured EtOH (Sigma) was injected through the application port onto the matrix, to absorb any contaminants. Again the MMEP was spun at 2000-2500 rpm for fifteen seconds. At fifteen seconds, the spinner was stopped and 1.0-1.5 mL of DC648 polysiloxane resin was quickly applied through the application port. The MMEP was immediately spun at 2000-2500 rpm for ten seconds, and allowed to remain in the ultra-pure nitrogen for an additional five to ten

seconds. This created a 2-4 μm thin insulation layer that covered the entire surface of the plate. In the meantime, the process began again with the removal of another MMEP in sequence from the 100% EtOH. The insulated MMEP was replaced by a non-insulated MMEP and the cycle was repeated. While the non-insulated MMEP was spinning, the freshly insulated MMEP was transferred to a covered glass container under a laminar flow hood, to prevent particulate contamination. Each complete cycle (one MMEP) required approximately 90-120 seconds.

After a typical batch of fifteen MMEPs were completed, they were removed from the laminar flow hood three at a time, beginning with the first insulated and following in sequence. Each individual MMEP underwent a quality control procedure prior to curing. Under the laminar flow hood, the MMEP was taken out of the closed glass container and the tape was carefully removed from the electrodes. A cotton swab saturated in 100% EtOH was used to clean off any debris or excess insulation on the electrodes or back of the MMEP. Finally, in groups of three, the MMEPs were placed flat on aluminum foil in clean Pyrex baking dishes and cured in a pre-cleaned oven using the long ramp and soak cycle previously described. The entire insulation process for a batch of fifteen MMEPs, beginning with the insulation of the first MMEP and ending with the quality control cleaning of the final MMEP, consumed approximately 60 minutes.

APPENDIX D

CURRENT GOLD ELECTROPLATING TECHNICAL DETAIL

In preparation, the CPGC electroplating solution was heated up to approximately 35-40ºC and maintained at this temperature throughout the plating process. The heated electroplating solution assisted in the removal of trapped air pockets in the deinsulation craters, which if present, prevented plating at the ITO cathode. The zebra connectors were thoroughly cleaned in 100% EtOH using the wooden shaft of the cotton swab. The gold wire anode was briefly cleaned in 100% EtOH. Prior to plating, each MMEP was subjected to a 2.5 minutes preconditioning acid strike using 3 N HCl diluted from concentrated 12 N HCl (36.5-38% assay strength). About 2 mL of the 3 N HCl was placed over the 64 ITO electrodes in the center of the MMEP and worked into the deinsulation craters. This was achieved by holding the MMEP horizontally and rapidly moving it up (10 cm) and down (10 cm) vertically to displace the air pockets. After 2.5 minutes, the acid solution was removed and the matrix was rinsed with UPH_2O for a few seconds. The purpose for the acid strike was to remove the oxidation layer from the ITO. The MMEP was transferred to a vertical flow hood next to the gold plating apparatus, and about 1.5 mL of warmed CPGC solution was pipetted over the 64 ITO electrodes on the matrix of the MMEP. As previously discussed with the acid strike, the air pockets were forced out with rapid vertical movements. The CPGC plating solution was allowed to settle on the MMEP for 4 to 8 minutes before electroplating to ensure no gas remained in the laser-deinsulated craters.

All pertinent information on the CPGC solution and electroplating apparatus was recorded into the MMEP Deinsulation and Gold Plating quality control form (Appendix

B). Depending on the MMEP type, the initial applied voltage was adjusted to compensate for the differences in surface area of the ITO cathodes and achieve similar current densities. For the Y3C and Y4A microelectrode designs, the voltages were approximately 2.1 and 2.2 volts, respectively.

The assembly of the electroplating sandwich occurred on the microscope stage. The MMEP to be electroplated, with the CPGC solution over the matrix, was placed on the non-conducting base plate of the sandwich and carefully centered. Zebra connectors were placed over the (32) ITO electrodes on the left and right side of the MMEP. The top conducting plate was lowered over the MMEP until it rested on the zebra conductors, and the thumbscrews were fastened. It was important that the base and top plate were in alignment to prevent changes in the position of the zebra strips.

After the ITO electrodes were surveyed for bubbles, the electrolytic lead was connected to the top plate of the assembled sandwich. The heat lamp was turned on to about 80ºC and directed towards the CPGC solution resting on the surface of the MMEP over the matrix. This type of thermal convection helped to agitate the CPGC solution, and was believed to allow more reactants and products to exchange at the electrode surface and reduce polarization at the cathode. The gold wire anode was lowered and submerged into the CPGC plating solution, and the timer was started. The ITO electrodes were briefly examined through the microscope to ensure that there was no cathodic electrolysis creating $H_{2(g)}$ gas pockets in the deinsulation crater. The current (1.0-1.3 μA for Y3C and 2.3-3.0 μA for Y4A) was monitored for several seconds. The total exposed ITO surface area and maximum current density for Y3C MMEPs was

roughly 0.0144 mm^2 and 90 $\mu A/mm^2$, and for Y4A MMEPs was 0.0452 mm^2 and 66 $\mu A/mm^2$. After 2.0 to 2.5 minutes, the electrodes usually had a significant layer of gold, and the anode (gold wire) was lifted out of the CPGC solution and wiped clean. The sandwich was disassembled, and the MMEP was rinsed for about 3 to 5 seconds with UPH_2O. Then, a brief quality control assessment took place using higher magnification with an additional light microscope. The gold plating parameters and electroplating variables were recorded into the MMEP Deinsulation and Gold Plating Records form (Appendix B).

Just before electroplating the next MMEP containing the CPGC solution, another MMEP was preconditioned with an acid strike. The acid strike solution was removed while that MMEP was electroplating. The brief qualitative observations of gold deposition and adhesion were also performed at the same time as the electrodes were plating. Hence, these processes were simultaneously cycled in accordance with the methods stated above until a typical batch of MMEPs was completed. The rate-limiting step was the assembly of the sandwich, electroplating, and disassembly of the sandwich, which required approximately seven minutes per MMEP. Once completed, the MMEPs were divided into culture or client reserves, depending on the overall quality of the MMEP.

REFERENCES

Cohen LB, Salzberg BM (1978) Optical measurement of membrane potential. Rev Physiol Biochem Pharmacol 78: 35-88.

Connolly P, Clark P, Curtis ASG, Dow JAT, Wilkinson CDW (1990) An extracellular microelectrode array for monitoring electrogenic cells in culture. Biosensors and Bioelectronics 5: 223-234.

Grinvald A, Salzberg BM, Lev-Ram V, Hildesheim R (1987) Optical recording of synaptic potentials from processes of single neurons using intracellular potentiometric dyes. Biophys J Apr;51(4): 643-51.

Gross GW, Rieske E, Kreutzberg GW, Meyer A (1977) A new fixed-array multi-microelectrode system designed for long-term monitoring of extracellular single unit neuronal activity in vitro. Neuroscience Letters 6: 101-105.

Gross GW (1979) Simultaneous single unit recording *in vitro* with a photoetched laser deinsulated gold multimicroelectrode surface. IEEE Transactions on Biomedical Engineering BME-26: 273-279.

Gross GW, Lucas JH (1982) Long-term monitoring of spontaneous single unit activity from neuronal monolayer networks cultured on photoetched, laser-deinsulated, gold multimicroelectrode surface. J Electrophysiol Tech 9: 55-67.

Gross GW, Wen WY, Lin JW (1985) Transparent indium-tin oxide electrode patterns for extracellular, multisite recording in neuronal networks. Journal of Neuroscience Methods 15: 243-252.

Gross GW, Kowalski JM (1991) Experimental and theoretical analysis of random nerve cell networks dynamics. In: Neural Networks: Concepts, Applications, and Implementations, Vol. 4 (P.Antognetti, V.Milutinovic, eds), pp 47-110. Englewood, N.J.: Prentice Hall.

Gross GW (1994) Internal Dynamics of Randomized Mammalian Neuronal Networks in Culture. In: Enabling Technologies for Cultured Neural Networks (Stenger DA, McKenna TM, eds), pp 277-317. New York: Academic Press, Inc.

Gross GW, Norton S, Gopal K, Schiffman D, Gramowski A (1997) Neuronal networks in vitro: applications to neurotoxicology, drug development and biosensors. Cell Eng 2: 138-147.

Hargis LG (1988) Electroanalytical Methods Based on Electrolysis. In: Analytical Chemistry: Principles and Techniques pp 350-358. Englewood Cliffs, N.J.: Prentice-Hall, Inc.

Israel DA, Barry WH, Edell DJ, Mark RG (1984) An array of microelectrodes to stimulate and record from cardiac cells in culture. Am J Physiol 247: 669-674.

Jimbo Y, Kawana A (1992) Electrical stimulation and recording from cultured neurons using a planar electrode array. Bioelectrochemistry and Bioenergetics 29: 193-204.

Kamioka H, Maeda E, Jimbo Y, Robinson HPC, Kawana A (1996) Spontaneous periodic synchronized bursting duing formation of mature patterns of connections in cortical cultures. Neuroscience Letters 206: 109-112.

Kandel ER, Schwartz JH, Sieglebaum SA (1991) Elementary Interactions Between Neurons. In: Principles of Neural Science (Kandel ER, Schwartz JH, Jessel TM, eds), pp121-234. East Norwalk, Connecticut: Appleton & Lange.

Kesselring RL, Howard LL (1986) Electrical Characteristics of Gold-Plated Indium-Tin-Oxide Microelectrode Arrays. (not published).

Nisch W, Boeck J, Egert U, Haemmerle H, Mohr A (1994) A thin film microelectrode array for monitoring extracellular neuronal activity in vitro. Biosensors and Bioelectronics 9: 737-741.

Palin GR (1969) Electroplating, Forming, Polishing and Machining. In: Electrochemistry for Technologists pp 154-180. Elmsford, New York: Pergamon Press Ltd.

Pine J (1980) Recording action potentials from cultured neurons with extracellular microcircuit electrodes. Journal of Neuroscience Methods 2: 19-31.

Rajagopal KS, Rajagopalan SR (1992) Selective gold plating on stainless steel components for space applications. Metal Finishing 90: 59-61.

Ransom BR, Neale E, Henkart M, Bullock PN, Nelson PG (1977) Mouse spinal cord in cell culture. I. Morphology and intrinsic neuronal electrophysiologic properties. J Neurophysiol 40: 1132-1150.

Sharma AK, Bhojaraj H (1990) Gold and black nickel plating on stainless steel for space applications. Metal Finishing 88: 115-116.

Skoog DA, West DM, Holler FJ (1996) Electrogravimetric and Coulometric Methods. In: Fundamentals of Analytical Chemistry pp 431-459. Orlando, Florida: Saunders College Publishing.

Skoog DA, West DM, Holler FJ (1996) Selected Methods in Analysis. In: Fundamentals of Analytical Chemistry p 820. Orlando, Florida: Saunders College Publishing.

Thomas CA, Springer PA, Loebe GE, Berwald-Netter Y, Okun LM (1972) A miniature micoelectrode array to monitor the bioelectric acivity of cultured cells. Exp Cell Res 74: 61-66.

Wenner P, Tsau Y, Cohen LB, Donovan MJ, Dan Y (1996) Voltage-sensitive recording using retrogradly transported dye in the chicken spinal cord: staining and signal characterisation. Journal of Neuroscience Methods 70: 111-120.